UC Berkeley
UC Berkeley Electronic Theses and Dissertations

Title

Telomerase and telomere length regulation in human disease

Permalink

https://escholarship.org/uc/item/6rr4f1ff

Author

Lorbeer, Franziska Katharina

Publication Date

2020

Peer reviewed|Thesis/dissertation

eScholarship.org Powered by the California Digital Library
University of California

Telomerase and telomere length regulation in human disease

By

Franziska Katharina Lorbeer

A dissertation submitted in partial satisfaction of the
requirements for the degree of

Doctor of Philosophy

in
Molecular and Cell Biology
in the

Graduate Division

of the

University of California, Berkeley

Committee in charge:

Professor Dirk Hockemeyer, Chair
Professor Robert Tjian
Professor David Raulet
Professor Britt Glaunsinger

Summer 2020

Abstract

Telomerase and telomere length regulation in human disease

By

Franziska Katharina Lorbeer

Doctor of Philosophy in Molecular and Cell Biology

University of California, Berkeley

Professor Dirk Hockemeyer, Chair

Telomere length shows a very wide distribution, from short to long, in the human population. Only at the extremes of the distribution are long or short telomeres associated with severe pathologies, such as cancer or bone marrow failure respectively. This variable constitutional telomere length provides a framework for the proliferative capacity of the cells of an individual. It thereby establishes the balance of enabling and limiting cell divisions required for tissue homeostasis. On the molecular level the key regulators of telomere length are the telomere binding protein complex shelterin and the telomere elongating enzyme telomerase.

Telomerase is expressed in embryonic and adult stem cells but downregulated upon differentiation. During tumorigenesis pre-malignant cells stabilize telomeres and acquire the capacity to proliferate indefinitely by various mechanisms. 90% of all cancers are immortalized by telomerase expression. Promoter mutations of the telomerase reverse transcriptase gene (TERT) are the most common non-coding mutations in cancer. However, the timing and consequences of *TERT* promoter mutations (TPMs) have not been fully established. I used a combination of melanoma patient samples and human embryonic stem cell (hESC) models to show that TPMs can occur before the loss of DNA damage checkpoints and do not prevent telomere shortening. *In vitro,* cells with TPMs proliferate for a prolonged time with ever shorter and partially deprotected telomeres. Thus, TPMs do not prevent bulk telomere shortening but extend cellular lifespan by healing the shortest telomeres for sustained proliferation. Over time cells with TPMs can gradually upregulate telomerase to levels sufficient to sustain all telomeres and thereby become immortalized as a bulk cell population.

The finding that TPMs occur very early during tumorigenesis of several cancers and provide a selective advantage for overcoming replicative senescence, led me to further investigate the role of telomere shortening as a tumor suppressive mechanism. However, pre-cancerous melanocytic neoplasms – dysplastic nevi – are widely believed to arrest due to oncogene induced senescence caused by the acquisition of an initial driver mutation. To assess when and how TPMs confer a selective advantage to melanocytes, I analyzed dysplastic nevi for melanoma-associated mutations and telomere length. I found that TPMs were detected with a higher frequency in older patients, indicating that not all melanocytes were arrested and that later in life telomere

length becomes limiting for proliferation. The analysis of telomere length revealed a dichotomy: melanocytes of samples with TPMs had relatively shorter telomeres than *TERT* promoter wild-type samples. In contrast, BRAF p.V600E-positive nevi had longer telomeres than nevi with other driver mutations and none of the BRAF p.V600E nevi harbored a TPM. This indicates that melanocytic growth can be restricted by either replicative senescence or oncogene induced senescence in a driver mutation dependent manner.

Telomere shortening acts as a tumor suppressor mechanism by restricting proliferation but in order to replenish tissues for homeostasis cells have to be able to undergo a sufficient number of cell divisions. In the short telomere disease Dyskeratosis congenita (DC) very short constitutional telomeres lead to severe pathologies of regenerating tissues like the bone marrow, lung and liver. 11 to 24% of DC cases are caused by heterozygous, autosomal dominant mutations in the shelterin component TIN2. We established a human embryonic stem cell (hESC) model system of TIN2 DC missense mutations, which recapitulates the short telomere patient phenotype. In hESCs the DC mutation leads to telomere shortening in a telomerase-dependent manner, while maintaining telomere protection. As a consequence, the differentiated daughter cells have a reduced proliferative capacity. Disruption of one allele of TINF2 restores telomere length and proliferative capacity. We conclude that TIN2-DC mutations exert their disease effect in the telomerase-positive stem cell compartments of the human body, such as hematopoietic stem cells, which could provide an attractive target for therapeutic intervention in the future.

Table of Contents

Acknowledgements iii

Chapter 1: Telomere length regulation in health and disease 1

Telomeres: The molecular clock of the cell 1

Molecular telomere length regulation by shelterin and telomerase 2

Regulation of *TERT* in cancer 3

Aberrant telomere length regulation leads to disease 4

Dissertation research questions 5

Figures 7

Chapter 2: Mutations in the promoter of the telomerase gene *TERT* contribute to tumorigenesis by a two-step mechanism 10

Abstract 10

Main 10

Supplemental Figures 18

Material and Methods 32

Chapter 3: Telomere shortening acts as a tumor suppressor mechanism in an oncogenic driver mutation dependent manner 37

Abstract 37

Introduction 37

Results 38

Discussion 41

Figures 43

Material and Methods 51

Chapter 4: Dyskeratosis congenita mutations in the shelterin component TIN2 affect telomere length in the stem cell compartment and lead to reduced proliferative capacity 53

Abstract 53

Introduction 53

Results 55

Discussion 57

Figures: 59

Supplemental Figures: 62
Material and Methods: 65
Chapter 5: Discussion and future directions 69
Summary 69
Why do cancer cells with TPMs generally have short telomeres and what are the implications? 69
TERT promoter mutations in precursor lesions 70
Molecular mechanisms of the mutant TERT promoter and ETS factor binding: An unresolved issue 71
Targetability and therapeutic relevance of TPMs: Short telomeres as a vulnerability 72
Long telomeres? Short telomeres? 72
References 74

Acknowledgements

I would like to thank all of you who have been part of this journey for the last 6 years:

First a big thank you to Dirk for being an inspiring thinker and always providing big visions of biology beyond individual experiments. Your enthusiasm for pure science is unparalleled. Thank you for always having an open office door and entertaining my wildest experimental dreams.

I am also grateful to have had a supportive and engaged thesis committee: Thank you Tij, Britt and David. Your input and comments during our meetings were invaluable and I appreciate your support beyond my thesis to become a successful scientist. Especially David, thank you for being out there on the basketball court every Friday morning for the past 6 years.

I would like to thank Kathy Collins and Roberto Zoncu for always being available for science and career discussions and sharing your passion for science, chocolates and drinks with me.

A special thank you also goes to my previous mentor Aurelio Teleman, who has taught me so much about how to think and do science.

I was so fortunate to work collaboratively with my partners in crime Sara Choo and Kunitoshi Chiba. I have spent most of my waking hours with you and I cannot imagine it any other way. I was also extremely lucky to be in the lab with the best possible lab mates especially John, John and Shirin. You have kept me sane this entire time and throughout the lockdown (!!) and thanks to you it has never felt like going to work but like “going to see my friends”. Also, Melissa and Paulina, you were the first friends I found in Berkeley, thank you for making me feel at home.

Berkeley has been the most supportive and inclusive community of grad students and faculty I have ever experienced. To my classmates and the movie night crew: Lydia, George, Tim, Dan, Eva, John. You have been the staple of my week for 126 movie nights and counting.

I cannot thank my friends enough for always having my back, countless sanity checks, journal clubs and sharing transcontinental adventures. And my friends who are my home and make sure that I never forget what actually matters: Catrine, Hanna, Kathy, Jule, Ferdl, Angi, Laura and das Känguruh.

My entire family who has always supported me no matter what:

Mama und Papa, ihr habt mir Wurzeln gegeben und Flügel.

Chapter 1: Telomere length regulation in health and disease

Portions of this chapter were published as "Lorbeer FK, Hockemeyer D: **TERT promoter mutations and telomeres during tumorigenesis**. *Curr Opin Genet Dev* 2020, **60**:56–62." [1]. It has been reproduced here in part with full permission of the authors.

Telomeres: The molecular clock of the cell

In eukaryotic cells, DNA, the genetic material, is organized into linear chromosomes. In order to protect and maintain the ends, the individual DNA molecules are capped by repetitive sequences called telomeres (Figure 1-1A). In humans, telomeres consist of tandem hexameric repeats ("TTAGGG") with a total length of 10-15kb. The repeats are bound by the six-member protein complex shelterin. Shelterin consists of TRF1, TRF2, RAP1, TPP1, POT1 and TIN2. The two DNA strands of each telomere have a 3' overhang of 50-500nt. With the help of the shelterin complex the overhang forms a duplex lariat structure, the t-loop, that arises from strand invasion of the overhang into the double-stranded telomeric DNA and creates the so-called displacement loop (D-loop) (Figure 1-1B, reviewed in de Lange 2009 [2]). This specific DNA architecture and binding of shelterin distinguish natural chromosome ends from internal DNA double-strand breaks. These protect chromosome ends against the activation of DNA damage checkpoints and aberrant repair by telomeric fusion [3,4]. By avoiding recognition as sites of DNA damage, telomeres help solve the end-protection problem, which arises from the organization of DNA into linear chromosomes.

Secondly, telomeres help solve the end-replication problem: DNA replication is bidirectional, but DNA polymerases can only proceed in a 5' to 3' direction and require an RNA primer with a free 3' end. Thereby it becomes impossible to fully replicate DNA without sequence loss. The solution to the end-replication problem is twofold: to protect the chromosomes from the loss of genetic information, the telomeric repeats serve as a sequence reservoir. To counteract sequence loss, some cells express the enzyme telomerase, which can synthesize new telomeric repeats and extends telomeres [5].

In the absence of telomerase, telomeres shorten on average 50-200nt with each cell division. This loss eventually triggers DNA damage signaling, leading to the arrest of cells in a state called replicative senescence. Telomeres thereby act as the molecular clock of the cell, which – by the decrease in length – count the cumulative population doublings. The number of divisions that cells can undergo before their telomeric repeats are depleted is referred to as the Hayflick limit [6]. This proliferative barrier can be delayed or overcome by the expression of telomerase [7]. Cells that constitutively express telomerase such as stem cells and cancer cells are immortal, meaning that their growth is not restricted by telomere shortening [8–11]. Telomere length and the telomerase expression status of cells together, therefore, determine how many cell divisions cells can undergo until they are restricted by replicative senescence (Figure 1-1D).

Molecular telomere length regulation by shelterin and telomerase

On a molecular basis, telomere length regulation is orchestrated by the interaction between shelterin and telomerase, and by the regulation of telomerase itself. While the shelterin components are found in all cell types, telomerase is only expressed in a subset of cells.

Regulation by shelterin

The proteins of the shelterin complex are anchored on telomeric DNA by the double-strand DNA binding components TRF1 and TRF2. Both TRF1 and TRF2 homodimerize and recruit the shelterin components TIN2, TPP1 and POT1 sequentially. TRF1, TRF2, TIN2 and POT1 are negative regulators of telomere length, while TPP1 acts as positive regulators (reviewed in Hockemeyer&Collins 2015 [12]). No role in telomere length regulation has been assigned to RAP1 [13]. The individual shelterin components can exert their roles as telomere length regulators in different ways: TRF1 and TRF2 occupy the double-strand portion of the telomere and control telomere accessibility for telomerase by transducing their occupancy status to the single-strand binding POT1, which results in steric blocking of access of the 3' end to telomerase [14–16]. To elongate telomeres, the single-strand DNA-binding protein POT1 is responsible for recruiting telomerase to the telomeres and POT1 together with the telomerase interacting protein TPP1 stimulate telomerase processivity *in vitro* [17,18]. Though the mechanism is not fully resolved, TIN2 may also regulate telomere length by stimulating telomerase recruitment [19]. Other proteins interacting with shelterin, such as the Apollo nuclease or CTC1-STN1-TEN1, have also been associated with changes in telomere length [20,21]. It has been speculated that they could be involved in telomere length regulation by processing the 3'-overhang and consequently also influencing the availability of the 3'-overhang for telomerase [12].

Taken together, telomere length regulation by the shelterin complex is achieved at two levels: by controlling whether individual telomeres are in an extendable state and by mediating the recruitment of telomerase.

Regulation by Telomerase

Telomere length control by telomerase regulation is mainly mediated by changes in telomerase acitivity. Telomerase is active during early development, human embryonic stem cells (hESCs), and adult stem cells but not in somatic, differentiated tissues [22–24] (Figure 1-1E). Telomerase consists of two components: the RNA component, Telomerase RNA (hTR), and the catalytic protein component, Telomerase Reverse Transcriptase (TERT). Overexpression of both components together leads to a dramatic elongation of telomeres [25,26]. Overexpression of the individual components leads to different outcomes depending on the targeted cell type/line: In naturally telomerase-positive human embryonic stem cells the overexpression hTR alone, but not TERT, can elongate telomeres [26]. In contrast, expression of TERT in fully differentiated telomerase-negative

cells leads to telomere elongation, while overexpression of hTR has no effect on telomere length [26,27].

This observation can be explained with the expression patterns of hTR and TERT. Regardless of telomerase activity hTR is highly expressed in all tissues [28]. In contrast, the mRNA expression of *TERT* is estimated at less than 1 to 5 copies per cell in telomerase-positive cells. Differences in telomerase activity are closely associated with *TERT* mRNA expression levels [29]. The transcriptional regulation of the *TERT* promoter has been studied extensively but no single factor has been identified as solely responsible for regulation. The *TERT* promoter is a TATA-less promoter, embedded in a CpG island, a region rich in transcription factor binding sites (E-box, ETS- and SP1-binding sites) [30] and also potentially repressor binding sites (MEN1) [31], which all appear to contribute to *TERT* regulation. How TERT expression levels are fine-tuned between stem cells and differentiated cells, therefore, remains unclear. Solving this question will be key for understanding the how telomere shortening acts as a tumor suppressor mechanism in different cell types (Figure 1-1E).

Regulation of *TERT* in cancer

In telomerase-negative cells, where TERT is undetectable, the induction of replicative senescence as a consequence of telomere shortening acts as a strong tumor suppressor mechanism. In order to overcome replicative senescence, cancer cells inactivate DNA damage signaling (e.g. p53 or CDKN2A) and stabilize telomeres (reviewed in Günes&Rudolph 2013 [32]). More than 90% of all human cancers overcome this proliferative barrier by expressing or re-activation of telomerase [33]. Several large scale chromosomal aberrations leading to aberrant *TERT* expression have been identified: amplifications of the *TERT* gene, transcriptional activation of the *TERT* gene through viral integrations [34,35], and rearrangements of the *TERT* locus [36–38]. Despite the discovery of these important mechanisms, it remained unresolved until recently how *TERT* is activated for a majority of cancer cases.

A major breakthrough came in 2013, with two studies in melanoma that identified three high frequency hotspot mutations in the *TERT* promoter at position -57A/C, -124C/T, -146C/T relative to the ATG start codon of the *TERT* gene [39,40] (Figure 1-2A). Systematic sequencing of the *TERT* promoter region of skin cancer samples further revealed less frequent tandem mutations in the *TERT* promoter (-124/125 CC>TT, -138/139 CC>TT) [41,42]. Several studies have worked on elucidating the molecular mechanism of *TERT* promoter mutations (TPMs). TPMs occur heterozygously and in a mutually exclusive fashion [43–45]. Each of the hotspot mutations creates a *de novo* ETS (E26 transformation specific) factor binding site. The ETS transcription factor family members share a conserved DNA binding domain that recognizes unique sequences containing GGA(A/T). While some to the of the ETS transcription factors are restricted to tissue specific expression, others are ubiquitously expressed [46].

Soon after the discovery of TPMs, a survey of 60 different tumor types confirmed their high prevalence in many other cancers, although they occurred with different

frequencies: for example, 51% in glioma and 44% in hepatocellular carcinoma (HCC) [47]. A comprehensive analysis of a TCGA data set of 9,127 patients and 31 cancer types determined that a remarkable 27% of all analyzed samples harbored one of these promoter mutations [48]. This extremely high prevalence makes TPMs the most frequent non-coding mutation in cancer and places them among the most frequent cancer mutations overall. Despite their ubiquity, TPMs are associated with a highly specific cancer spectrum. They are much more frequently found in cancers originating from tissues with low-self renewal rates such as melanomas, liposarcomas, and subtypes of gliomas, but are rare in cancers originating from highly regenerative tissues such as the intestine or blood [47]. In a matched data set of whole genome sequencing data and RNA-sequencing from 14 different cancer types, TPMs show an association with elevated *TERT* mRNA expression levels [49]. Additionally, when engineered into an isogenic hESC model, TPMs led to a failure of transcriptional downregulation upon differentiation [26]. The aberrant TERT expression in *TERT* promoter mutant cells and the pattern of TPM presentation suggests that TPMs do not provide a selective advantage in tumors initiating from naturally telomerase-positive cells. The mutation rather confers an advantage to cancer cells that initiate from tissues with low or typically no TERT expression [26] (Figure 1-2B).

Aberrant telomere length regulation leads to disease

Both cancer cells and embryonic as well as adult stem cells, are immortal. In immortal cells, telomere elongation is required to ensure continuous regeneration. Once stem cells have differentiated into telomerase-negative somatic cells, telomere shortening acts as a mechanism to limit the number of cell divisions and suppress aberrant proliferation. The constitutional “starting” telomere length of a human, which is set in the telomerase-positive cells, has to be within a certain range to balance both processes. Large population studies of telomere length of different blood cells of individuals of all age groups revealed that telomeres shorten with increasing age. Telomere length drops rapidly during early childhood, followed by a slow by steady decline [50–53] (Figure 1-3). While telomere length of all cells in the body may not necessarily behave the same way, it has been shown that leukocyte telomere length is correlated with telomere length in other cell types [54]. At the extremes of the telomere length distribution - regardless of age – are patients with a genetic deposition for either familial cancer (long telomeres) or short telomere diseases (reviewed in Savage 2018 [55]).

Familial cancers have been associated with mutations in both telomerase and shelterin genes (Figure 1-3A,B): rare cases of families with germline TPMs suffer from familial melanoma and other cancer types and patients present with longer telomeres than non-carriers [56]. Similarly, cancer-associated mutations in the shelterin proteins POT1 and TIN2 lead to telomere elongation and a broad variety of cancers (Kim et al. 2020, Schmutz et al. 2020, under review). Mutations in other shelterin components (TPP1, RAP1 [57]) have been identified in familial cancers but their effect on effect on telomere length has not been established. On the opposite end of the spectrum of telomere length related diseases are short telomere disorders, such as Dyskeratosis

Congenita (DC), Hoyerson-Hreidarsson syndrome (HHS), Pulmonary Fibrosis (PF) (Figure 1-3A,B). While cancer is a disease caused by the uncontrolled overproliferation of cells, short telomere diseases are characterized by defects of regenerative tissues, presumably due to a lack of proliferative capacity. Mutations that have been associated with these diseases generally fall into genes within the telomere maintenance pathways such as telomerase biogenesis and shelterin (reviewed in Savage 2018 [55]). Patients diagnosed with DC have a lymphocyte telomere length below the first percentile for their age and present with symptoms of varying severity, including bone marrow failure and severe liver disease [58]. Stronger telomere shortening is associated with an even increased disease severity [59]. Interestingly, patients with short telomere diseases also have an increased risk of developing acute myeloid leukemia, myeloid dysplastic syndrome, and solid cancers [60–62].

On a population-wide level, the genetic determinants of long telomeres are also associated with an increased risk for melanoma, lung cancer, breast and ovarian cancer and an increased overall cancer risk [63–66]. On the other hand, short telomeres are associated with a decreased risk of melanoma development [67,68]. Retrospective cancer studies, however, have reported that telomere length of cancer tissue was shorter compared to normal tissue [44]. Since both patients with short telomere disorders as well as increase telomere length, both have elevated risk for developing cancers, how is telomere length thus connected to each disease?

Dissertation research questions

While GWAS studies have been very powerful in identifying genetic variants associated with long and short telomeres, gaining a functional understanding of how the genetic variants are connected to the diseases, has remained a challenge. While a lot of progress has been made with the help of mouse models and cancer cell lines, their lack of physiological telomerase and telomere length regulation has limited the experimental possibilities to address: 1) In which cell-type does telomere length regulation take place? 2) What is the effect of a mutation, in an otherwise normal genetic background, on different cell types?

For my dissertation research presented here, I have studied the effects of two different mutations, which were identified in patients with telomere-related disorders. In order to understand how disease-associated mutations affect telomere length and consequently support disease formation, I have used a combination of hESC-based model systems and patient samples. hESCs are telomerase-positive and maintain a stable telomere length but can be readily differentiated into somatic, telomerase-negative cells. In contrast to cancer cells, they do not harbor other mutations and are genomically stable. The recent advances in genome-editing by site-specific nucleases and homologous recombination have made it possible to perform targeted gene knockouts but also repair and introduce point mutations (reviewed in Johnson 2015 [69]). To establish model systems for the individual mutations, we can now engineer hESCs and compare isogenic cell lines. This allows us to study the mutations in the context of

physiological telomere length and telomerase regulation and controls for genetic variability.

Specifically, I have addressed the following questions:

1) Are TPMs sufficient for immortalization during tumor formation and what is their effect on telomere length?
2) Do telomere-shortening and replicative senescence act as tumor suppressors during melanoma formation?
3) Which cells are affected by TIN2-DC mutations and can we counteract the short telomere disease phenotype?

In Chapters 2 and 3, I aim to elucidate the role of TPMs during early tumorigenesis and designed a study assessing the role of telomere shortening as a tumor suppressor mechanism in melanoma formation. In Chapter 4, I describe the establishment of an hESC-based model system to study the causes and consequences of DC mutations in the shelterin component TIN2. In the last chapter of my thesis I will provide concluding remarks to summarize my findings and present them in the broader context of telomere length regulation in health and disease.

Figures

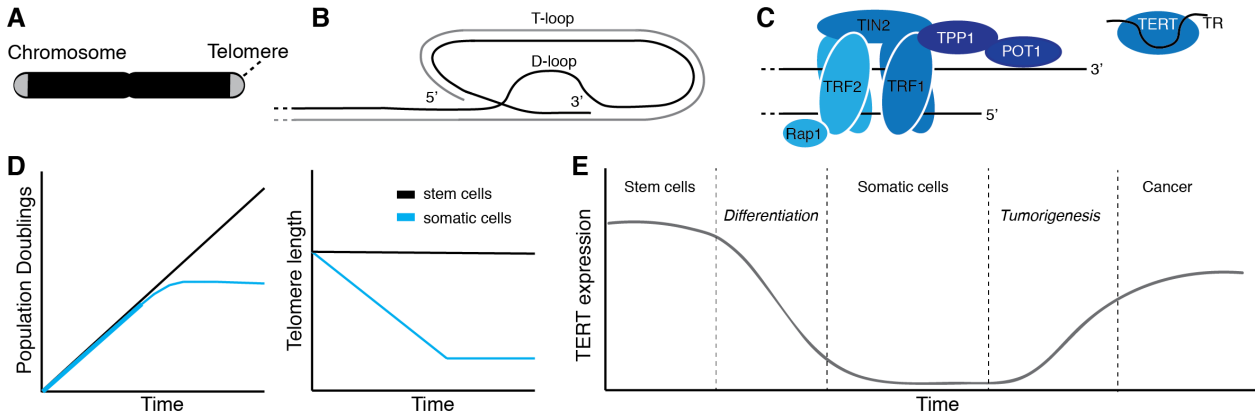


Figure 1-1: Telomeres, telomerase and proliferative capacity. *(A) Telomeres are the repetitive sequences capping the ends of linear chromosomes (B) Telomeric DNA forms a double lariat structure as protection against recognition as a site of DNA-damage. The 3' overhang invades the double-stranded portion of the telomere to form the T-loop (telomeric loop) and by displacing itself also creates the D-loop (displacement loop). (C) The shelterin complex is bound to the telomeres, suppresses the DNA damage response and recruits the telomere elongating enzyme telomerase comprised of the protein component TERT and RNA component TR. Shelterin consists of three DNA binding components TRF1, TRF2, and POT1. TIN2 binds TRF1, TRF2, and TPP1 which connects the complex to POT1. RAP1 is bound to TRF2. (D) Stem cells and somatic cells show different growth behaviors based on their ability to maintain their telomeres. Stem cells are immortal, telomerase-positive cells and proliferate indefinitely because they can maintain their telomeres. Somatic cells are telomerase-negative and undergo replicative senescence (plateau) because their telomeres shorten with each cell division. (E) TERT expression strongly correlates with telomerase activity. Telomerase is active in stem cells but downregulated during differentiation. In 90% of all cancers, telomerase is expressed.*

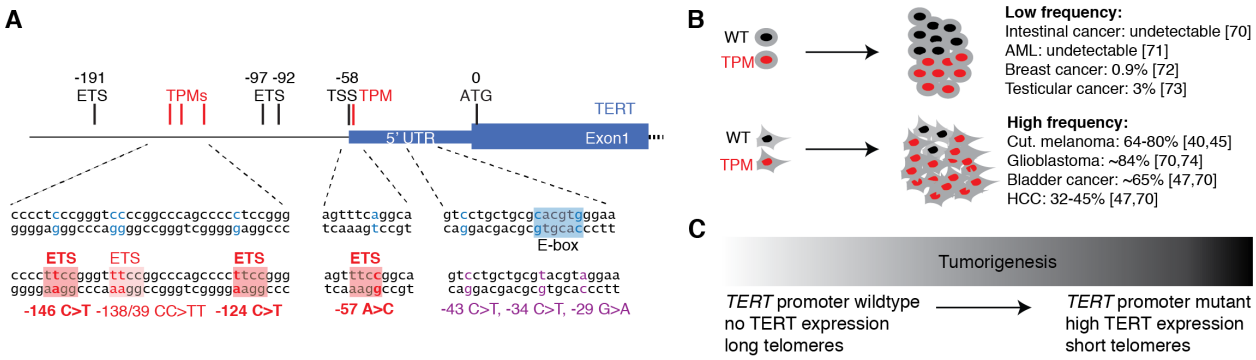
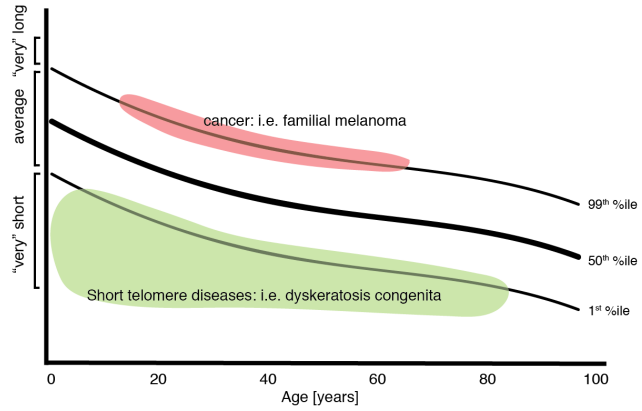


Figure 1-2: TERT promoter mutations are close to the transcription start site and occur with a high frequency in tissues of low self-renewal capacity. *(A) Schematic overview of the TERT promoter with the endogenous ETS factor binding sites (black), TERT promoter mutations (TPM, red) and 5 0 UTR mutations (purple). All numbers are relative to the first ATG of the TERT gene. (ETS = E26 transformation specific, TPM = TERT promoter mutation, TSS = transcription start site, 5 0 UTR = 5 0 untranslated region, E-box = enhancer box). (B) Model for TERT promoter mutations leading to a selective advantage depending on the telomerase status of the cell of origin of the cancer. In telomerase-positive cells there is no selective pressure from shortening telomeres, TERT promoter mutant (TPM, red) and wild-type (WT, black) can proliferate equally well. Cancers originating from tissues of high self-renewal have a low rate of TPMs. In telomerase-negative cells, telomeres shorten and act as a strong tumor suppressor mechanism. Cells that have acquired a TPM (red) have a selective advantage over WT (black) cells, which undergo replicative senescence. Cancers originating from tissues with low self-renewal capacity have TPMs with a high frequency. Low frequency: Intestinal cancer [70], acute myeloid lymphoma (AML) [71], breast cancer [72], testicular germ cell cancer [73]. High frequency: Cutaneous melanoma [40,45], glioblastoma [70,74], bladder cancer [47,70], hepatocellular carcinoma (HCC) [47,70]. (C) Over the course of tumorigenesis, cells that start with a wild-type TERT promoter, no TERT expression, and long telomeres turn into cancerous cells with high TERT expression and short telomeres.*

A



B

Gene	Cancer	Short telomere disease
TERT	TPMs: Familial melanoma, basal cell carcinoma, bladder tumor [39,75]	Point and missense mutations: DC, HH, AA, PF [79]
TR		Point mutations, promoter mutations: DC, AA, PF [80-83]
TINF2	Truncating and missplicing: Vatious cancers	Point mutations, missense mutations: DC, HH, RS [84, 85]
TPP1	Nonsense mutations: Familial melanoma [57]	Small deletion: AA, HH [86]
POT1	Point mutations: Familial melanoma, CLL, Li-Fraumeni like syndrome [76-78]	Substitution: CP [87]

Figure 1-3: Telomere length is widely variable in the population with extremely short and long telomeres leading to disease. *(A) Schematic representation of the connections between telomere length, age, and disease (adapted from Savage 2018 [55]) Clinically significant telomeres associated with telomere biology disorders are generally at or below the first percentile for age (green shape). Some studies have identified rare families with germline mutations in components of the shelterin telomere protection complex as associated with longer telomeres (red shape). (B) Table of familial mutations associated with long and short telomere disorders. Familial cancers: TERT [39,75], TIN2 (Schmutz et al. 2020), TPP1 [57], POT1 [76–78]. Short telomere diseases: TERT [79], TR [80–83], TIN2 [84,85], TPP1 [86], POT1 [87]. (AA = Aplastic anemia, CLL = Chronic Lymphoid Leukemia, CP = Coats Plus, DC = Dyskeratosis Congenita, HH = Hoyerson-Hreidarsson Syndrome, PF = Pulmonary fibrosis, RS = Revesz Syndrome)*

Chapter 2: Mutations in the promoter of the telomerase gene *TERT* contribute to tumorigenesis by a two-step mechanism

This Chapter was published as “Chiba K, Lorbeer FK, Shain AH, McSwiggen DT, Schruf E, Oh A, Ryu J, Darzacq X, Bastian BC, Hockemeyer D: **Mutations in the promoter of the telomerase gene TERT contribute to tumorigenesis by a two-step mechanism**. *Science* 2017, **357**:1416–1420.[88]” It has been reproduced here in part with full permission of the authors.

Abstract

TERT promoter mutations (TPMs) are the most common non-coding mutations in cancer. The timing and consequences of TPMs have not been fully established. Here we show that TPMs acquired at the transition from benign nevus to malignant melanoma do not support telomere maintenance. In vitro experiments revealed that TPMs do not prevent telomere attrition, resulting in cells with critically short and unprotected telomeres. Immortalization by TPMs requires a gradual upregulation of telomerase, coinciding with telomere fusions. These data suggest that TPMs contribute to tumorigenesis by promoting immortalization and genomic instability in two phases. In an initial phase, TPMs do not prevent bulk telomere shortening but extend cellular life-span by healing the shortest telomeres. In the second phase, the critically short telomeres lead to genome instability and telomerase is further upregulated to sustain cell proliferation.

Main

Mutations in the promoter region of the gene coding for the reverse transcriptase component of telomerase (TERT) [5,89] are found at high frequency in various human tumor types [39,40,47,90]. These *TERT* promoter mutations (TPMs) have been detected both in early- and late-stage tumors, consistent with the possibility that they play a role early in tumorigenesis [39,40,47,90,91]. However, tumor cells with TPMs have short telomeres despite exhibiting increased telomerase expression [44,92,93], an observation arguing that the critical functional effects of TPMs may occur at a later time point after telomeres have become critically short. Critically short telomeres can trigger a DNA damage response and replicative senescence, which can be bypassed by the loss of DNA damage checkpoints. This allows cells to continue proliferating until they enter a state called crisis, where telomeres become dysfunctional leading to chromosome end-to-end fusions and cell death. Cancer cells can emerge from crisis by reactivating telomerase [94]. Through the genomic instability that occurs during crisis, short telomeres can drive cancer [67,94–96]. Nevertheless, individuals with constitutionally shorter telomeres have a decreased cancer risk [64,67,68]. The current model of telomerase reactivation during crisis fails to explain these contradictory observations. Moreover, it is not understood why tumors with TPMs are associated with a poor prognosis [93,97].

To determine the role of TPMs in telomere maintenance during tumor formation, we followed the intratumoral changes in telomere length in tumors with TPMs. TPMs occur with high frequency (60-85%) in cutaneous melanoma [39,40,45]. We took

advantage of a subset of human melanomas, which arose from adjacent pre-neoplastic lesions such as nevi [91]. This allowed us to compare genetic alterations and telomere length in four melanomas that acquired TPMs as they arose from nevi (Figure 2-1 and Supplementary Data Figure 2-1). Using structured illumination microscopy, we acquired large, high-resolution telomere and centromere fluorescence in situ hybridization images of melanoma and nevus in the same tissue section and quantitatively analyzed telomere length (Figure 2-1A,B and Supplementary Data Figure 2-1). Multiple iterations of random sampling of normalized telomeric signals showed that in all four cases telomeres were significantly shorter in the melanoma than in the nevus (reduced normalized signal intensity in melanoma compared to the nevus, Figure 2-1C,D, Supplementary Data Figure 2-1D). These data highlight that in vivo, TPMs do not induce TERT expression levels sufficiently to counteract or reverse telomere shortening.

To explore the long-term effects of TPMs on telomere length and genomic stability in a genetically defined setting, we engineered the three most frequent TPMs de novo into human embryonic stem cells (hESCs) using CAS9 mediated genome editing [26] (Figure 2-2A and Supplementary Data Figure 2-2A-D). We started the "experimental clock" by differentiating the parental cell lines into fibroblasts, which are normally telomerase-negative. We assayed the proliferative capacity of hESC-derived fibroblasts with and without a single TPM using three distinct conditions: (i) fibroblasts transduced with Simian virus 40 large T antigen (SV40 TAg, inactivating pRb and p53 signaling) (Figure 2-2B, Supplementary Data Figure S2-2B), (ii) fibroblasts with intact cell cycle and DNA damage checkpoints (Figure 2-2C), and (iii) fibroblasts with inactivated cell cycle and DNA damage checkpoints, achieved by deletion of p14/p16 function (CDKN2A Δ/Δ) (Figure 2-2D, Supplementary Data Figure 2-2C). In all cell lines the TPMs extended the proliferative capacity significantly past the proliferative barrier of wild-type cells. Cells with TPMs proliferated without signs of crisis or a strong decrease in doubling rate at the time when wild-type cells arrested in a telomere length dependent manner [9] (Figure 2-2B-D, Supplementary Data Figure 2-2E,F). Overall, these data demonstrate that TPMs promote the immortalization of bulk cell populations.

Telomere maintenance is essential for cancer cell immortalization [33]. To investigate whether TPMs prevented telomere shortening, we measured telomere length over time in the fibroblast model system (Figure 2-2E-G and Supplemental Data Figure 2-3A,B). In wild-type cells, telomeres shortened progressively. Surprisingly, telomeres in cells with TPMs initially also shortened and stabilized only after approximately 70 population doublings (PD) at a length of 2.5-4.5 kb. The stabilized mean telomere length in the TPM cells was shorter than telomere length in wild-type control cells at the time of crisis (Figure 2-2E-G). The analysis of the telomere length distribution of cells with TPMs revealed that the mean length shifted from long to short telomeres and then stabilized (Figure 2-2H and Supplemental Data Figure 2-3C), suggesting that short telomeres were preferentially maintained, while long telomeres continued to shorten.

Unprotected short telomeres can lead to genomic instability through telomere fusion events, which have been detected in a variety of tumor samples and cell lines [94–

96,98–100]. To assess whether the chromosome ends are protected in cells with TPMs, we used a PCR-based method to quantify telomere-telomere fusion events over the course of a year after cell differentiation [98]. We detected fusions in SV40 TAg cells with the -124 and -146 TPMs when telomere length stabilized (Figure 2-3A,B and Supplemental Data Figure 2-4A,B). These fusion events were suppressed by overexpression of TERT (Supplemental Data Figure 2-4C), showing that they were driven by telomere attrition. Cells with the -57 TPM showed fewer fusions, presumably due to their slightly longer telomeres (Figure 2-2E). Thus, TPMs not only promote cancer cell immortalization but might also drive cancer cell evolution via dysregulation of telomere protection.

To determine the effect of TPMs on telomerase levels, we assayed enzymatic activity and TERT mRNA expression over time (Figure 2-3C, Supplemental Data Figure 2-4D,E). Shortly after differentiation, telomerase activity and *TERT* mRNA expression levels were higher in cells with TPMs than in wild-type cells, consistent with previous reports [26]. However, telomerase levels rapidly fell below the detection limit of the assay in both cell types (Figure 2-3C and Supplemental Data Figure 2-4D). Nevertheless, cells with the TPM proliferated at a similar rate as cells overexpressing TERT (Supplemental Data Figure S5A-C), demonstrating that TERT expression levels were not limiting for proliferation when telomeres were long. To examine whether TERT was fully transcriptionally silenced, we overexpressed POT1ΔOB, an allele sensitizing cells to low telomerase levels [16]. The expression of the allele induced significant telomere elongation specifically in cells with TPMs (Supplemental Data Figure 2-5D-G). Therefore, telomerase was not fully transcriptionally silenced but TPMs initially lead to telomerase activity below the detection threshold. At the time when telomere length in TPM cells had stabilized, telomerase expression became detectable again and activity rose as high as 5-10% of that found in hESCs and established cancer cell lines (Figure 2-3C and Supplemental Data Figure 2-6). To exclude the possibility that this upregulation of telomerase was the result of an outgrowth of a small subpopulation of cells with preexisting high telomerase activity, we performed subcloning experiments. Individual cell clones recapitulated the behavior of the bulk population (Supplemental Data Figure 2-7). Like the bulk cell population, individual clones also first had low telomerase levels, which became elevated with increasing PDs. This confirmed that TERT upregulation was the consequence of an additional event occurring when telomeres became critically short. At the time point of the acquisition of a TPM telomeres did not immediately stop shortening. The time lag until telomerase activity increased sufficiently to maintain all telomeres could provide a rationale for the cancer-protective function of constitutionally short telomeres and explain how the cellular context influences the immortalization process. We hypothesize that: (i) telomere length at the time when a cell acquires a TPM determines the number of cell divisions a cell can undergo before telomeres become critically short and (ii) once telomeres have become critically short the ability to upregulate telomerase determines whether a cell with a TPM becomes immortalized or ceases to proliferate. To test these hypotheses, we generated hESCs with shorter telomeres by modulating TERT expression. We attenuated the effect of TPMs by mutating the three endogenous ETS-

factor binding sites in the TERT promoter (E3), which facilitate binding of the GABPα - as a heterodimer with GABPβ−w [101,102] (Figure 2-4A), and which we show to be essential in hESCs (Supplemental Data Figure 2-8A,B). hESCs with a TPM and the E3 mutation (E3-124 and E3-146) had lower TERT expression and stably maintained shorter telomeres in comparison to hESCs with only a TPM (-124 and -146) (Figure 2-4B,C and Supplemental Data Figure 2-8C-F). From this allelic series we generated SV40 Tag-transduced fibroblasts and monitored proliferation, telomere length, and frequency of telomere fusions (Figure 2-4B, and 2-4D-E). Fibroblasts without the TPM, but with the three ETS mutations (wt-E3), had the shortest telomeres and died shortly after differentiation. In accordance with our first hypothesis, -124-E3 and -146-E3 cells with constitutionally shorter telomeres showed a high frequency of fusion events, much earlier than -124/-146 cells (Figure 2-4D and Supplemental Data Figure 2-8G). Both -124-E3 and -146-E3 cells initially proliferated despite their short telomeres (Figure 2-4E), arguing that they retained low levels of telomerase activity. Although they harbored TPMs, both -124-E3 and -146-E3 cells upregulated telomerase to only low levels; these cells entered crisis and did not become immortalized, confirming our second hypothesis.

In summary, we propose that TPMs drive cell immortalization in two phases (Figure 2-4F). TPMs that arise in early phases of tumorigenesis result in telomerase activity that is insufficient to prevent bulk telomere shortening, preferentially acting on critically short telomeres and thereby delaying replicative senescence (Phase 1). During subsequent divisions, the number of critically short telomeres increases, and telomerase activity becomes rate-limiting, causing telomere-driven genomic instability and selective pressure for telomerase upregulation by yet to be characterized factors (Phase 2). In contrast to crisis, where genomic instability arises as an acute and pronounced phenomenon, the genomic instability in cells with TPMs is reduced and persists over a longer period. Thus, TPMs play a dual role in tumorigenesis by enabling not only cancer cell immortalization via upregulation of TERT but also by promoting genome instability.

The finding that TPMs can become selected at the transition from pre-neoplastic to cancerous lesions indicates that telomere shortening acts as a critical barrier early during the neoplastic transformation of some cancers [91]. Together with our findings that TPMs are necessary but not sufficient to maintain telomere length this might explain why individuals with constitutionally short telomeres have a decreased rate of melanoma incidence [64,67,68]. Variation in constitutional telomere length likely limits the numeric expansion of early neoplastic cells at a precancerous stage. By characterizing the TPM-driven immortalization process over extended periods of time, we were able to reconcile the seemingly contradictory observations that short telomeres can initially protect against cancer formation [66,63], yet have a cancer promoting effect and can be associated with a poor prognosis [93,97] by later fueling genomic instability [94,95,99].

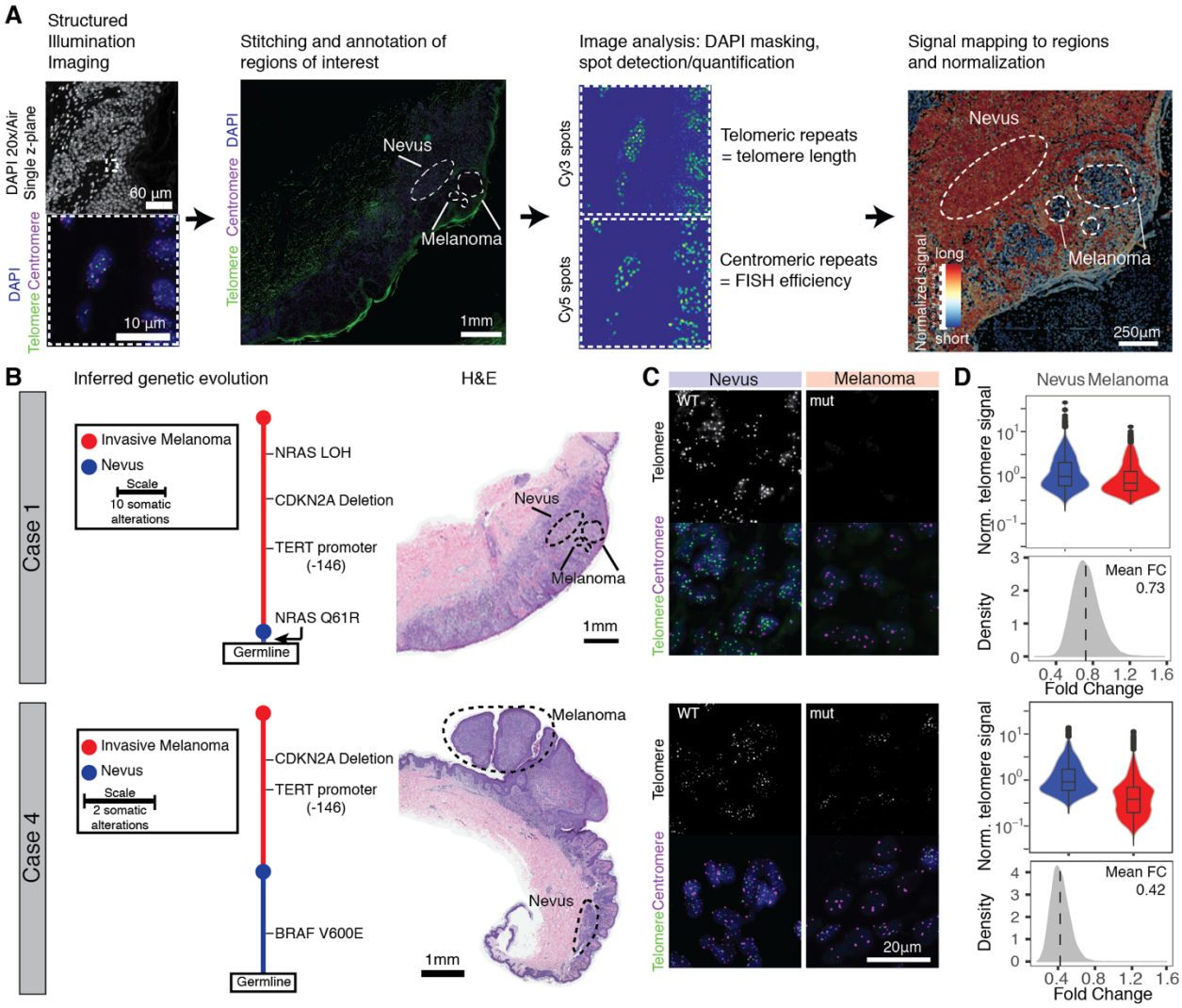


Figure 2-1: Telomeres shorten during progression from nevus to melanoma despite acquisition of a TPM *(A) Schematic overview of workflow. Melanoma progression samples from four patients were imaged using structured illumination microscopy. Acquired images were stitched and regions of interest were annotated. Telomeric and centromeric repeat FISH signals were detected and mapped back on pre-defined regions of interest. The relative telomere length was calculated by normalization to the closest centromeric signals. (B) The genetic evolution of each progression case, rooted at the germline shows how each case evolves from a wild-type nevus to a melanoma with TPM (nevus in blue, melanoma in red). Adjacent is the H&E staining of the analyzed sections of each case (Scale bar 1mm). (C) Magnification of the FISH image resolving individual telomere and centromere spots in nevus/melanoma area (DAPI = blue, telomere = green, centromere = magenta). TPM status is noted as wild-type (WT) or mutant (mut) (Scale bar 20 µm). (D) Violin plots of normalized telomere signal (telomere/centromere) with an inset boxplot indicating the median and quartiles of the signal. Histograms show the fold change of telomere spot intensity after random sampling (fold change melanoma/nevus).*

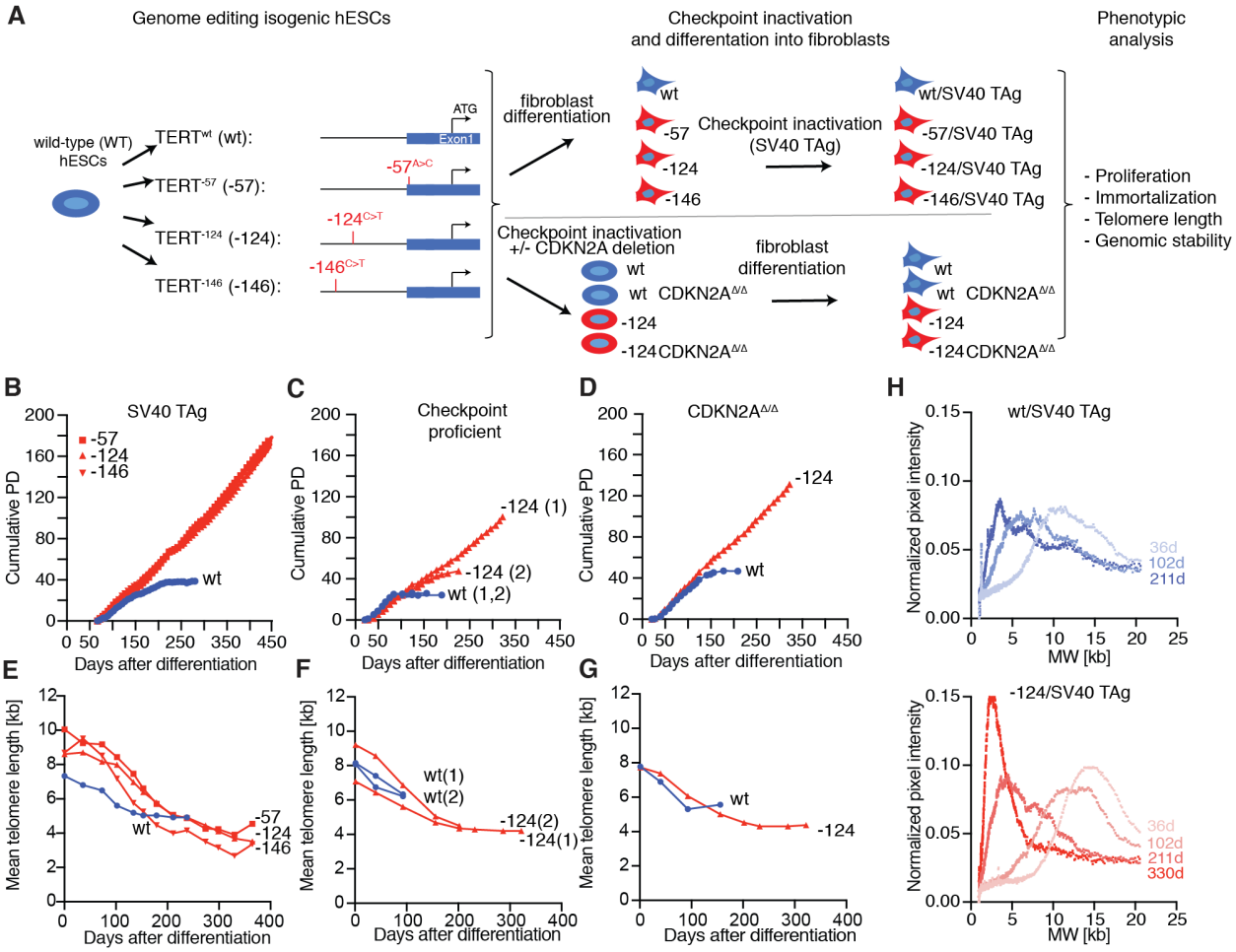


Figure 2-2: TPMs support cellular immortalization in vitro but do not prevent telomere shortening *(A) Experimental overview: Isogenic hESCs with the TPMs were differentiated into fibroblasts. To inactivate cell cycle and DNA damage checkpoints, either CDKN2A function was deleted in hESCs prior differentiation or fibroblasts were infected with SV40 TAg. (B-D) Growth curves of cumulative PDs over days after differentiation. (B) SV40 TAg fibroblasts with (red, -57, -124, -146) or without (blue, wt) TPMs (C) DNA damage checkpoint proficient cells with (red, -124) or without (blue, wt) TPM. (1), (2) indicate two independent experiments. (D) CDKN2AΔ/Δ cells with (red, -124) or without (blue, wt) TPM (E-G) Quantification of mean telomere length over time after differentiation. (H) Accumulation of shorter telomeres over time shown by visualization of telomere length distribution of images shown in Figure S3A. Quantification of the normalized pixel intensity over molecular weight per lane for the indicated time points after differentiation.*

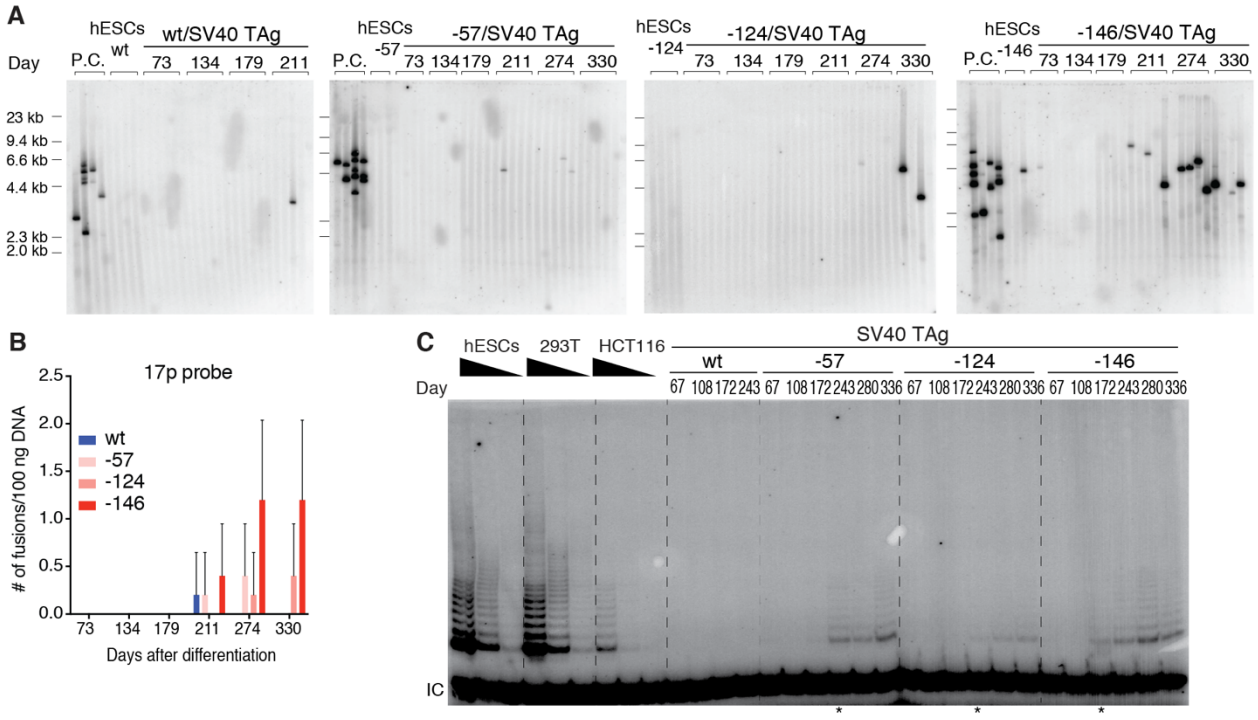


Figure 2-3: TPMs do not fully protect against genomic instability and mutant cells gradually increase telomerase expression *(A) Detection of interchromosomal telomere fusions over time in SV40 TAg fibroblasts by PCR of specific subtelomeric regions. Fusions were detected by probes against the 17p subtelomeric regions [98]. DNA from cells in crisis served as a positive control (P.C.: TERT, p53 and p16 triple knockout fibroblasts cultured into crisis). (B) Quantification of fusion events shown in Figure 3A. (C) Telomerase activity assay of the indicated cell lines over time. IC: internal control. * indicates time points when telomerase activity became detectable.*

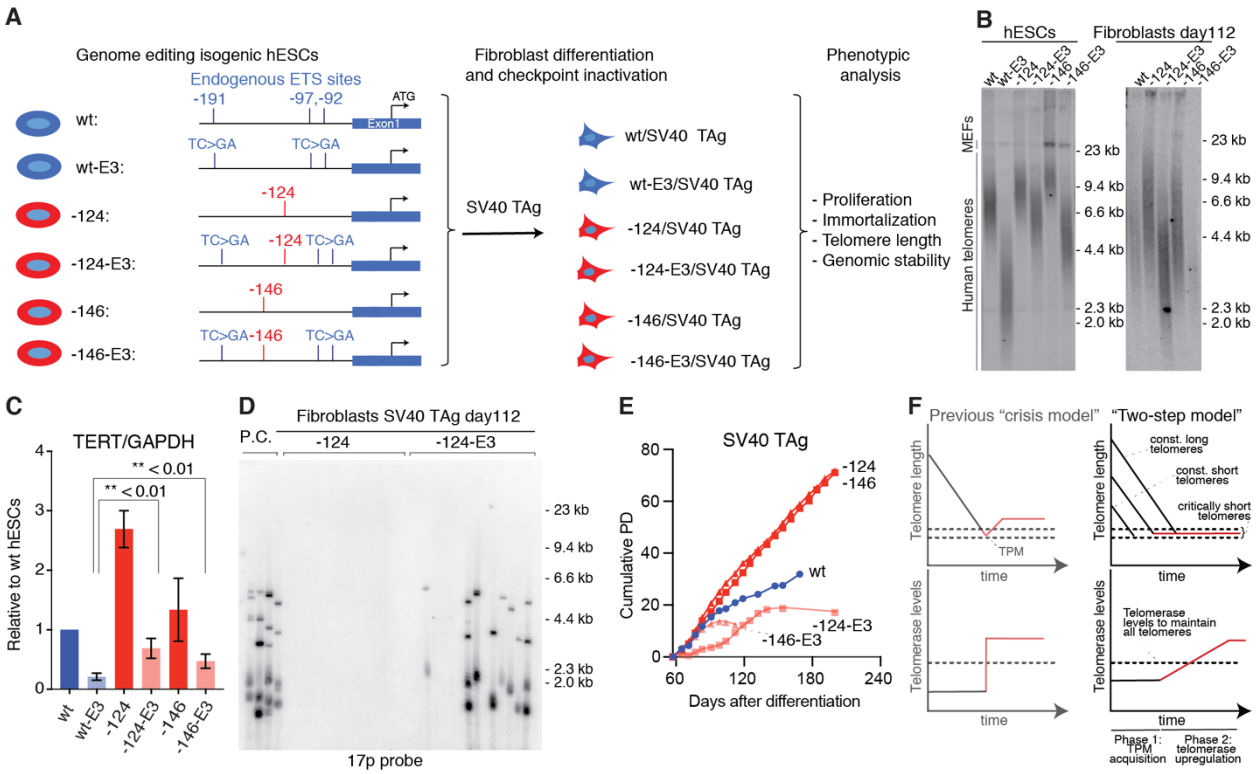
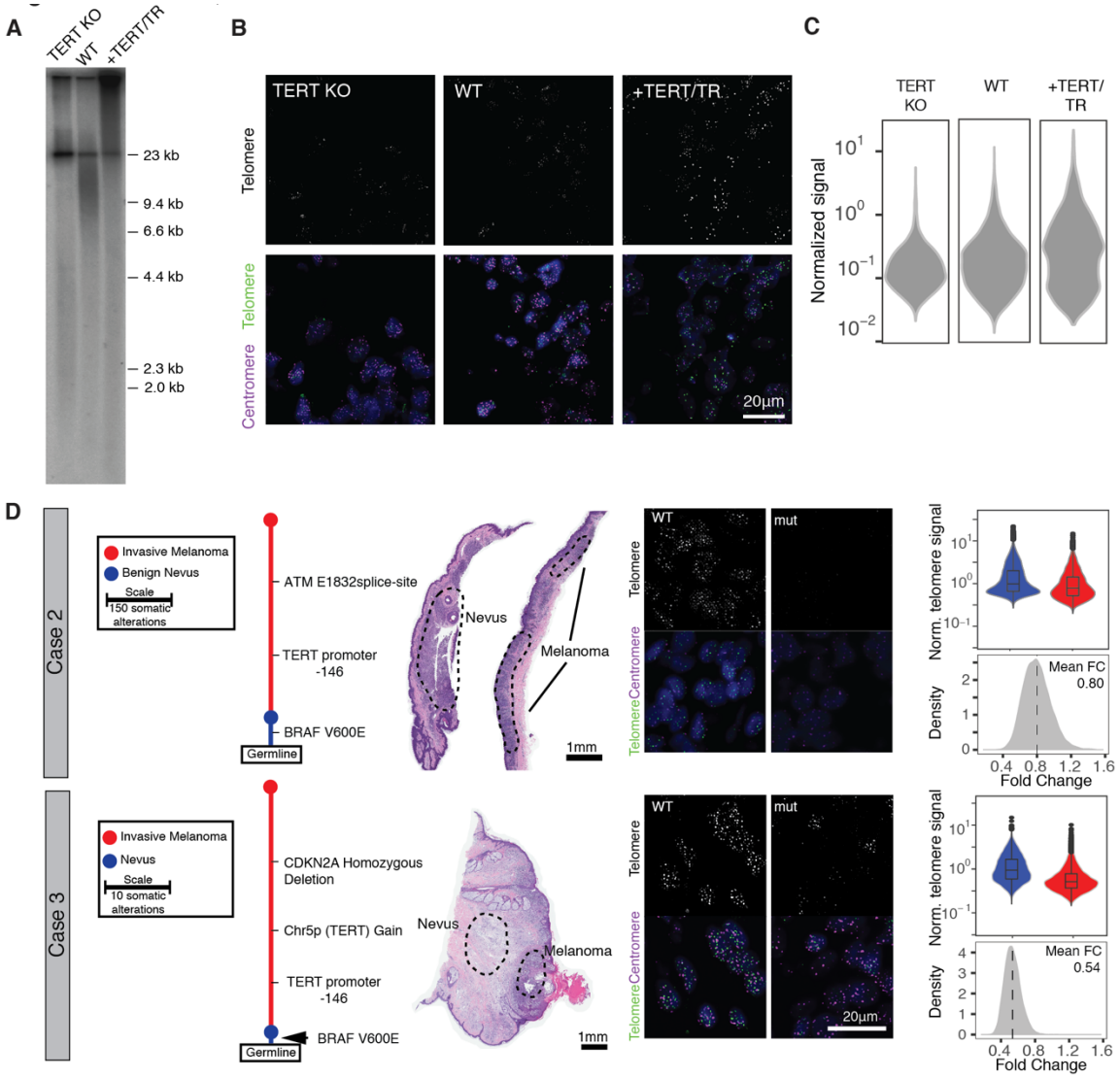


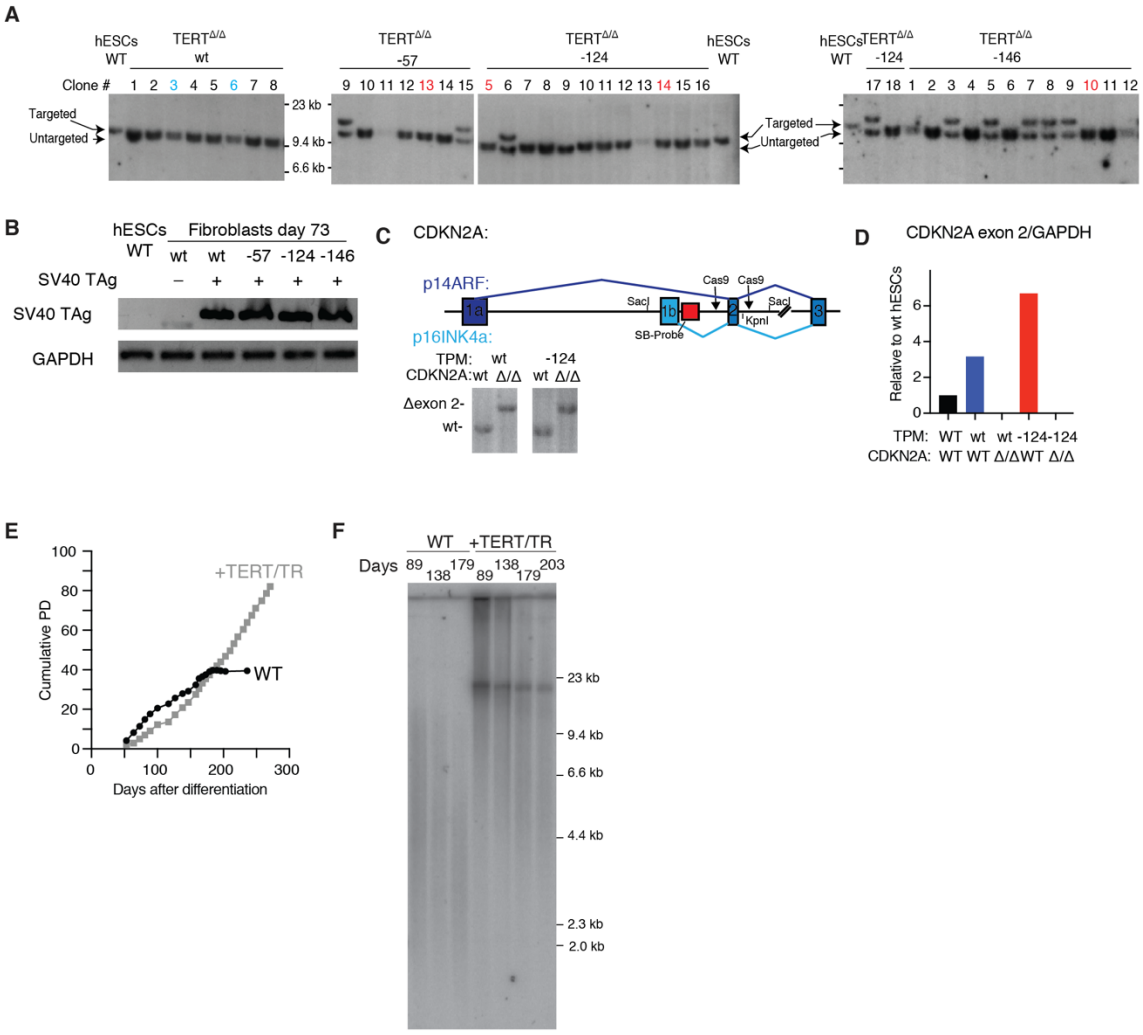
Figure 2-4: Short telomeres and low telomerase levels protect cells from immortalization by TPMs *(A) Schematic overview of allelic series of cells carrying TPMs (red) and/or endogenous ETS site mutations (E3: mutated TC>GA, blue) in the TERT promoter. E3 refers to the simultaneous mutations of all three endogenous ETS sites (-191, -97 and -92 from the translational start site: ATG). (B) Telomere length analysis for hESCs and fibroblasts with TPMs and ETS mutation combinations. (C) TERT expression normalized to GAPDH relative to wt hESC. Error bars: SEM, two-sided student t-test, n = 3. (D) Telomere fusions detected in -124 and -124 E3 fibroblasts with 17p. (E) Growth curve of fibroblasts with or without TPMs and/or ETS mutations. (F) Telomere length (top) and TERT expression (bottom) in a revised model for immortalization by TPMs. In the classic crisis model, TERT expression is acquired during crisis as a single event (left panel). In the biphasic model (right panel), TPMs can be acquired in a telomere length independent manner at any time (Phase 1). In phase 2 cells are required to gradually upregulate telomerase. Due to unprotected telomeres cells can acquire genomic instability.*

Supplemental Figures



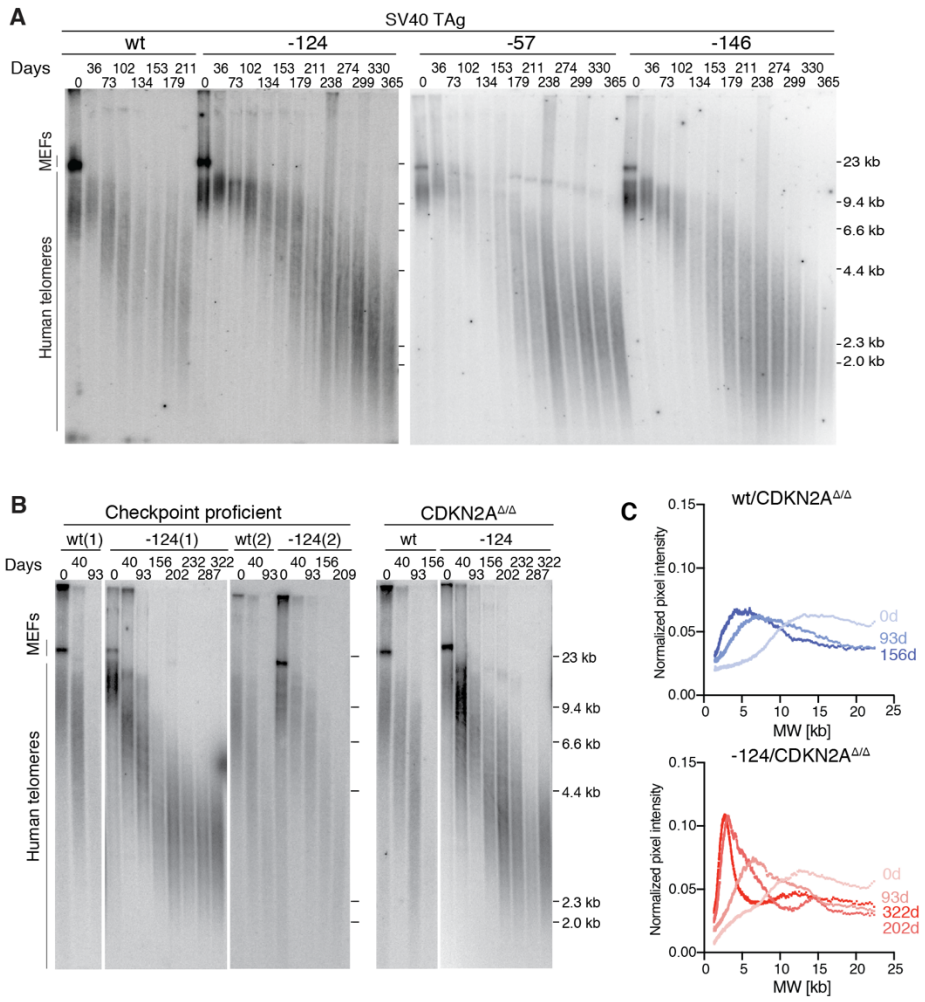
Supplemental Data Figure 2-1: *Structured illumination microscopy allows for quantitative comparison of telomere length (A) Telomere restriction fragment analysis of telomere length analysis of hESCs of different telomere length. (B) Magnification of structured illumination FISH images of the same hESCs fixed and embedded in paraffin (DAPI = blue, telomere FISH = green, centromere FISH = magenta). (C) Quantitative analysis of telomeric and centromic signal accurately depicts telomere length differences in the analyzed hESCs. (D) Panels as described in Figure 1: The genetic evolution of each progression case, rooted at the germline, shows how each case evolves from a wild-type nevus to a melanoma with TPM (nevus in blue, melanoma in red). Adjacent is the H&E staining of the analyzed sections of each case (Scale bar 1mm). Magnification of the FISH image resolving individual telomere and centromere spots in nevus/melanoma area (DAPI = blue, telomere = green, centromere = magenta). TPM status is*

noted as wild-type (WT) or mutant (mut) (Scale bar 20 μm). Violin plots of normalized telomere signal (telomere/centromere) with an inset boxplot indicating the median and quartiles of the signal. Histograms show the fold change of telomere spot intensity after random sampling (fold change melanoma/nevus).

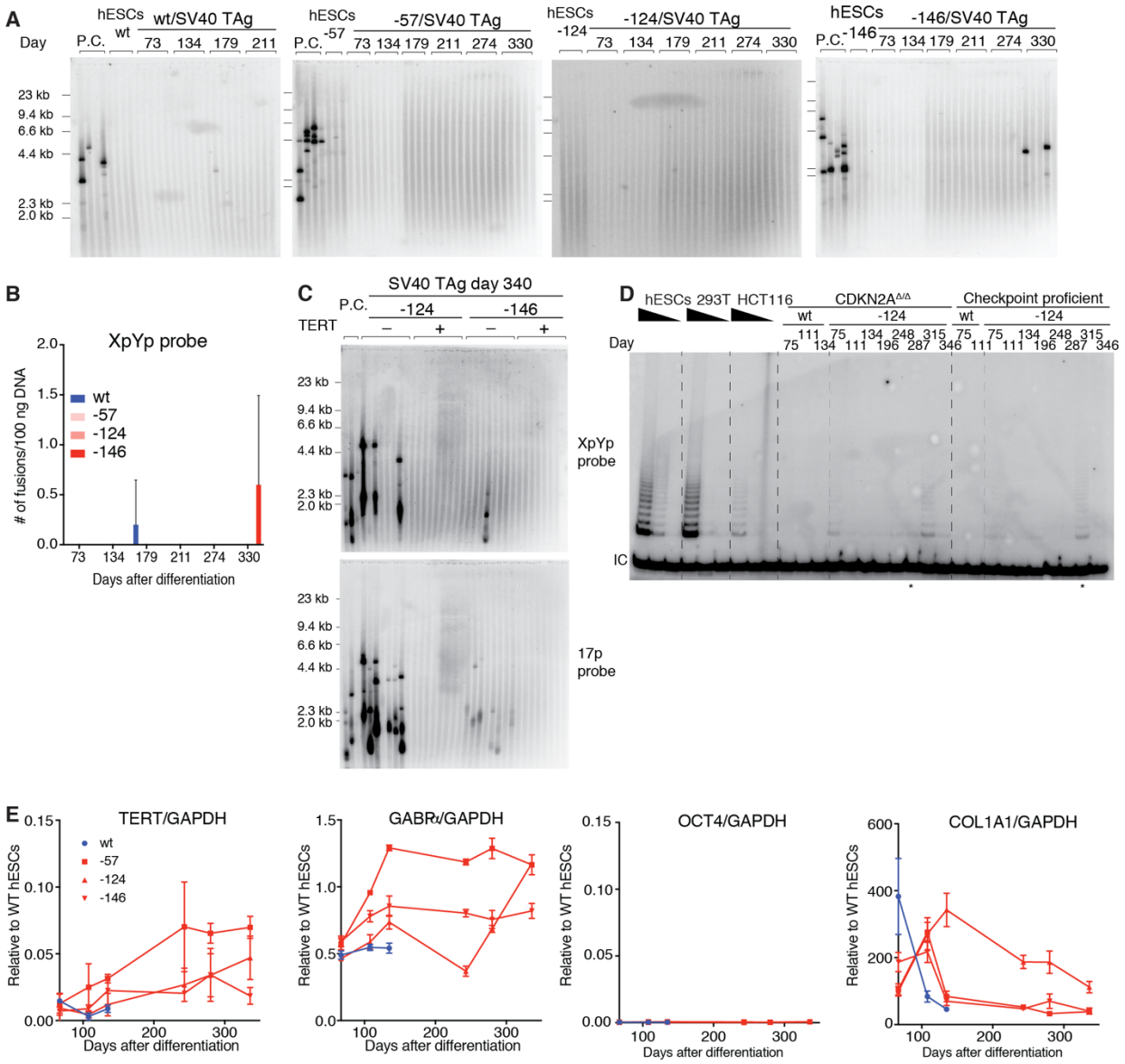


Supplemental Data Figure 2-2: *Genotyping and characterization of cells used in this study (A) Genotyping of single cell derived isogenic hESC clones with and without TPMs by Southern blotting as previously described in (35). The correctly targeted allele is 11 kb and untargeted is 9.6 kb. The highlighted correctly targeted clones were used for further analysis (wt-6 and -124-14 for checkpoint proficient cells and for the deletion of CDKN2A Δ/Δ; wt-3, -57-13, -124-5 and -146-10 for the SV40 TAg experiments) (B) Expression of SV40 TAg and GAPDH after transduction. (C) Targeting schematic for the generation of CDKN2AΔ/Δ hESCs. Deletion of exon2 of p16 and p14 in the CDKN2A locus was obtained by the simultaneous expression of two Cas9/sgRNAs. For Southern blot analysis, genomic DNA was digested with SacI and KpnI. (D) Confirmation of CDKN2A exon 2 deletion by measuring relative mRNA expression of exon 2. (E) To confirm that arrest of the wild-type cells was due to progressive telomere shortening, TERT and TR, the RNA component of telomerase, were constitutively overexpressed from the AAVS1 locus in hESCs. In fibroblasts, overexpression of telomerase was sufficient to rescue the arrest phenotype and support indefinite proliferation. Growth curves show cumulative PDs over days after differentiation*

(Wild-type: grey, Overexpression of TERT/TR: black). (F) Telomere length analysis of WT cells and TERT/TR overexpressing cells.

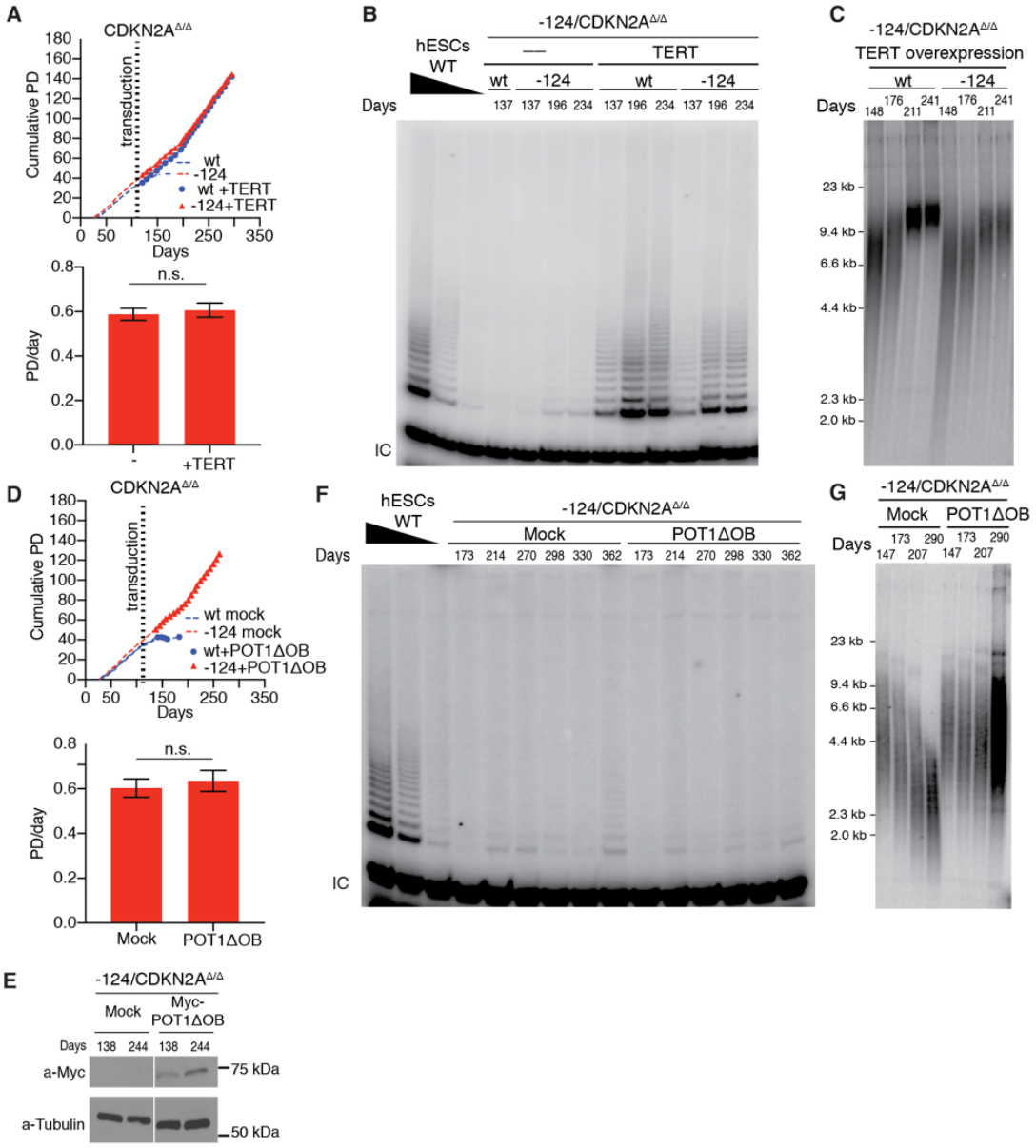


Supplemental Data Figure 2-3: *Telomeres shorten in the presence of TPMs in both checkpoint proficient and deficient cells (A) Analysis of telomere length in SV40Tag fibroblasts. Day 0 refers to hESCs at the day of differentiation initiation. hESCs are cultured on mouse embryonic fibroblasts (MEFs), the telomeric signal of these MEFs is indicated. Quantification of mean telomere length is shown in Figure 2E. (B) Analysis of telomere length over time of the cells and experiment shown in Figure 2C and 2D. From the left: Checkpoint proficient cells with or without -124 TPM (two independent -124 TPM clones are shown), CDKN2AΔ/Δ cells with or without -124 TPM. The days post-differentiation are shown above each lane. (C) Accumulation of shorter telomeres over time shown by visualization of telomere length distribution of images shown in panel (B). Quantification of the normalized pixel intensity over molecular weight per lane for the indicated time points after differentiation.*



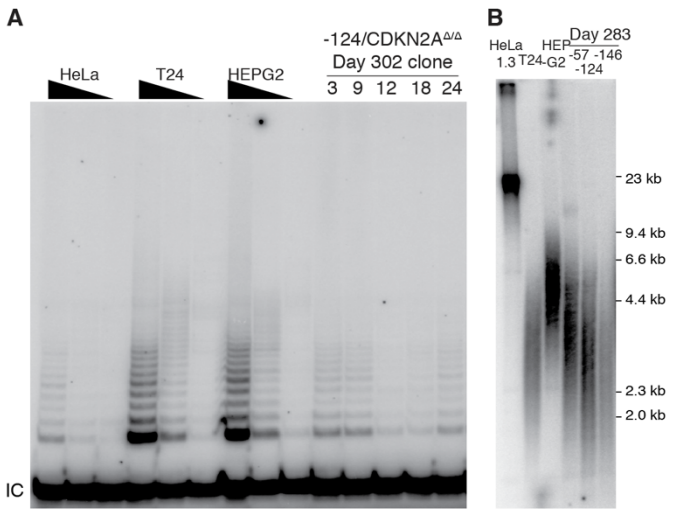
Supplemental Data Figure 2-4: *Gradual telomerase increase is checkpoint independent and via upregulation of TERT mRNA expression (A) Detection of interchromosomal telomere fusions over time in SV40 TAg fibroblasts by PCR of specific subtelomeric regions. Fusions were detected by probes against the XpYp subtelomeric regions (23). DNA from cells in crisis served as a positive control (P.C.: TERT, p53 and p16 triple knockout fibroblasts cultured into crisis). (B) Quantification of fusion events shown. (C) TERT overexpression suppressed telomeric fusions in TPM cells, demonstrating that fusions are driven by telomere attrition. Telomere fusion PCR was performed in TPM cells with or without overexpression of TERT at day 340. -124 and -146 TPM cells were retrovirally transduced at day 289 with TERT. (D) Telomerase activity assay of the cells shown in Figure 2C-D over time. IC: internal control for the assay, * indicates time points when telomerase activity becomes detectable. (E) Relative expression levels of TERT, GABPα, OCT4 and COL1A1*

mRNA in SV40 Tag cells over time. Expression is relative to WT hESCs and normalized to GAPDH. Error bars show the standard error of the mean (SEM), n = 3.

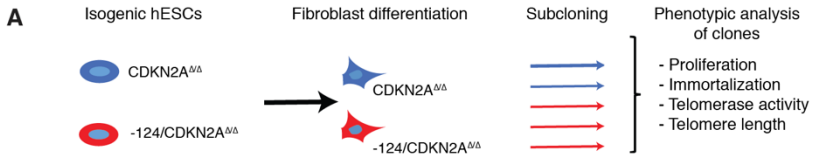


Supplemental Data Figure 2-5: TERT expression is not limiting for proliferation of TPM cells with sub-threshold telomerase activity (A) Growth curve and proliferation rate of uninfected and TERT overexpressing cells shown as cumulative PDs over days after differentiation. Cells were infected on day 108 after differentiation (dashed line). PD/day were calculated after each passage between day 129 and 296. Error bars show SEM two-sided student t-test, p = 0.66, n = 24. No significant difference in growth rate was observed indicating that telomerase levels were not limiting for proliferation in TPM cells while telomeres were long. (B) Telomerase activity of TERT overexpressing cells. Uninfected cells were compared with TERT overexpressing cells at 137, 196, and 234 days after differentiation. (C) Telomere length analysis showed telomere elongation by TERT overexpression in wt and -124 TPM cells. (D-G) Telomerase positive cells are highly

sensitive to the expression of POT1ΔOB (26), an allele of the shelterin protein POT1 (41), that leads to telomere elongation, but not in telomerase-negative cells. Exploiting this feature, we investigated whether telomere shortening in early phase was due to complete absence of TERT expression or TERT was expressed at low levels that were insufficient to maintain telomere length. (D) Cumulative PDs of cells retrovirally infected with POT1ΔOB or mock infected cells. No difference in proliferation rate of PD/day was observed after each passage between day 145 and 262. Error bars: SEM, two-sided student t-test, $p = 0.61$, $n = 19$. Cells were infected on day 103 after differentiation. (E) Western blot analysis of retrovirally transduced cells with Myc-POT1ΔOB. (F) Telomerase activity of POT1ΔOB and mock-infected cells at indicated time points after differentiation. (G) Telomere length analysis of POT1ΔOB and mock-infected cells showed expression of POT1ΔOB induced significant telomere elongation in cells with TPMs, indicating telomerase activity that was below the detection limit of our method.

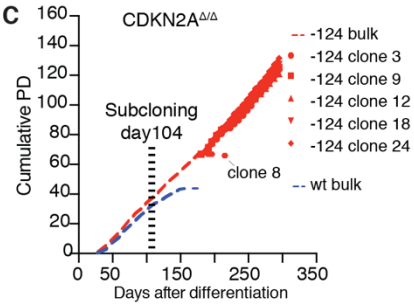


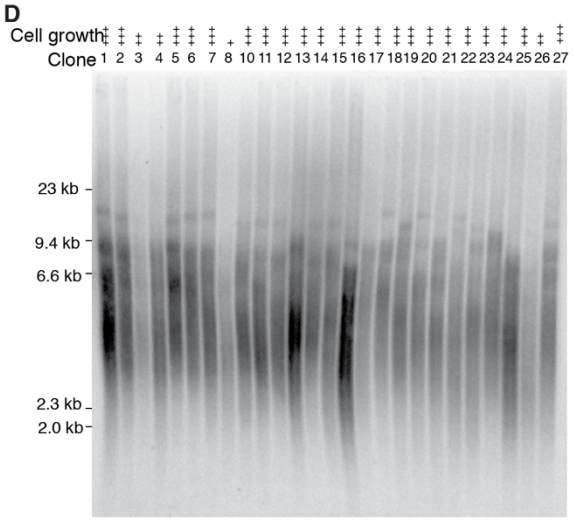
Supplemental Data Figure 2-6: *Telomerase activity and telomere length are not correlated in established cancer cell lines (A) Comparison of telomerase activity between cancer cell lines and clones of -124 CDKN2AΔ/Δ at day 302. For cancer cell lines, 200, 40, 8 ng of lysate were used for the assay. For -124 CDKN2AΔ/Δ, 200 ng of lysate was used. (B) Comparison of telomere length between the indicated cancer cell lines and SV40 Tag transduced fibroblasts with a TPM at day 283.*

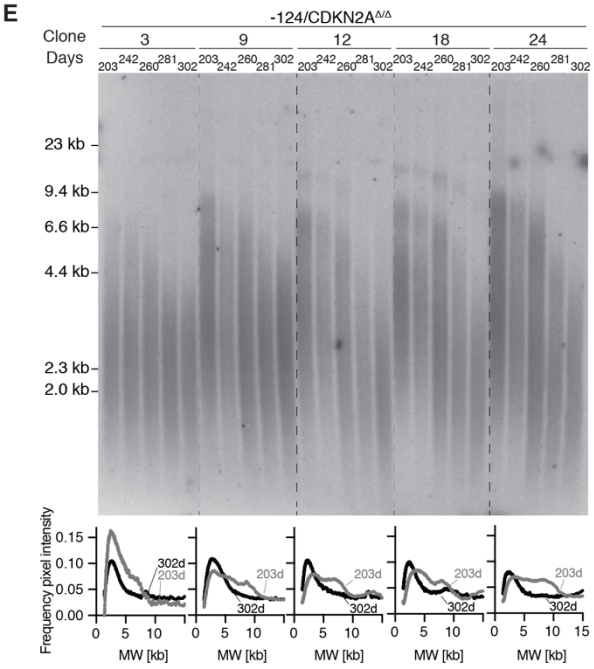


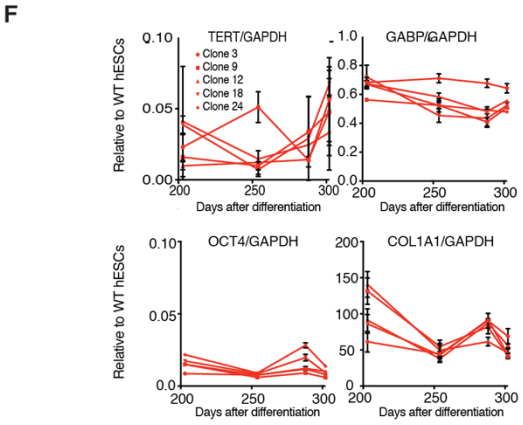
B

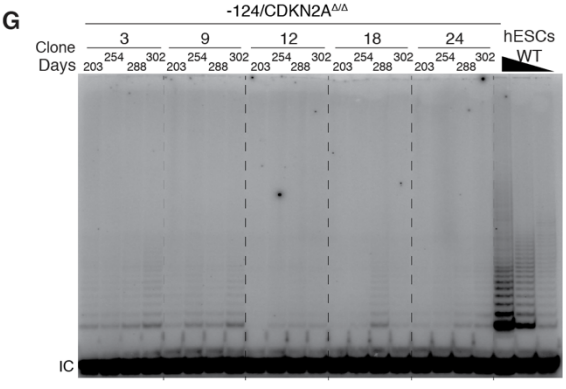
Density	Visible outgrowth wt/CDKN2A$^{\Delta/\Delta}$	Visible outgrowth -124/CDKN2A$^{\Delta/\Delta}$
0.5 cells per well	11 of 96	27 of 96
1 cell per well	10 of 96	38 of 96
2 cell per well	17 of 96	62 of 96
4 cell per well	47 of 96	90 of 96



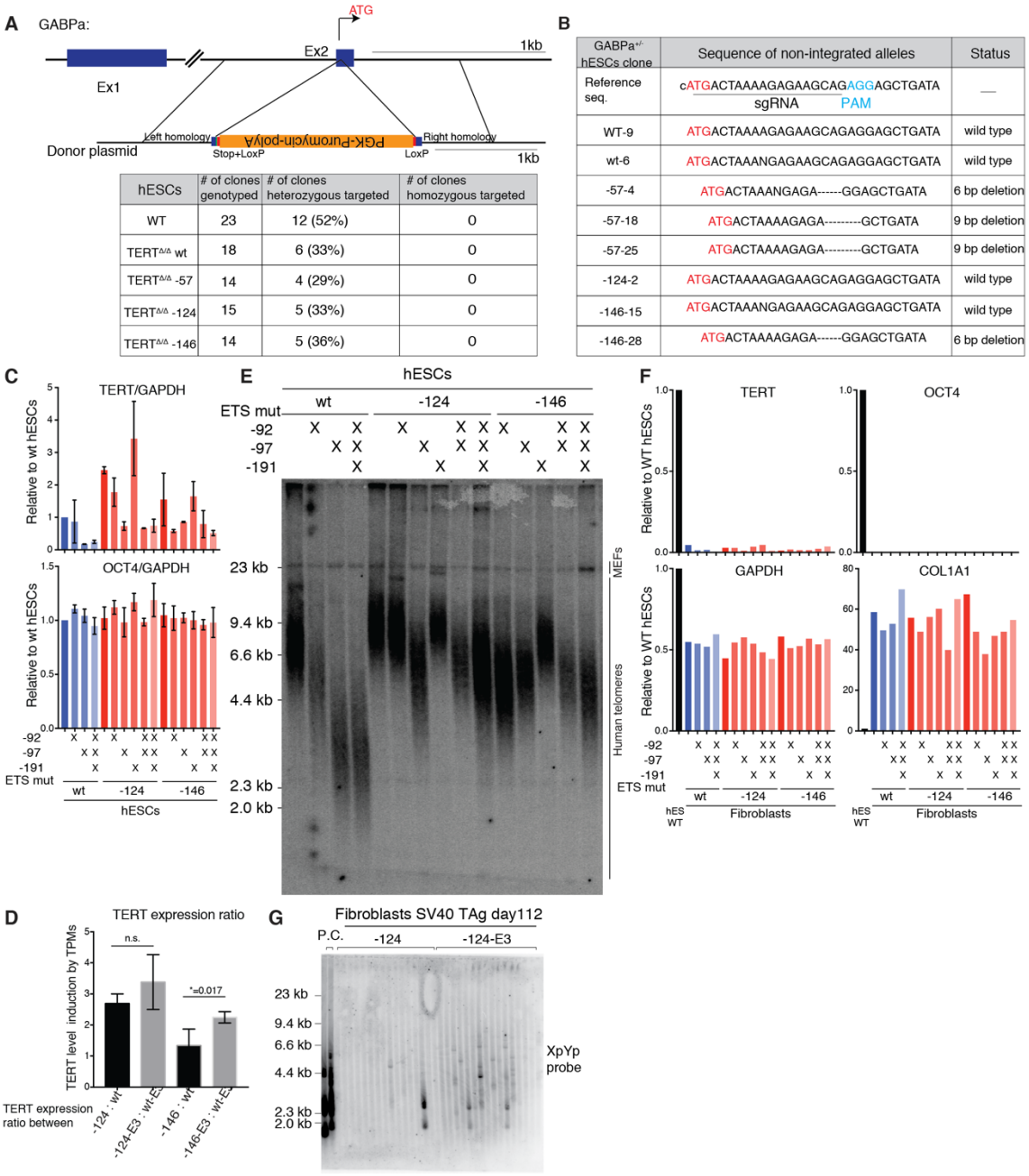








Supplemental Data Figure 2-7: *A large fraction of cells with a TPM are poised to immortalize and exhibit the same telomere length dynamics as the bulk population, yet a small fraction of individual cell clones failed. (A) Experimental overview: To assess the potential of individual cells within a population to stabilize their telomeres and immortalize, we isolated subclones of -124 TPM (CDKN2AΔ/Δ) and wild-type (CDKN2AΔ/Δ) cells at day 104 after differentiation, before the upregulation of telomerase. (B) Table of frequency of successful subcloning by limiting dilution. We isolated 11 clones from wild-type and 27 clones from cells carrying the -124 TPM. Both sets of clones grew in parallel for 45 days before all wild-type clones ceased to proliferate. (C) Telomere length analysis of all TPM clones at day 149. Evaluation of cell growth is indicated above each clone ranging from poor growth (+) to excellent growth (+++). Six cell lines were chosen for long-term analysis. (D) Growth curve showing cumulative PDs over time of the six of the subcloned lines. Five out of six clones proliferated more than 70 PDs beyond the proliferative capacity of wild-type cells. However, one of the six clones (#8), stopped proliferating with morphology and culture characteristics of cells in crisis. (E) Telomere length analysis of the clones analyzed for proliferation. Plotted below the autoradiogram are the telomere length distributions (frequency of pixel intensity over molecular weight) of the earliest and latest time point (Day 203, grey line and 302, black line). (F) Relative expression levels of TERT, GABPα, OCT4, COL1A1 mRNA in each clone between days 203 and 302. Expression was normalized by GAPDH. Error bars show SEM, n = 3. (G) Telomerase activity assay of the TPM -124 clones at indicated time points after differentiation.*



hESCs	# of clones genotyped	# of clones heterozygous targeted	# of clones homozygous targeted
WT	23	12 (52%)	0
TERT$^{\Delta/\Delta}$ wt	18	6 (33%)	0
TERT$^{\Delta/\Delta}$ -57	14	4 (29%)	0
TERT$^{\Delta/\Delta}$ -124	15	5 (33%)	0
TERT$^{\Delta/\Delta}$ -146	14	5 (36%)	0

GABPa$^{+/-}$ hESCs clone	Sequence of non-integrated alleles	Status
Reference seq.	cATGACTAAAAGAGAAGCAGAGGAGCTGATA (sgRNA / PAM)	—
WT-9	ATGACTAAAAGAGAAGCAGAGGAGCTGATA	wild type
wt-6	ATGACTAAANGAGAAGCAGAGGAGCTGATA	wild type
-57-4	ATGACTAAANGAGA------GGAGCTGATA	6 bp deletion
-57-18	ATGACTAAAAGAGA--------GCTGATA	9 bp deletion
-57-25	ATGACTAAAAGAGA--------GCTGATA	9 bp deletion
-124-2	ATGACTAAAAGAGAAGCAGAGGAGCTGATA	wild type
-146-15	ATGACTAAANGAGAAGCAGAGGAGCTGATA	wild type
-146-28	ATGACTAAAAGAGA------GGAGCTGATA	6 bp deletion

Supplemental Data Figure 2-8: *Modulation of TERT expression by attempted GABPα knockout and mutation of endogenous ETS sites in the TERT promoter (A) Schematic overview of GABPα knockout strategy and frequency of successful targeting determined by Southern blot genotyping. (B) PCR genotyping of non-integrated alleles of GABPα+/- clones. Note: All alterations of the non-targeted allele are in-frame deletions. These in-frame deletions are expected to retain GABPα function, suggesting an essential role for GABPα in hESCs. Using an alternative approach, we mutated the three endogenous ETS-factor binding sites in the TERT promoter (E3), which have been proposed as binding sites of the GABPα/β heterodimer. (C) Relative expression levels of*

TERT and OCT4 for the indicated combinations for mutations in the endogenous ETS sites with or without TPMs. Expression levels are relative to hESCs and normalized to GAPDH. Mutations in the ETS sites decrease TERT expression in wt hESCs, indicting a contribution of these ETS sites to TERT transcription even in the absence of the TPMs. Moreover, the endogenous ETS sites did not act cooperatively but rather additively with the TPMs, as TPMs were able to increase TERT transcription in the presence of the triple ETS mutation.(D) Fold change of TERT expression for the indicated comparisons (Error bars: SEM, two-sided student t-test, n = 3). TPMs can equally upregulate TERT expression in the absence of the endogenous ETS sites. (E) Telomere length analysis of hESCs carrying individual and combinatorial mutations in the endogenous ETS sites with or without TPMs. (F) Relative expression levels of TERT, OCT4, GAPDH and COL1A1 in fibroblasts differentiated from hESCs. Samples were collected at day 21 after differentiation. (G) Telomere fusions detected in -124 and -124 E3 fibroblasts with probe XpYp in subtelomeric regions at day 112.

Material and Methods

hESC culture and genome editing

Genome editing experiments were performed in WIBR#3 hESCs [103], NIH stem cell registry # 0079. Cell culture was carried out as previously described [104]. hESCs engineered to carry a TPM were subcloned and genotyped as previously reported . Exon2 of *CDKN2A* was deleted using accattctgttctctctggc and cgcggaaggtccctcaggtg as sgRNA target sites. Targeting was confirmed by Southern blotting with using probe amplified from genomic DNA with primers: Fw: (ggggaaatgatgttggcttagaatcct) and Re: (caatgaagtccttcgtcttggtca). TERT and TR were overexpressed by engineering hESCs to express both from the AAVS1 [26].

Southern blot analysis was performed as previously described [105–107]. Combinatorial mutations in the *TERT* promoter were introduced using a two-step scarless editing approach [26]. All comparisons were made between the wild-type *TERT* promoter element (wt) or the respective TPMs (-57A/C, -124 C/T, -146C/T) as described previously [26]. Cells were cultured for more than 90 days after the targeting and no obvious growth defect was observed in the hESCs.

Differentiation to fibroblast-like cells

Fibroblast-like cells were derived from embryoid bodies (EBs). To form EBs, hESC colonies were grown on petri dishes in fibroblast medium (DMEM [Lifetech]) supplemented with 15% fetal bovine serum [Lifetech], 1 mM glutamine [Lifetech], 1% non-essential amino acids [Lifetech], and penicillin/streptomycin [Lifetech]). After 9 days, EBs were transferred to tissue culture dishes to attach for 6 days. Fibroblast-like cells were passaged with Trypsin EDTA ([Lifetech], 0.25%), triturated into a single-cell suspension and plated on tissue culture dishes.

Growth curve for fibroblasts

Cells were trypsinized, counted and plated at a density of 250,000 cells per 10 cm dish. Medium was changed every 3-4 days and cells were passaged every 5-8 days. Growth curves are presented by plotting cumulative PD against days after differentiation. Most data analysis shown is in reference to the time after differentiation. PDs of experiments initiated at a given time point are extrapolated by adding the PD of the parental cell line at the time point of the manipulation.

Generation of cDNA overexpression cell lines and viral infections

For TERT cDNA overexpression, the expressing vector along with lentiviral packaging vectors Delta-VPR and CMV-VSV-G were transfected into HEK293FT cells using calcium phosphate. For POT1 ΔOB cDNA overexpression, the retroviral plasmid was transfected into Phoenix A cells. Media was changed 12 hr after transfection. The virus-containing supernatant was collected 48 and 72 hr post transfection and passed

through a 0.45 μm filter to eliminate cells. Target cells were plated in 10 cm plates in media containing 2 μg/ml polybrene. After infection, virus was removed, and cells were selected with puromycin or hygromycin. Cells were validated for protein expression via immunoblotting or telomerase activity assay. To transduce cells with SV40 TAg, fibroblasts were infected with pBABE-SV40 large T-Neo at 55 days (for TPMs cells) or 25 days (for TPMs/E3 cells) after differentiation and selected with neomycin.

qRT-PCR

RNA was extracted with TRIzol [Lifetech] and treated with DNaseI [NEB]. 600 ng RNA were converted to cDNA with the iScript Reverse Transcriptase [BioRad] and random and poly(A) priming. qRT-PCR was performed with KAPA SYBR fast [KAPA Biosystems] in 384-well format with a total reaction volume of 10 μl. 2 μl cDNA from the iScript reaction mixture was used for the detection of TERT mRNA. For measuring the expression levels of all other genes, cDNA was diluted 1:10 and 2 μl were used for qPCR. Relative expression levels were calculated based on Δ/ΔCt and/or ΔCt analysis. qRT-PCR primers used in this study were:

TERT fw (TGTCAAGGTGGATGTGACGG),
TERT rev (GAGGAGCTCTGCTCGATGAC),
GAPDH fw (CAGTCTTCTGGGTGGCAGTGA),
GAPDH rev (CGTGGAAGGACTCATGACCA),
OCT4 fw (CGTTGTGCATAGTCGCTGCT),
OCT4 rev (GCTCGAGAAGGATGTGGTCC),
COL1A1 fw (GTCACCCACCGACCAAGAAACC),
COL1A1 rev (AAGTCCAGGCTGTCCAGGGATG),
GABPα fw (CATCAATGAACCAATAGGCAAT),
GABPα rev (GGTCAAATAAACTTCGTTCTGGA),
SV40 TAg fw (GGTGGGTTAAAGGAGCATGA),
SV40 TAg rev (TAGTGGCTGGGCTGTTCTTT)
CDKN2A ex2 fw (CAACGCACCGAATAGTTACGG),
CDKN2A ex2 rev (ACCAGCGTGTCCAGGAAG)

Telomeric repeat amplification protocol

PCR-based telomeric repeat amplification protocol (TRAP) was performed as previously described using TS (AATCCGTCGAGCAGAGTT) and ACX (GCGCGGCTTACCCTTACCCTTACCCTAACC) for amplification of telomeric repeats and TSNT (AATCCGTCGAGCAGAGTTAAAAGGCCGAGAAGCGAT) and NT (ATCGCTTCTCGGCCTTTT) as an internal control [33]. Cell extract was generated using hypotonic lysis buffer (20 mM HEPES, 2 mM $MgCl_2$, 0.2 mM EGTA, 10% Glycerol, 1 mM DTT, 0.1 mM PMSF) supplemented with 0.5% CHAPS and samples were normalized using the Bradford assay (BioRad). 200 ng of total protein were used for detection of fibroblasts telomerase activity. For hESCs and cancer cell lines, a series of diluted lysate, 200, 40 and 8 ng was used. Throughout the figures, the same hESCs WT lysate was

used as a standard. The TRAP products were resolved on a 10% polyacrylamide /1xTAE gel. Dried gels were visualized by phosphor imaging.

Immunoblotting

Protein samples were extracted by hypotonic lysis, normalized for protein concentration and mixed with Laemmli buffer. After heating to 95 °C for 5 min they were resolved by SDS-PAGE. The protein was then transferred to nitrocellulose membrane and subsequently incubated with mouse α-tubulin (1:20000, DM1A [Calbiochem]) and mouse α-Myc (1:20000, [Santa Cruz]) in 4% nonfat milk [Carnation] in TBS-T buffer (150 mM NaCl, 50 mM Tris pH 7.5, 0.1% Tween 20) overnight at 4 °C. The membrane was washed in TBS-T and incubated with goat α-mouse HRP (1:5000, [BioRad]) in 4% nonfat milk in TBS-T for 1 hr at room temperature. After washing with TBS-T, the membrane was visualized using ECL.

Detection of telomere length

Genomic DNA was prepared as described previously (*36*). Genomic DNA was digested with MboI, AluI and RNaseA overnight at 37 °C. The resulting DNA was normalized and 2 µg of DNA was run on 0.75% agarose [Seakem ME Agarose, Lonza], dried under vacuum for 2 hr at 50 °C, denatured in 0.5 M NaOH, 1.5 M NaCl for 30 min, shaking at 25 °C, neutralized with 1 M Tris pH 6.0, 2.5 M NaCl shaking at 25 °C, 2x for 15 min. Then the gel was pre-hybridized in Church buffer (1% BSA, 1 mM EDTA, 0.5M $NaP0_4$ pH 7.2, 7% SDS) for 1 hr at 55 °C before adding a ^{32}P-end-labeled $(T_2AG_3)_3$ telomeric probe. The gel was washed 3x 30 min in 4x SSC at 50 °C and 1x 30 min in 4x SSC + 0.1% SDS at 25 °C before exposing on a phosphorimager screen. Mean telomere length was quantified as described previously (*37*) using the following equation: Mean telomere length = $\Sigma(OD_i \times L_i)/ \Sigma(OD_i)$. OD_i = optical density at position i, L_i= telomere length at position i. To exclude skewing by MEF telomeres, signals above 23 kb were not incorporated into the quantification. Normalized pixel intensity showing the accumulation of short telomeres was calculated by quantifying pixel intensity and normalizing to the area under the curve for each lane using ImageJ and Prism7.

Fusion PCR

Fusion PCR was performed as previously described [87,98] with the following modifications. Briefly, genomic DNA was extracted using phenol chloroform following overnight proteinase K digestion. Isolated DNA was solubilized by EcoRI and RNaseA digestion and phenol chloroform extracted followed by ethanol precipitation. Purified DNA was resolved in TE buffer and quantified. 100 ng of digested DNA were used per 25 µl Failsafe PCR reaction mix (Buffer H) with mixed primers of XpYpM (ACCAGGTTTTCCAGTGTGTT), 17p6 (GGCTGAACTATAGCCTCTGC) and 21q1 (CTTGGTGTCGAGAGAGGTAG). PCR was conducted at the following condition [95 °C for 2 min, (95 °C for 15 sec, 58 °C for 20 sec, 68 °C for 9 min) x35 cycles, 75 °C for 5 min]. PCR products were detected by southern blotting using probes amplified with the following primers: 17p probe: 17p7**(**CCTGGCATGGTATTGACATG) and 17p2

(GAGTCAATGATTCCATTCCTAGC), XpYp probe: XpYpE2 (TTGTCTCAGGGTCCTAGTG) and XpYpB2 (TCTGAAAGTGGACC(A/T)ATCAG).

Telomeric and centromeric fluorescence in situ hybridization in FFPE samples from patients with melanoma

Tissue sections were deparaffinized with histoclear and rehydrated through a graded alcohol series. They were placed in deionized water followed by permeabilization in water with 0.1% Tween-20 for 2 min. Slides were then placed in 10mM sodium citrate pH 6.5 at 85 °C for 15 min. After rinsing with water, they were treated with 0.4% pepsin for 10 min (pre-warmed to 37 °C). Following another water rinse, slides were dehydrated in a graded alcohol series and air-dried. 100 μl of hybridization buffer (70% formamide, 1 mg/ml blocking reagent [Roche], 10 mM Tris-HCl, pH 7.2, PNA probes [TelC-Cy3, CenpB-Cy5, PNA Bio]) were applied to each section and denaturation was performed by incubation at 75 °C for 10 min. Slides were then moved to a dark container for incubation for 2 hr at room temperature. Slides were washed 3 times in wash buffer (70% formamide, 10 mM Tris-HCl, pH 7.2), followed by 3 washes with PBS. To stain DNA, DAPI (100 ng/mL) was added to the second of the PBS washes.

Image analysis

Image analysis was performed using custom written scripts in Matlab (Mathworks). First, individual high-resolution fields of view were stitched together to generate a single high-resolution file of the tissue sample for each channel: DAPI (nucleus), Cy3 (telomere), and Cy5 (centromere). ROIs were generated by hand to identify relevant tissue types within the images. Individual spots in the Cy3 or Cy5 channels were identified using an adaptation of the MTT detection algorithm, based on maximum likelihood fitting to a two-dimensional Gaussian [108]. Because of the large size of each image, the stitched high-resolution image was subdivided into 512-by-512 pixel boxes for analysis by MTT, and the detected spots mapped back into the original spatial coordinates. For both channels, the following detection parameters were used: NA: 1.4; detection box: 9 pixels; error rate: 3; deflation loops: 0. Synthetic Aperture Optics (SAO) reconstruction in StellarVision instrument can introduce periodic structures into low- or homogenous-signal areas of an image [109]. In order to ensure that only bona fide telomere or centromere spots were being counted, a number of additional filters were applied. First, spot detection was confined only to annotated ROIs. Second, a binary mask was generated using the DAPI channel to only count and include spots that fell within a nucleus. Third, a signal intensity threshold was applied to all detections to remove any detections stemming from periodic fluctuations in the image background. Intensity thresholds varied from patient to patient but were held constant for all the images analyzed form the same hybridization. Using these steps, a list of high confidence spots was generated for the telomere channel and the centromere channel. The centromere channel was included in the analysis as an internal normalization for the telomere signal, particularly in order to control for differences in staining and fluorescence signal between tissue types and to control for changes in illumination intensity across a field of view. The closest n centromere spots were identified

using ‘knnsearch’ functions in order to generate a normalized telomere signal for each detected telomere spot. Normalized telomere signal was determined as the telomere intensity divided by the median of those 10 closest centromeres.

A random subsampling was performed to compare telomere lengths between different tissue types within a given sample, and to make an estimate of the magnitude of difference between telomeres in the melanoma and nevus. 50 telomeres from each tissue were randomly sampled, the median calculated, and the signals compared as the ratio between the two. This random resampling was performed for 10,000 iterations with replacement. In the null hypothesis, the two sampled populations would have similar spot intensities, and thus the ratio of the two would be centered around unity.

Statistics

All numerical results are presented as mean and SEM of at least three independent biological or experimental replicates unless stated otherwise. Statistical significance between experimental and control groups was assessed by a two-tailed unpaired Student’s *t*-test. A confidence coefficient of 0.05 was used for all tests.

Patient information and data availability

Case 1: Age 52, female, melanoma on posterior shoulder

Case 2: Age 64, male, melanoma on lower back

Case 3: Age 78, male, melanoma on scalp

Case 4: Age 37, male, melanoma on axillary vault

Patient sequencing data is available within the Short Read Archive with the accession number SRP113411. Authors can confirm that all other relevant data are included in the paper and or its supplementary information files. The research was approved by the UCSF human research protection program (institutional review board #11-07951).

Inferred genetic evolution

Phylogenetic trees were constructed as previously described in [91]. The sequence analysis of Case 2 has been previously reported as Case 9 in [91].

Code availability

MATLAB code used for image analysis is available under https://gitlab.com/tjian-darzacq-lab other data are available from the corresponding author.

Chapter 3: Telomere shortening acts as a tumor suppressor mechanism in an oncogenic driver mutation dependent manner

Abstract

The acquisition of an initiating oncogenic mutation stimulates proliferation of otherwise normal cells, but the cells rarely become malignant. A hyperproliferation of melanocytes forms nevi, which are precursor lesions of melanoma. In nevi melanocytes are halted in a senescence-like state, which is widely attributed to oncogene induced senescence caused by the initiating mutation. However, rare mutations in the promoter of the telomerase reverse transcriptase gene (TERT), which support the immortalization of a cell population, and may be found in early stages of melanoma development before full malignant transformation. This suggests that in at least a subset of nevi melanocyte replication occurs and *TERT* promoter mutations (TPMs) confer selective advantage in overcoming replicative senescence.

To address what role telomere shortening plays in tumor suppression and how TPMs are selected for in pre-cancerous melanocytic neoplasms we analyzed dysplastic nevi, a precursor of cutaneous melanoma for mutations and telomere length. We found that TPMs were detected with a higher frequency in older patients, indicating that later in life telomere length becomes limiting for the proliferation of melanocytes. Telomere length analysis showed that melanocytes of samples with TPMs had relatively shorter telomeres than wildtype samples. Oncogenic BRAF p.V600E mutations were detected frequently and preferentially in nevi of younger patients and none of the BRAF p.V600E-positive cases had TPMs. Telomere length analysis resolved by driver mutations showed that telomeres of BRAF p.V600E-positive nevi were longer than all other driver mutations, which indicates an earlier and telomere length independent arrest.

Introduction

Somatic mutations in signaling pathways that promoter cell division arise early in many neoplastic conditions and often result in self-limited proliferation of mutant cells that leads to the formation of benign neoplasms (Figure 3-1A). Oncogene-induced senescence (OIS) is considered as the dominant mechanism that restrains cell proliferation initiated by such oncogenic mutations. OIS is caused by unphysiologically strong and sustained growth signals resulting from a constitutively activated oncogene such as RAS of BRAF p.V600E [110–112]. The aberrant signaling leads to cellular stress and the induction of cell cycle inhibitory factors [110,113]. Cells can escape from OIS when genes encoding components of these checkpoints such as CDKN2A, pRb, and p53 become compromised [114].

Replicative senescence is an independent tumor suppressive mechanism that caps the total number of divisions of cells. Cells progressively shorten their telomeres with each cell division, ultimately triggering a DNA damage signal that induces cell-cycle arrest and senescence once telomeres become too short [6,115,116]. The enzyme telomerase can prevent this shortening [5,89], but in human somatic cells its expression

is normally silenced. This repression can be overcome by genetic alteration – structural rearrangements, amplifications or promoter mutations – of the *TERT* gene that allow telomerase to become expressed and bestow cells with the capacity to proliferate [39,40,47,117,118]. Telomerase expression is detected in 90% of all cancers [33]. *TERT* promoter mutations (TPMs) may occur early during cancer formation [91,119] and can support the immortalization of pre-cancerous cells [88].

Studying the early evolution of neoplastic growth is difficult for most cancer types as they are detected at advanced stages. Cutaneous melanomas present as atypically pigmented lesions that are visible on the skin and often are removed at very early stages, making them a useful model to study the early phases of cancer evolution [91,120]. Approximately 30% of cutaneous melanomas arise from melanocytic nevi [121,122]. These nevi constitute clonal proliferations of typically a few hundred thousand melanocytes that harbor a proliferation-inducing mutation such as BRAF p.V600E or various types of NRAS mutations known to induce senescence [112,123,124]. Dysplastic nevi are histologically or clinically defined lesions that are associated with an increased melanoma risk.

Comparison of the genetic alterations in melanomas and their adjacent precursor nevi has revealed that progression to melanoma is driven by the accumulation of additional driver mutations in the nevus cells by UV radiation induced mutagenesis [91]. TPMs and inactivating mutations of CDKN2A feature as the most common mutations during the progression to melanoma [91]. Surprisingly, TPMs can already be detected in 60% of precursor lesions that gave rise to a melanoma. TPMs provide a selective advantage to cells only when telomeres have shortened enough to induce replicative senescence. Therefore, the early selection of TPMs in premalignant lesions calls attention to replicative senescence as a tumor suppressor mechanism for some benign tumors, which are not or no longer constrained by OIS. Identifying the existence of such unstable lesions and characterizing their features would allow for the prospective removal and prevent melanomas to form. To address the role of telomere length in tumor suppression of premalignant lesions, we analyzed relative telomere length and the mutational status of the TERT promoter and melanoma-relevant genes in dysplastic nevi prospectively collected from a cohort of patients across a wide age range.

Results

BRAFV600E is more commonly found in younger patients, TERT promoter mutations are selected for in older patients

We successfully sequenced 89 lesions from patients ranging from 9 to 84 years in age (Supplemental Data Figure 3-1A). BRAF p.V600E was the most common pathogenic mutation in the cohort (64%) and was the dominant alteration in lesions from younger patients (Figure 3-1C, Supplemental Data Figure 3-1B). TPMs were present in 8 lesions (11.3%) and occurred in a mutually exclusive pattern with BRAF p.V600E mutation (χ^2-test $p<0.05$, Supplemental Data Figure 3-2C,D) and were found only in patients over the age of 50 (Figure 3-1C, Supplemental Data Figure 3-1C). Lesions with TPMs harbored

alternative drivers mutation of the MAP-kinase pathway that commonly seen in melanomas on chronically sun-damaged skin [125,126]. The type of mutations found in the lesions, BRAF p.V600E or alternative mutations activating the MAP-kinase pathway and TPMs, were similar to those catalogued in cutaneous melanomas. In cutaneous melanomas BRAF p.V600E constitutes the most common driver of the MAP-kinase pathway in patients younger than 55 years, whereas in older patients other mutations in the pathway predominate [125,127–129].

However, the mutually exclusive distribution of BRAF p.V600E mutations and TPMs in our cohort of premalignant lesions differs markedly. While TPMs are found in up to 80% of cutaneous melanomas, they occur irrespective of their BRAF mutation status [44]. We analyzed a previously published data sets of cutaneous melanoma patients for the occurrence of BRAF p.V600E and *TERT* promoter mutations [44,91,129]. A comparison of TPM frequency in nevi with primary melanoma and metastasis showed that TPMs are strongly selected for at the progression from nevus to melanoma (Figure 3-2). A test for independence of the two variables (BRAFV600E status/TPM status) showed that after progression to melanoma in both primary and metastatic tumors TPMs occurred with a high frequency regardless of the oncogenic driver mutation (Figure S2E-H).

Our data indicates an unappreciated heterogeneity in dysplastic nevi that points towards different categories of lesions in the young and old. The dysplastic nevi in younger patients are genetically similar to common acquired nevi, in which BRAF p.V600E mutation is the sole detectable alteration [130–133]. This is in concordance with the model that these nevi arise early in life, persists for several decades and then involute and disappear. However, the data indicates the existence of a separate type of lesion that emerging later in life and is genetically characterized by a different set of MAP-kinase pathway driver mutations that can be accompanied by additional pathogenic mutations that include TPMs. TPMs become a selective advantage for cells, only when their telomeres had become sufficiently short to trigger replicative senescence. The complete absence of TPMs in BRAF V600E driven nevi is consistent with the model that they ceased proliferation due to OIS. This would mean that their telomere length would be longer than in cells that underwent replicative senescence.

Deriving cell type specific telomere length measurements

To test this hypothesis, we measured the telomere length of neoplastic melanocytes by fluorescence *in situ* hybridization and structured illumination microscopy. As individual telomeres of a cell shorten by 50-200 nucleotides with each division, cellular telomere length clocks the number of cell divisions that a cell has undergone. However, telomere length does not provide an absolute measurement of past divisions, as the starting lengths of telomeres varies among individuals. To compensate for such inter-individual differences and any variability in hybridization efficiency of tissues, we normalized the telomeric signals of neoplastic melanocytes to that of epidermal keratinocytes within the same lesion. To obtain cell type specific measurements, we lined

up DNA staining images with images from hematoxylin and eosin (H&E) stained tissue sections and annotated melanocytes and epidermal keratinocytes (Figure 3-3A-D, Supplemental Data Figure 3-3A). We derived a "normalized telomere length" measurement for melanocytes relative to the average keratinocyte telomere length signal per patient. In total we successfully derived normalized telomere length measurements for 59 patient cases and variations in staining efficiency and constitutive telomere length influence telomere length measurements were successfully removed by the normalization (Supplemental Data Figure 3-3C). To ensure the consistency of the normalized telomere length measurement we additionally analyzed three consecutive sections of one patient and found the normalized telomere length measurement to be highly similar (Figure 3-3F). Neither before nor after normalization was the mean telomere length correlated with patient age (Figure 3-3G, Supplemental Data Figure 3-3B).

The combination of driver mutations and TPMs dictates the proliferation of dysplastic melanocytes

In the 59 lesions in which telomere length could be measured we found that those with TMPs had short telomeres with lengths similar to that of melanomas with TPMs (Figure 3-4A). This is expected, because TPMs only become a selective advantage when telomeres are short. Once telomerase becomes expressed by TPMs its action maintains telomeres at a short length rather than re-extending them [88]. By contrast, dysplastic nevi with BRAF V600E mutations had a significantly longer average relative telomere length than other nevi (two-sided t-test, $p = 0.007694$). The distribution of individual telomeric signals of neoplastic melanocytes normalized to the average keratinocyte signal was shifted towards shorter length in lesions with TPMs (Figure 3-4B), with a compressed spread for the lower quartile (Figure 3-4A, Supplemental Data Figure 3-4A,B), likely reflecting that telomere length had reached a minimum.

The long telomeres in BRAF p.V600E mutated lesions therefore confirm the notion that their cells had undergone growth arrest before running out their replicative lifespan and reached a stable state maintained by OIS. Lesions with TPMs either never reached such a state or escaped from it, as their cells must have continued to proliferate when their telomeres became critical short. At that point, the presence of a TPM did become a selective advantage and enabled their cells to continue dividing in spite of their short telomeres. Lesions without TPMs that had MAP-kinase pathway mutations other than BRAF p.V600E had telomere lengths that ranged between the longer telomeres of the BRAF p.V600E mutated cases and the very short telomeres of lesions with TPMs. The normalized telomere length of these three groups were significantly different from each other (ANOVA, $p < 0.05$). This suggests that the cells of dysplastic nevi in older individuals that do not have TPMs may also not be arrested and continue to divide and thus poised to select for any TPMs in the future.

In summary, the findings suggest that premalignant lesions with strong MAP-kinase pathway mutations such as BRAF p.V600E are kept in check by different mechanisms of tumor suppression than those with other BRAF mutations or inactivation

of NF1. If true, this would impact the type and number of additional genetic alterations necessary for transformation and likely the sequential order in which they have to occur in these two settings. Nevi kept in check by OIS would have to overcome this first barrier first, before telomere length could become rate-limiting and impose an additional barrier. By contrast, precursors that are unconstrained by OIS would face replicative senescence as their first barrier towards transformation. In this scenario, melanomas that evolved from precursors constrained by OIS would be expected to acquire genetic alterations that override OIS first, before they go on and acquire TPMs to break through the second barrier imposed by replicative senescence (Figure 3-4C).

Discussion

Empirical clinical observation indicates that melanocytic nevi that arise in the first two decades of life, persist for some time but then slowly regress later in life [134]. During their lifespan the majority of these lesions are stable and do not change their appearance in longitudinal studies with dermoscopy, but the subset that does undergo phenotypic changes is enriched for nascent melanomas [135]. The molecular underpinnings underlying the differences between these lesions are currently not known. Our results indicate that indeed microscopically defined dysplastic nevi are genetically heterogeneous, shedding some light on the conflicting findings (Figure 3-4C). Dysplastic nevi in younger patients had a pattern of somatic mutations similar to that of common acquired nevi, BRAF p.V600E mutation as the sole genetic alteration. The longer telomere length in these lesions supports the notion that they are kept in check by growth arrest, consistent with OIS. Our data also reveal a separate type of lesion, which emerges at around age 60. It is genetically characterized by different MAP-kinase pathway driver mutations that similar to BRAF V600E mutations are also commonly found in cutaneous melanomas. The age-dependent distribution of mutations in our cohort mirrors that found in cutaneous melanoma. Melanomas in patients under the age of 55 frequently have BRAF p.V600E mutations, whereas melanomas in older patients have other BRAF mutations, mutations KIT, and inactivation NF1 [125,127,129,136].

This age-dependent variation of MAP-kinase pathway mutations that affects both nevi and melanomas, points towards two distinct evolutionary trajectories towards cutaneous melanoma. One starts with BRAF p.V600E, early in live that lead to the formation of nevi, lesions that are constrained by OIS. In our follow-up analysis we will determine whether these lesions first select for the inactivation of CDKN2A, or equivalent genetic alterations to override OIS. Only then does replicative senescence emerges as the next barrier to full transformation, selecting for TPMs as the third step. The trajectory of the other subset of nevi begins with other MAP-kinase pathway driver mutations or NRAS but likely begins decades later, as their distribution is mainly confined to older patients. These lesions thus already start with age-dependent shorter telomeres, acquire TPMs faster and probably only subsequently lose cell cycle checkpoints.

Finally, both OIS and replicative senescence converge on the same DNA damage sensing pathways. The tumor suppressive effects, which are mediated by varying

degrees of DNA damage signaling could lead to qualitative differences in cell cycle arrest and require the loss of different checkpoints for cancer progression. Others have proposed that the DNA damage signaling pathways are even physically intertwined at telomeres as major sites of DNA-damage during replication stress [137,138]. When BRAFV600E mutant melanocytes escape arrest, they equally require immortalization, which is then also often mediated by the acquisition of TPMs. Future studies will have to clarify under which circumstances melanocytes with different driver mutations can overcome growth inhibition.

Figures

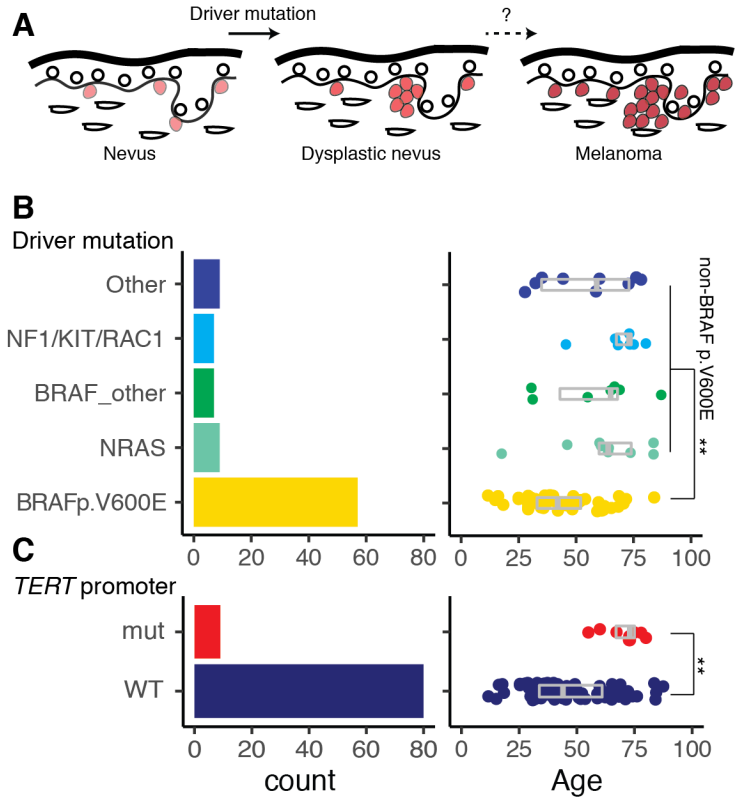


Figure 3-1: Distribution of TPMs and driver mutations detected in the patient cohort. *(A) Overview of early tumorigenesis of melanoma. Following an initial oncogenic mutation, melanocytes proliferate to form a dysplastic nevus but do not yet progress to melanoma. (B-C) Frequency of oncogenic driver mutations/TPMs and age distribution in dysplastic nevus cohort.*

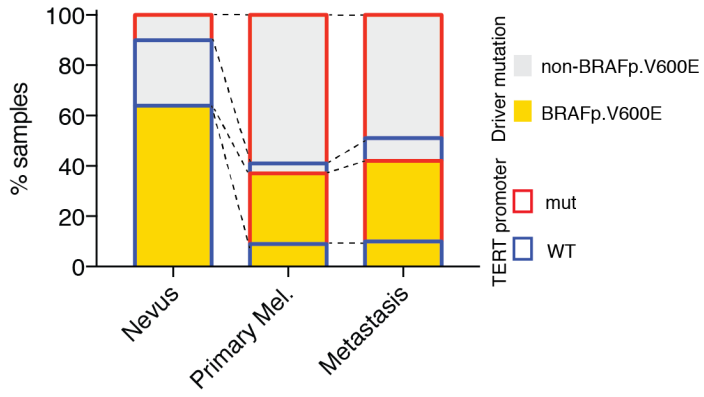


Figure 3-2: Driver mutations and TPM status in nevi, primary cutaneous melanoma and metastasis

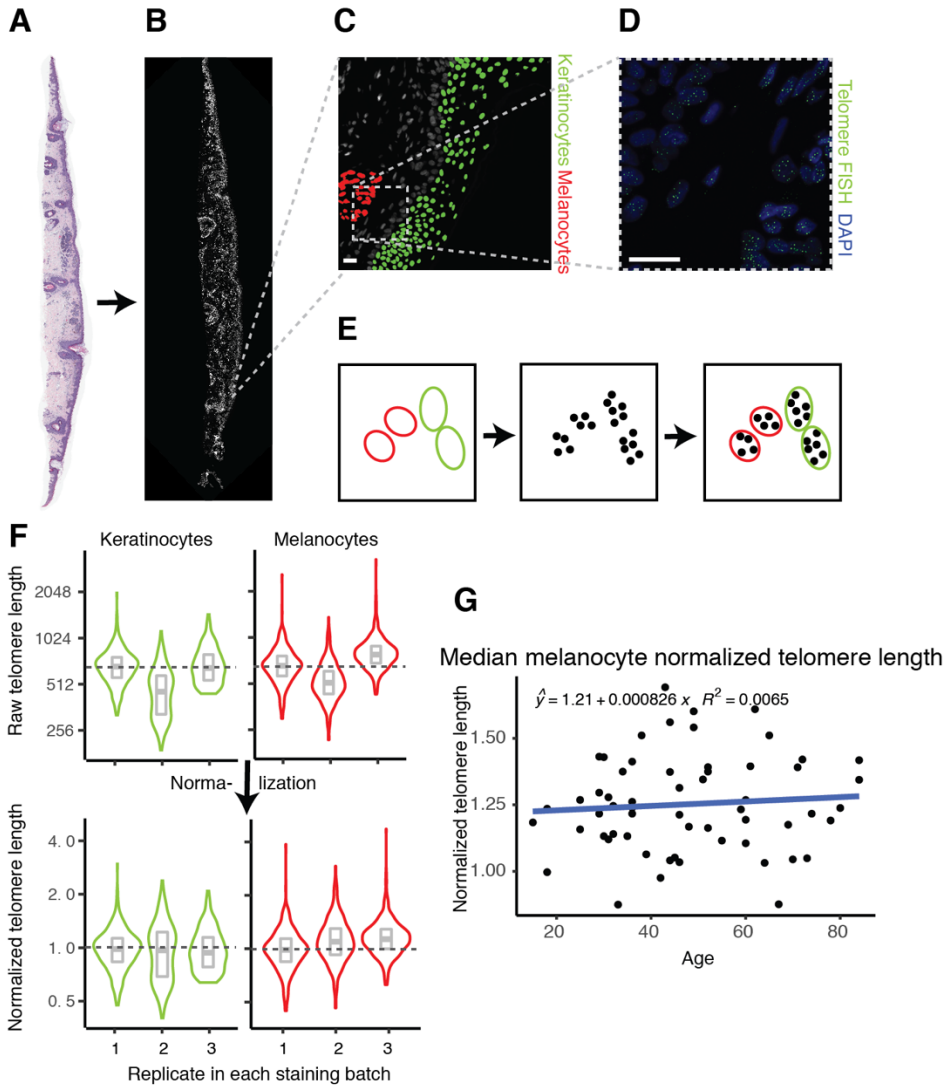


Figure 3-3: Telomere length measurements in nevi using structured illumination microscopy and qFISH. *Workflow for spot detection and image analysis: (A) H&E staining of a nevus sample. (B) Stitched 4,6-diamino-2-phenylindole (DAPI) image of the same nevus. (C) Annotation of the DAPI image based on the H&E image. (D) Telomere FISH image of the same tissue is used for telomeric spot detection. (E) Schematic overview of the process of overlay of cell annotations with detected spots to extract cell type specific telomere length measurements. (F) Violin plots of one nevus case stained, imaged and annotated in each batch. Upper panel: Telomere length measurements per cell for keratinocytes and melanocytes before normalization (Raw telomere length). Lower panel: Relative telomere length measurements after normalization (Normalized telomere length). (G) Linear correlation of median normalized telomere length measurements per patient against patient age.*

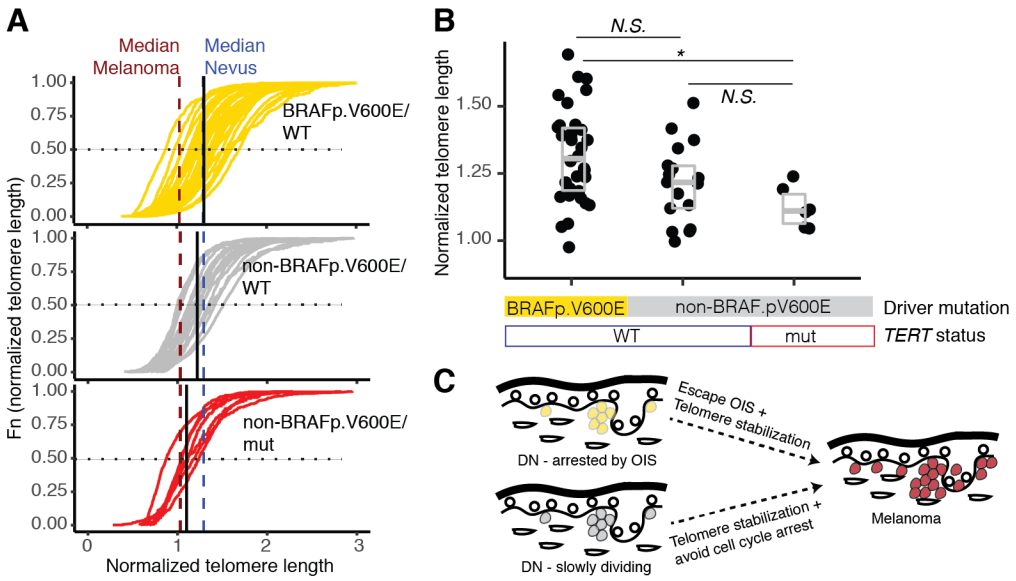
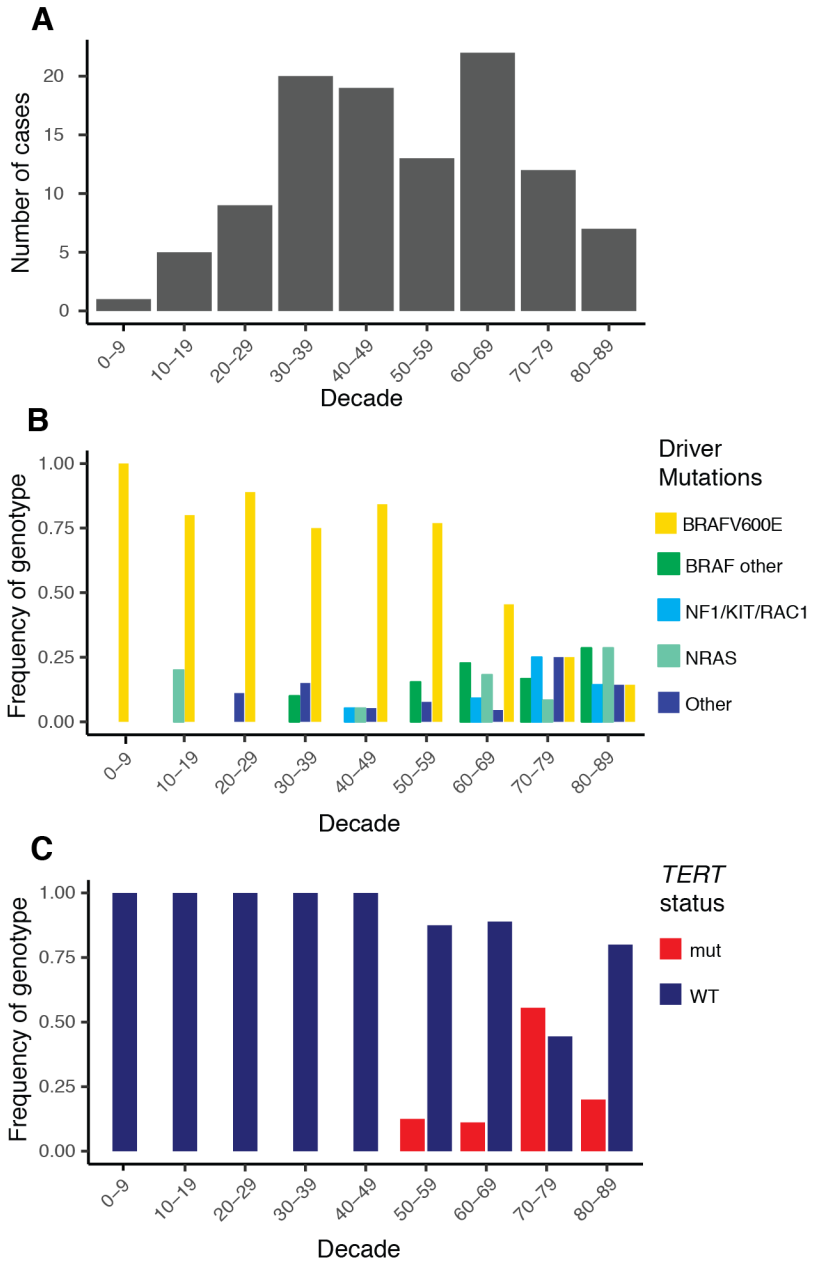
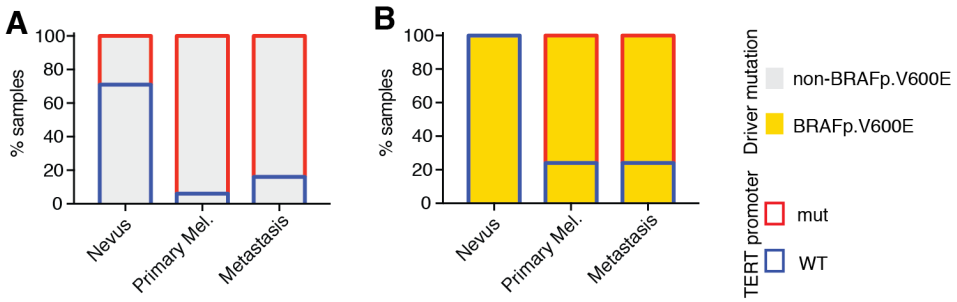
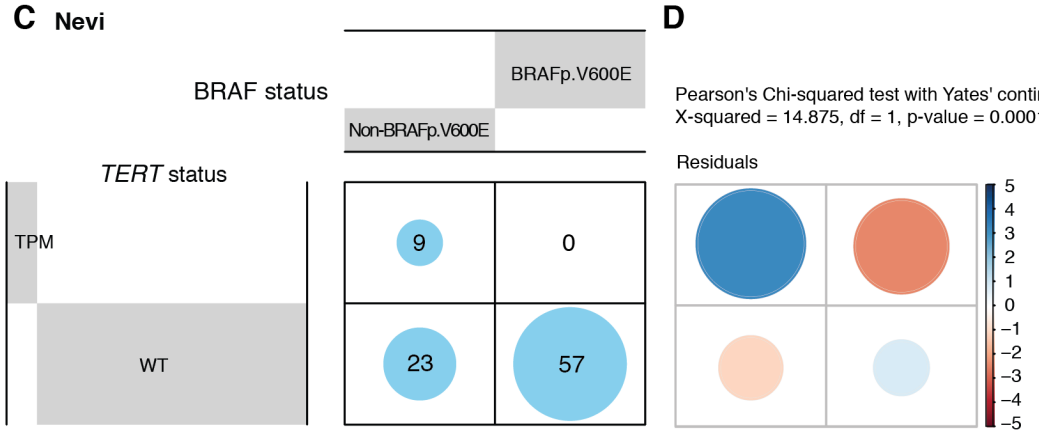


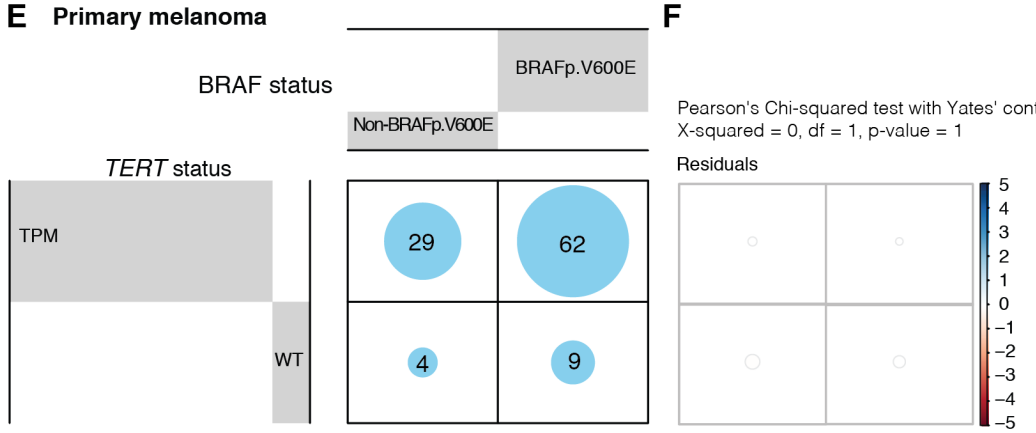
Figure 3-4: Relative telomere length of TPM mutant nevi is shorter than that of wildtype nevi. *(A) Empirical cumulative distribution function (ECDF) depicting the distribution of normalized telomere length of each patient case grouped by driver mutations and TPM status. Dotted reference lines for average median nevus telomere length and matched melanoma. (B) Comparison of medians grouped by driver mutations and TPM status (**p = 0.008, one-sided ANOVA, individual p-values Tuckey HSD annotated in plot). (C) Model of different driver mutations leading to tumor suppression by different mechanisms. BRAF p.V600E mutant melanocytes are stalled by OIS (yellow), while melanocytes with weaker driver mutations (grey) experience telomere shortening and are arrested by replicative senescence.*

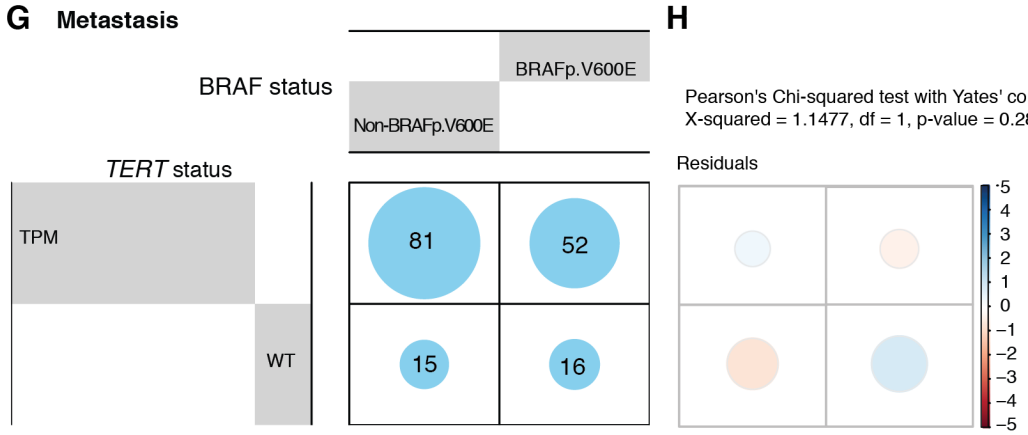


Supplemental Data Figure 3-1: *(A) Age distribution of the nevus samples collected and analyzed. (B) Frequency of mutations per decade of different driver mutations and (C) for TPMs.*

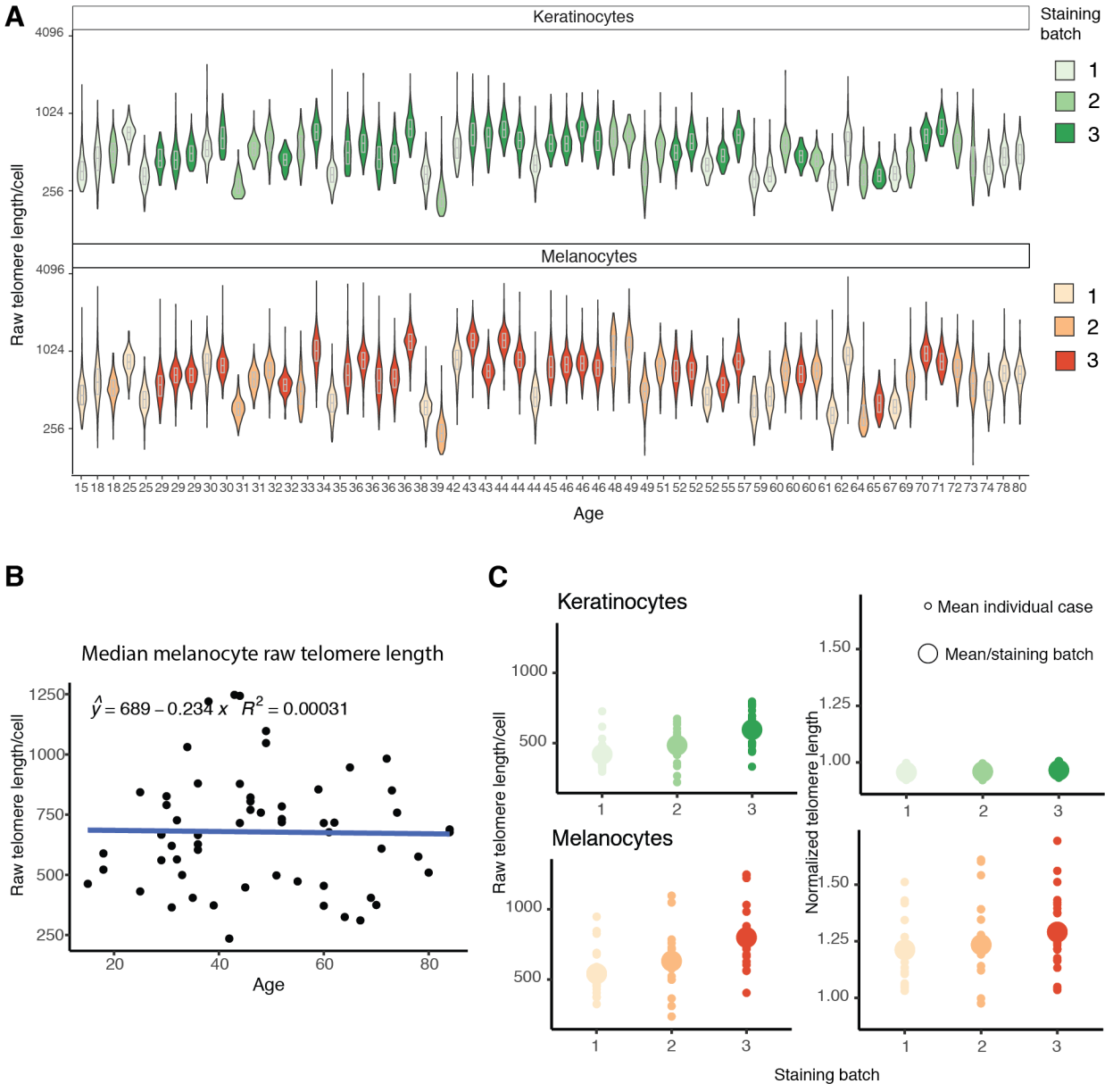

A
B
% samples
100
80
60
40
20
0
Nevus
Primary Mel.
Metastasis
Driver mutation
non-BRAFp.V600E
BRAFp.V600E
TERT promoter
mut
WT


C Nevi
BRAF status
BRAFp.V600E
Non-BRAFp.V600E
TERT status
TPM
WT
9
0
23
57
D
Pearson's Chi-squared test with Yates' continuity correction
X-squared = 14.875, df = 1, p-value = 0.0001149
Residuals
5
4
3
2
1
0
−1
−2
−3
−4
−5

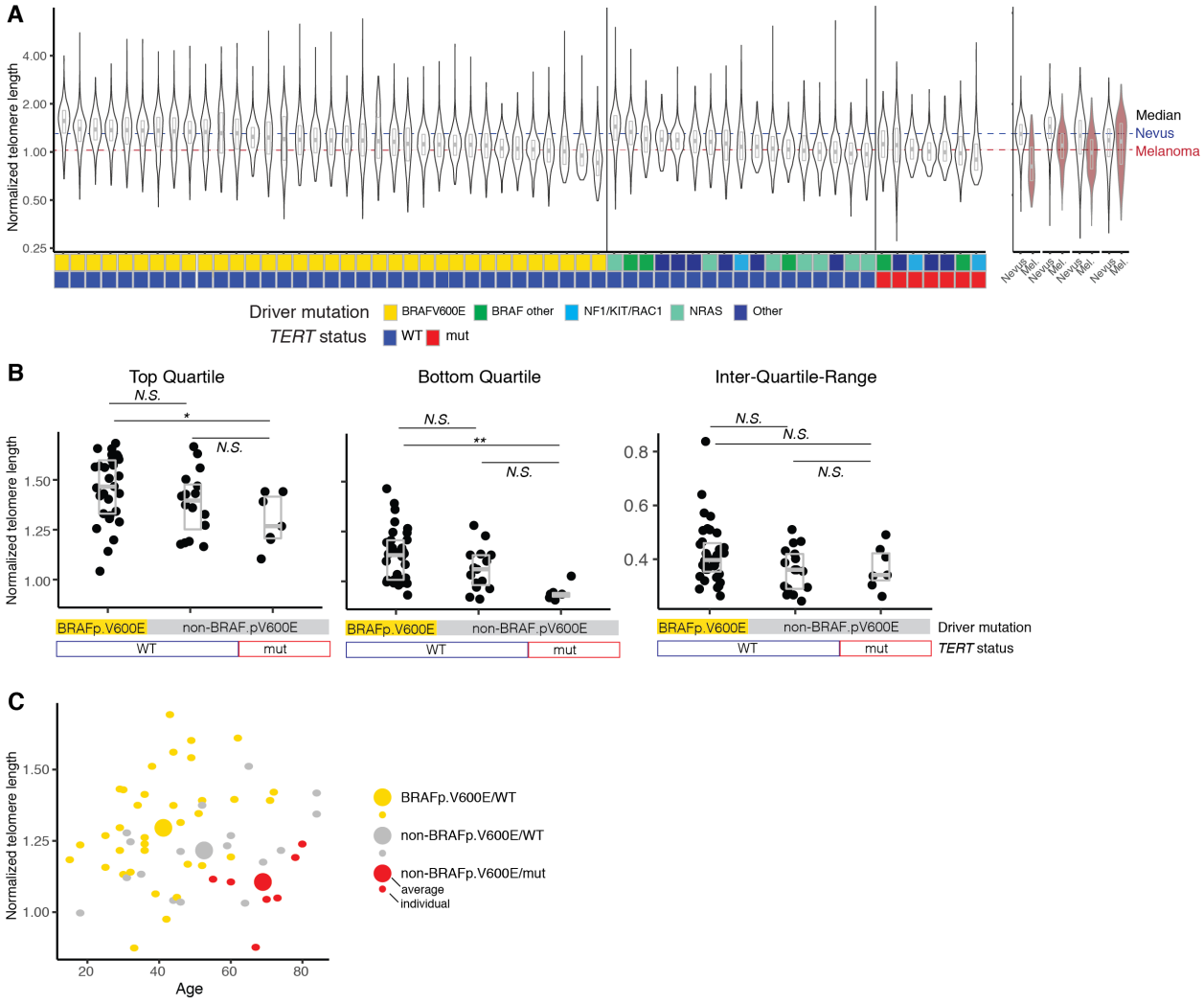

E Primary melanoma
BRAF status
BRAFp.V600E
Non-BRAFp.V600E
TERT status
TPM
WT
29
62
4
9
F
Pearson's Chi-squared test with Yates' continuity correction
X-squared = 0, df = 1, p-value = 1
Residuals
5
4
3
2
1
0
−1
−2
−3
−4
−5


G Metastasis
BRAF status
BRAFp.V600E
Non-BRAFp.V600E
TERT status
TPM
WT
81
52
15
16
H
Pearson's Chi-squared test with Yates' continuity correction
X-squared = 1.1477, df = 1, p-value = 0.284
Residuals
5
4
3
2
1
0
−1
−2
−3
−4
−5

Supplemental Data Figure 3-2: *TPM status grouped by driver mutation status (A) BRAF p.V600E and (B) all other driver mutations for nevi, primary and metastatic cutaneous melanoma. (C) Balloon plot representing the relative magnitude of the case numbers of the contingency table of nevi found with BRAFV600E vs. all other mutations and TERT promoter mutant vs. wildtype. Pearson residuals. The size of the circle is relative to the amount of the contribution. (D) Residuals of the contingency table: Blue positive association = more than expected, red negative association = less than expected. (E,G) Graphic representation of the contingency table of the representation of BRAFV600E vs. all others and TPMs in primary and metastatic cutaneous melanoma (F,H) Residuals of primary melanoma/metastasis contingency table.*



Supplemental Data Figure 3-3: Normalization of batch effects and individual telomere length differences by normalization to keratinocyte telomere signal. *(A) Violin plot with box plot inset of raw telomeric signals before normalization (red = melanocytes, green = keratinocytes, shades indicate staining batches) (B) Linear correlation of raw median telomere length measurements per patient against patient age. (C) Jitter plot of median telomeric signal per patient/case (small circle) and the average of all cases (big circle) per staining batch for melanocytes and keratinocytes before (Raw telomere length) and after normalization (relative telomere length).*



Supplemental Data Figure 3-4: *(A) Violin plot with boxplot inset. Tiling below indicates the driver mutation and TPM status. To the right: TPM melanoma cases with adjacent WT nevi. Average telomere length of all melanoma/nevus cases is indicated by the dashed line. (B) Jitter plot of top quartile, bottom quartile and inter-quartile-range (IQR) of normalized telomere length distribution of all cases grouped by driver mutations and TPM status (one-sided ANOVA, individual comparisons annotated). (C) Median telomere length per case relative to age (small dot) and group average (big dot).*

Material and Methods

Patients

We prospective collected nevi with histopathological features of so-called Clark's or dysplastic nevi during the routine diagnostic sign-out process from patients ranging in age ranging from the 9 to 84 (Figure 4-1B). Cases either received a benign diagnosis (ICD-10 D22.9) or a diagnosis of neoplasm of uncertain behavior (ICD-10 D48.5). Histopathological features for inclusion were the presence of broad silhouette with lateral extension of the junctional component, eosinophilic or lamellar fibroplasia of the papillary dermis, patchy lymphocytic infiltrates, random cytologic atypia, or scattered melanocytes with dusty melanin pigmentation [139]. Cases had to have sufficient tumor cell content to be micro-dissected to be included.

Next-generation sequencing

Microdissection of unstained 10 µm sections of leftover formalin-fixed paraffin-embedded tissue was performed under a dissection microscope using routinely stained as guidance. DNA was extracted and libraries constructed for targeted next generation sequencing (NGS) as previously reported [91]. Libraries were pooled and captured with baits for the coding region 79 genes and promoter region of 3 genes known or suspected to be involved in the pathogenesis of melanocytic neoplasia. Mutations were called against a normal human reference genome. Cases in which no pathogenic mutation in any of the genes could be detected were subsequently excluded from the study as we could not definitely ascertain that sufficient neoplastic melanocytes were present in the sample.

Telomeric and centromeric fluorescence in situ hybridization in FFPE patient samples

Telomere FISH was performed in three batches on three separate days. Tissue sections were randomly selected from all age groups for each staining batch. For each round the staining was performed as described in Chiba et al. [88]. Briefly, tissue sections were deparaffinized with histoclear and rehydrated through a graded alcohol series. They were placed in deionized water followed by permeabilization in water with 0.1% Tween-20 for 2 min. Slides were then placed in 10mM Sodium Citrate pH 6.5 at 85 °C for 15 min. After rinsing with water, they were treated with 0.4% pepsin for 10 min (pre-warmed to 37°C). Following another water rinse, slides were dehydrated in a graded alcohol series and air-dried. 100 ml of hybridization buffer (70% formamide, 1 mg/ml blocking reagent [Roche], 10 mM Tris-HCl, pH 7.2, PNA probes [TelG-Cy3, CenpB-Cy5, PNA Bio]) were applied to each section and denaturation was performed by incubation at 75°C for 10 min. Slides were then moved to a dark container for incubation for 2hr at room temperature. Slides were washed 3 times in wash buffer (70% formamide, 10 mM Tris-HCl, pH 7.2), followed by 3 washes with PBS. To stain DNA, DAPI (100 ng/mL) was added to the second of the PBS washes. Samples were mounted using Prolong gold and imaged

within a week following staining using structured illumination microscopy with the Stellarvision synthetic aperture optics custom microscope.

Cell type specific telomere length analysis

Spot detection was performed using custom Matlab software provided by the Stellarvision company.

Annotations

To create annotations of individual cells, regions of interest (ROIs) were created around nuclei using thresholding of the DAPI signal. DAPI images were then lined up with H&E images of each case and ROIs were color coded based on cell type as determined by nuclear morphology and histopathology of the region using Fiji. To avoid annotating melanocytes residing in the keratinocyte layer only the outer layers of keratinocytes were used. Annotations were then translated into spatial information for each image and lined up with the detected telomeric spots using Matlab. Spots were then matched with ROIs representing individual cell outline and the cell type information for select each ROI and saved as individual annotation text files for each analyzed image. The subsequent data processing and normalization of telomere length was performed in R. To calculate relative telomere length, the mean telomeric signal per cell was calculated to ensure that the cell population measured was normally distributed and no clonal subpopulations were detected. To derive the relative telomere length, melanocytic telomere length measurements were divided by the mean of the keratinocyte telomere signal for each patient. Statistical analysis was performed using the base R and the coin package, plots were generated with ggplot2 and corrplot.

Chapter 4: Dyskeratosis congenita mutations in the shelterin component TIN2 affect telomere length in the stem cell compartment and lead to reduced proliferative capacity

Abstract

Dyskeratosis congenita (DC) is a rare but severe bone marrow failure syndrome caused by defective telomere maintenance. Whole exome sequencing studies have identified disease-linked mutations in genes involved in telomere maintenance, with 11 to 24% of DC cases being caused by mutations in the shelterin component TIN2. The DC-linked mutations in the *TINF2* gene are nonsense or missense mutations found in the so-called 'DC cluster' in exon 6. The mechanism by which the TIN2 DC mutations lead to short telomeres remains largely elusive. Here, we establish a human embryonic stem cell (hESC) model system of TIN2 DC missense mutations, which recapitulates the short telomere patient phenotype. We show that introducing the mutation leads to telomere shortening in a telomerase-dependent manner in hESCs while maintaining telomere protection. As a consequence of the mutation TIN2-DC hESC-derived, differentiated daughter cells had a reduced proliferative capacity. Disruption of one allele of TINF2 restored telomere length and proliferative capacity. We conclude that TIN2-DC mutations exert their disease effect in the telomerase-positive stem cell compartments of the human body, such as hematopoietic stem cells, which could provide an attractive target for therapeutic intervention.

Introduction

Telomeres are the capping structure at the end of linear chromosomes and are composed of telomeric DNA repeats and telomere-binding proteins. The telomere-binding protein complex called shelterin has multiple functions: It inhibits a DNA damage response at the telomeres and controls the amount of DNA lost due to the end replication problem and nucleolytic degradation. On the other hand, it also facilitates telomere elongation by recruiting the enzyme telomerase to telomeres. Telomerase is a ribonucleoprotein that adds telomere repeat sequence to the 3' end of telomeres [5,89]. Together shelterin and telomerase function to tightly regulate telomere length in humans in telomerase-positive cells, such as the early embryo, and adult stem cell populations. In contrast, fully differentiated telomerase-negative somatic cells shorten telomeres during each round of cell division until telomeres become critically short and signal as sites of DNA damage. This signal leads to a cell cycle arrest referred to as replicative senescence. Dysregulation of telomere length in the stem cell compartment is associated with disease: Exceptionally long telomeres allow for many rounds of cell divisions and can lead to over-proliferation and cancer [63]. Contrarily aberrantly short telomeres greatly restrict the number of cell divisions and therefore often manifest as adult stem cell depletion syndromes, affecting the regenerating tissues, particularly the hematopoietic system [55].

Short telomere diseases do not only display a broad range of clinical symptoms but also vary in their age of onset and severity. Milder versions such as idiotypic lung fibrosis, liver cirrhosis, aplastic anemia and myeolodysplastic syndrome often are later onset. Rarer but more severe diseases such as Coats Plus, Hoyerson Henderaal, Revesz and Dyskeratosis Congenita tend to occur earlier in life. Dyskeratosis congenita (DC) is a bone marrow failure and premature tissue aging syndrome, which is additionally characterized by the mucocutaneous triad of clinical symptoms (oral leukoplakia, nail dystrophy and skin pigmentation) (reviewed in Bertuch 2016 [140,141] Townsley 2014). The genetic link of DC to telomeres was established when the first disease-causing allele was mapped to the Dyskerin locus (DKC1) [142–144]. In later studies, mutations in other telomerase subunits (TERT [79,145], TERC [80,81], NOP10 [146], NHP2 [147]) as well as in the telomerase biogenesis pathway (TCAB1 [148], PARN [149]) and in telomere binding proteins (RTEL1 [150], TPP1 [151] and TIN2 [84]) have been identified.

TINF2, coding for the TIN2, protein has been reported as the second most mutated gene in all DC cases [152]. TIN2 is important for maintaining the integrity of the shelterin complex and for telomere length regulation: By bridging between the double strand-binding shelterin proteins TRF1/TRF2 and the TPP1/POT1 heterodimer [153] it affects telomere length regulation. With its interaction with TRF1 TIN2 stabilizes TRF1 on the telomeres, which is a negative regulator of telomere length [154]. Additionally, the telomerase-interacting TPP1/POT1 heterodimer requires TIN2 to be recruited to telomeres, thus making TIN2 also an important player for telomere elongation [155]. The majority of TIN2 DC-mutations reported to date are heterozygous missense and nonsense mutations, found in a cluster of 30 amino acids located in exon 6. This so-called “DC cluster” is adjacent to the TRF1-interaction domain in exon 6 but lies in a region of unknown function [84,156,157]. TIN2 DC mutations do not affect the interactions of TIN2 with its binding partners TRF1, TRF2 and TPP1 suggesting that the assembly of shelterin complex remains intact [158–160]. Furthermore, the mutations were shown to neither affect telomerase expression levels nor cause differences in telomerase activity [19].

The mode-of-action of the mutation – whether it causes telomere-shortening in a telomerase-dependent or independent manner – remains unresolved. In a conditional TIN2-DC knock-in mouse model, accelerated telomere shortening was observed in DC mutant, telomerase-deficient mice, suggesting that telomere shortening was exacerbated independent of telomerase activity [160]. Contrarily, in a human DC mutant knock-in cancer cell lines telomeres shortened due to impaired telomerase recruitment [19]. Therefore, it remains an open question where and by which mechanism the disease mutations manifest first. Progress in understanding TIN2-DC has been hampered by the limitations of mouse and cancer cell models in recapitulating the physiological telomerase and telomere length regulation. Telomere length regulation takes place during the self-renewal of telomerase-positive stem cells and the progressive telomere shortening of telomerase-negative differentiated cells. Therefore, understanding how telomere shortening is caused by the disease mutations in both compartments is important. A model system that adequately represents all affected cell types will help us to address

the unknown aspects of the disease and will allow us to identify potential therapeutic strategies.

Here we report the development of an endogenous, isogenic model system in human embryonic and hematopoietic stem cells that allows us to study the disease *in vitro* as well as *in vivo*. We found that while the TIN2 DC mutations have been classified as autosomal dominant mutations [55,140], overexpression of the disease-relevant mutant forms of TIN2 did not recapitulate the telomere shortening phenotype observed in patients. Instead the overexpression of the long isoform - of both the mutant and wild-type - caused telomere elongation, not acting as a dominant negative. By using CAS9 mediated genome editing of human embryonic stem cells (hESCs) we successfully generated a model of the short telomere phenotype observed in DC patients. We found that the short telomeres resulted from mutant protein expression from the endogenous locus. Short telomeres did not exhibit signs of DNA damage or exacerbated telomere shortening, instead we could show that telomeres shortened in a telomerase-dependent manner. The phenotype could be rescued by a disruption of the *TINF2* mutant and wild type allele, which lead to telomere elongation and could restore replicative potential.

Results

Editing of the endogenous TINF2 locus in hESCs recapitulates the short telomere patient phenotype

The heterozygous germline mutations of *TINF2* cause DC patients to have short telomeres in all tissues. hESCs can function as a model of self-renewal and regeneration as they are telomerase-positive but can readily be differentiated into various telomerase-negative cell types. In order to establish an hESC-based model system and to assess the effect of the DC mutant protein, we initially examined the consequences of the overexpression of wild-type and DC-mutant, short ($TIN2S_{1-354}$) and long ($TIN2L_{1-451}$) TIN2 isoforms in wild-type hESCs with regards to telomere length (Figure 1A). Following viral transduction, both the wild-type and mutant $TIN2L_{1-451}$ lead to pronounced telomere elongation compared to control cells (Median length: GFP control 9.6 kb versus 11.1 and 11.3 kb WT/mutant $TIN2L_{1-451}$ respectively). Overexpression of $TIN2S_{1-354}$ only had minor effects on telomere length, with telomeres being slightly shorter (Median length 8.6 kb). While this finding was in agreement with previous reports of TIN2 overexpression in cancer cells [159,161], it showed that the TIN2 DC mutation did not act as a dominant negative allele for telomere shortening. We concluded that the telomere elongating effect of the overexpression was masking the expected shortening effect of the disease mutation. Therefore, in order to obtain expression levels that would allow us to faithfully recapitulate the difference between wild-type and mutant, we decided to generate the TIN2-T284R mutation endogenously. Using CRISPR/Cas9 mediated genome editing we obtained isogenic heterozygous and homozygous TIN2-T284R containing hESC lines (Figure 4-1B,C). We confirmed expression of both alleles by Sanger Sequencing of a cDNA PCR amplicon from the heterozygous cell line (Supplemental Figure 4-1A). Furthermore, in both the heterozygous and homozygous cell lines, TIN2 localized to

telomeres normally as shown by immunofluorescence (IF) of TIN2 in conjunction with the shelterin component TRF1 (Figure 4-1D). To assess telomere length, we serially passaged wild-type, heterozygous and homozygous hESCs for 150 days and collected DNA samples. Throughout this time course, the average telomere lengths of heterozygous and homozygous hESCs were shorter (Mean: 5.8kb and 5.6kb respectively) than that of wild-type cells (Mean: 7kb) and were stable over time (Figure 4-1E).

Telomere shortening is telomerase-dependent and reduces the proliferative capacity of TIN2 mutant cells

The short telomeres observed in the mutant hESCs could be due to excessive nucleolytic degradation caused by increased DNA damage at telomeres or due to defective telomerase recruitment. Expression of the mutant protein did not induce a DNA damage response at telomeres, as demonstrated by the absence of telomere dysfunction-induced foci in mutant cells (TIFs) compared to the positive control (Figure 4-2A). To test whether telomere shortening occurred in a telomerase-dependent manner, we differentiated telomerase-positive hESCs into telomerase-negative fibroblasts. If the shortening occurred in a telomerase-dependent manner, we would expect to observe similar telomere shortening rates in telomerase-negative fibroblasts. If telomerase-independent excessive nucleolytic degradation was the cause of telomere shortening, we would expect to see increased telomere shortening rates in telomerase-negative mutant cells. We confirmed that the levels of telomerase activity were undistinguishable between hESC lines by telomerase repeat amplification protocol (TRAP) and it was undetectable after differentiation into fibroblasts (Figure 4-2C). The isogenic fibroblasts lines were serially passaged until they reached replicative senescence. Fibroblasts derived from the mutant hESCs had a reduced proliferative capacity of about 10 PD compared to 25 PD of wild-type cells (Figure 4-2B). This difference was exclusively attributed to different starting telomere lengths not to differences in the shortening rate, which was similar in all three cell lines (Figure 4-2D, Supplemental Data Figure 4-2A,B). This finding refutes the idea that telomere shortening is exacerbated by the TIN2 mutations and is in agreement with a previously published study suggesting that short telomeres are a result of impaired telomerase recruitment [19]. By overexpressing the limiting telomerase RNA component hTR from the AAVS1 safe-harbor locus [26], we could confirm that telomeres are not defective but remain in an extendable state despite the TIN2 DC mutation. Following targeting, telomeres in wild-type as well as in mutant hES cell lines elongated rapidly providing further evidence that the short telomeres were a result of a telomerase-dependent defect (Supplemental Figure 4-2C,D). The disease-relevant telomere shortening therefore occurred exclusively in the telomerase-positive stem cell compartment, leading to a reduced proliferative capacity of the cell progeny. Any therapeutic intervention to counteract the disease outcome would therefore have to address the short telomere phenotype in the telomerase-positive/stem cells.

Telomere length and proliferative capacity can be restored by hemizygous disruption of TINF2

In order to develop a strategy to restore telomere length in the stem cell compartment we needed to understand the genetics of the disease mutation. While the heterozygosity of the disease mutations suggested that the mutations could be dominant, the lack of a phenotype from overexpression of mutant TIN2 argued otherwise (Figure 4-1). If the allele were dominant, a disruption of the mutant allele would restore telomere length, while the disruption of the wild-type allele should not have an effect. If it were a loss of function mutation, the disruption of the mutant allele would have no effect on telomere length. To resolve this, we excised the region spanning exons 4 to 7 of TIN2 (a TIN2 [155] disruption strategy successfully used in mouse) using CRISPR/Cas9 to generate TIN2 hemizygous cell lines (Figure 4-3A). Disruption of TIN2 in a wild-type background led to telomere elongation in agreement with previous reports [153] (Figure 4-3B). The removal of exon 4-7 in heterozygous cells lead to cell lines of two genotypes: hemizygous wild-type or hemizygous mutant (Figure 4-3A). Regardless of whether the wild-type or mutant allele was deleted, we found that TIN2 hemizygous cells elongated telomeres (Figure 4-3B, Supplemental Data Figure 4-3C). This showed that the DC-causing TIN2-T284R mutation was not acting as a dominant negative allele or as a loss of function allele. The elongated telomeres of hemizygous cells showed no signs of increased DNA damage (n=1, preliminary results), leading us to speculate whether this telomere elongation could be used to restore the proliferative capacity of mutant hESCs and thereby alleviate the consequences of the TIN2 DC mutations (Figure 4-3C, Supplemental Data Figure 4-3B). For better efficiency, we developed a TIN2 disruption strategy reliant on a single cut and NHEJ in exon 2 resulting in premature stop codons downstream and thereby disruption of TIN2 expression (Figure 4-3D). We targeted heterozygous mutant hESCs and genotyped using PCR. The disruption of TIN2 in exon 2 of the mutant allele similarly led to telomere elongation. This elongation was sufficient to fully restore the proliferative capacity of the cell line to wild-type levels (Figure 4-3E, Supplemental Data Figure 4-3C).

Discussion

By gene editing the endogenous TIN2-DC cluster region in hESCs we established a model system of DC telomere shortening in telomerase-positive cells capable of differentiation into telomerase-negative cells. In these model systems we could directly compare the effect of the mutations in stem cells with isogenic differentiated cells. Using hESCs we found that the telomere shortening effect of TIN2-DC mutations was telomerase-dependent and affected solely the stem cells, consistent with the model that the effect of the TIN2-DC mutations is affecting solely the role of TIN2 for telomerase recruitment [19]. Additionally, in a longitudinal study we were able to determine that TIN2-DC cells had a drastically reduced proliferative capacity following differentiation. The replicative potential of mutant cells could be restored - together with telomere length - by the disruption of one allele of *TINF2*. Thereby, we showed that combining the hESC model and humanized mouse model is a powerful approach that connects the

mechanistic insights to the consequences for differentiated tissues and highlights the potential targets for therapeutic intervention.

Restoring telomere length in the stem cell compartment could alleviate the downstream consequences of a limited proliferative capacity in the differentiated tissues. Despite the fact that the TIN2-DC mutations are autosomal dominant mutations [55,140] we made the observation that overexpression of the disease mutant did not lead to telomere shortening and was indistinguishable from wild-type overexpression. Other groups have previously reported similar findings that overexpression of TIN2S wild-type and mutant (K280E, R282H, R282S) only led to very subtle but equal shortening in telomere length in HCT75 cancer cells [159]. Similarly, following overexpression of TIN2S wild-type and mutant in HT1080 telomere length remained constant but the overexpression of TIN2L elongated telomeres [161]. Differences between the isoforms, which are hard to address on the endogenous level due to the splicing pattern could be involved in telomere length regulation. While all isoforms stimulate telomerase activity to similar levels [162], differential interaction of the C-terminus of the long isoform with TRF2 could affect telomere length through accessibility [161]. The fact that TIN2-DC mutations are not dominant opens up new avenues for therapeutic intervention. While it had previously been shown that reduction of TIN2 levels could lead to telomere elongation in HT1080 TIN2 wild-type cancer cells [160], we found that hemizygous loss of TIN2 restores telomere length and proliferative capacity even in the TIN2-DC mutant cells. This rescue of the disease phenotype occurred without a significant DNA damage response meaning that telomeres were not deprotected following hemizygous loss of TIN2. Similar results have been reported by Schmutz et al., where heterozygous loss-of-function cancer mutation in TINF2 led to excessively long, but fully protected telomeres.

The tissue, which is most severely affected in its regeneration by the TIN2 DC mutations is the hematopoietic system. To be able to translate the findings of our hESC-based DC model system we aim to establish an *in vivo* model of how the mutations affect hematopoiesis in DC patients. Previously the effects of DC-causing mutations in the hematopoietic system has been achieved by either *in vivo* subcutaneous transplantation of patient bone marrow stromal cells or *in vitro* differentiation of mutant hESCs to human hematopoietic stem cells (HSCs) [163,164]. The former showed defects of patient stromal cells in forming the hematopoiesis-supporting structure *in vivo* but did not show the hematopoietic potential of the cells. The latter showed defects of DC-mutant stem cells in definitive hematopoiesis *in vitro* but did not show the engraftment potential and proliferative capacity *in vivo*. To overcome the limitations of those model systems we propose to establish a humanized mouse model by introducing the disease mutations in normal HSCs and engrafting them. In contrast to patient HSCs, which can only exhibit the late consequences of the short telomere phenotype, editing normal HSCs will enable us to understand how the disease takes its course following the induction of the mutation. In this model system we will track telomere shortening but could also test whether the restoration of telomere length by disruption of TIN2 will provide edited cells with a proliferative advantage *in vivo*.

Figures:

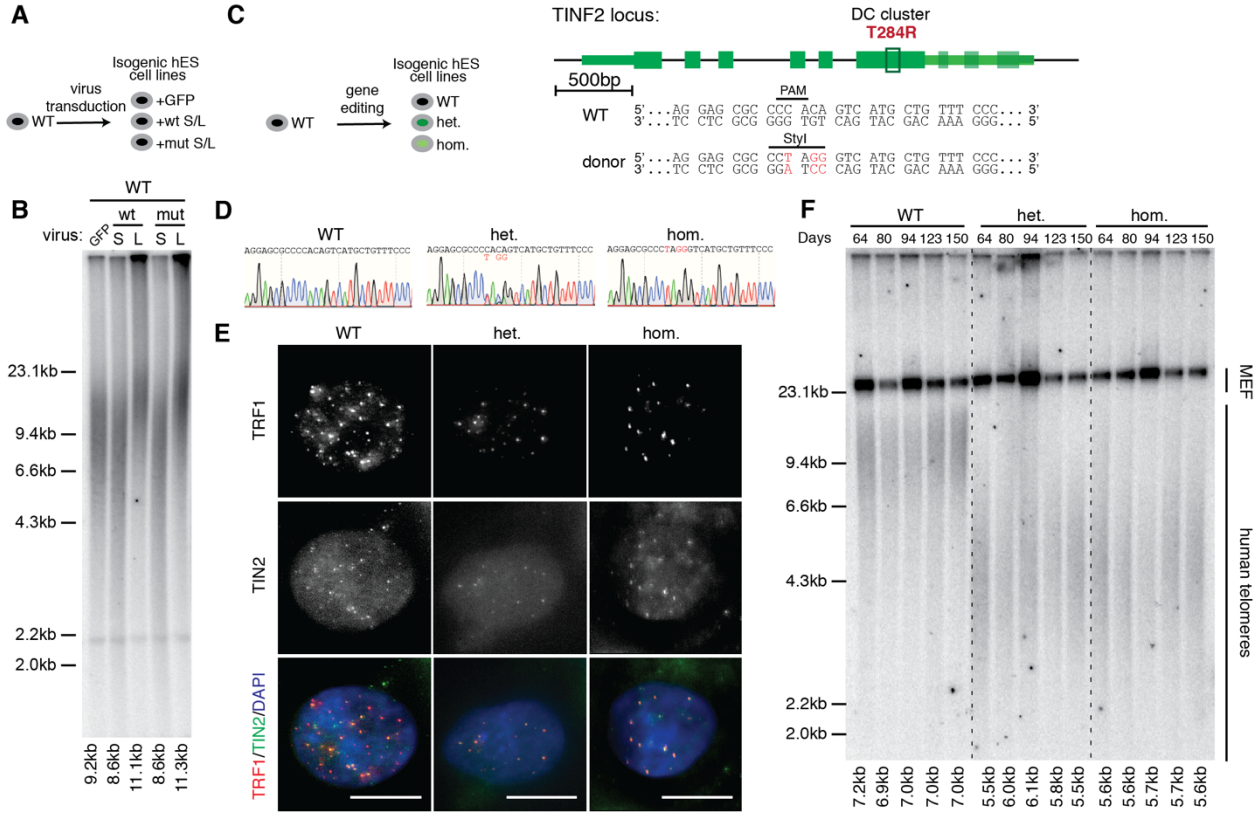


Figure 4-1: Introduction of a TIN2 DC disease mutation at the endogenous TINF2 locus recapitulates the short telomere phenotype observed in patients. *(A) Experimental overview of viral overexpression of wild-type (wt) and TIN2T284R mutant (mut) TIN2 isoforms (short S and long L) in wild-type (WT) hESCs. (B) Telomere length analysis of WT hESCs overexpressing GFP (control), TIN2S1-354 (S) and TIN2L1-451 (L). (C) Experimental overview: Generation of isogenic cell lines by CAS9 mediated double strand break introduction and homologous recombination in presence of mutation containing repair template. Successful targeting results in the ablation of the PAM site and de novo generation of a StyI site. (D) Chromatogram of Sanger sequencing traces of PCR of genomic DNA from wild-type (WT), heterozygous (het T284R) and homozygous (hom T284R/T284R) hESC lines. (E) IF for telomeric binding proteins TRF1 (red) and TIN2 (green) in WT, het and hom hESCs. DNA was stained with 4,6-diamino-2-phenylindole (DAPI; blue). Scalebar: 10μm. (F) Telomere length analysis of WT, heterozygous and homozygous hESCs at indicated timepoints after targeting.*

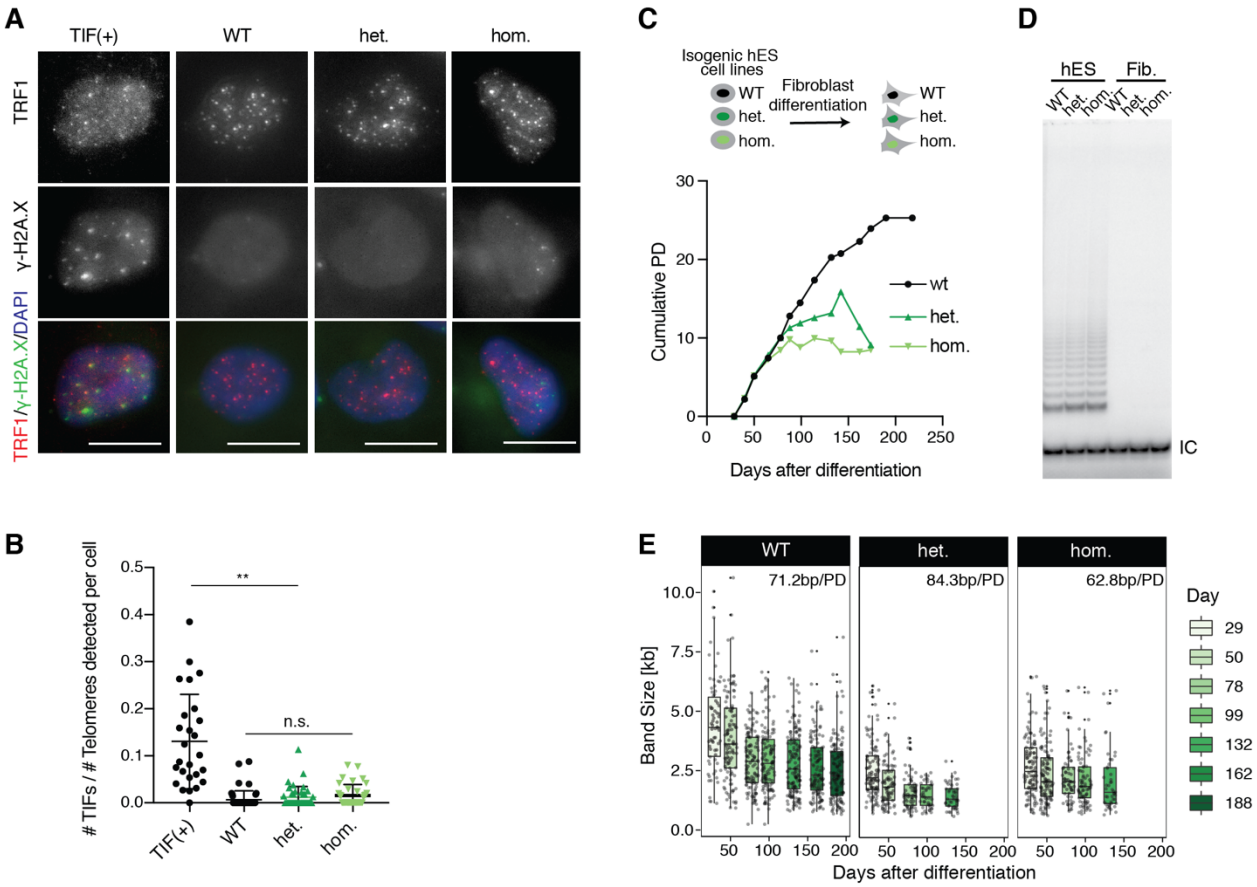


Figure 4-2: Telomeres of DC mutant hESCs were shortened in a telomerase dependent manner leading to a decrease of proliferative capacity. *(A) IF of TRF1 (red) γ-H2A.X (green) of positive control (TIF+, TPP1$^{M87I/-}$ [165]), WT, heterozygous and homozygous hESCs. DNA was stained with DAPI (blue) (Scalebar 10μm). (B) Quantification of TIFs detected per telomeres per cell (n = 1, TIF(+) = 26 cells, WT = 40 cells, het. = 49 cells, hom. = 35 cells). (**) p < 0.05 (Mann-Whitney test) (C) Experimental overview of fibroblast differentiation and growth curves of cumulative population doublings (PDs) over days after differentiation. (D) Telomerase activity assay of the indicated cell lines as hESC or fibroblast 30 days after differentiation. IC: internal control. (E) Quantification of size of TeSLA PCR products (n=8) of fibroblasts at indicated timepoints after differentiation and derived telomere shortening rate in base pairs per PD (bp/PD).*

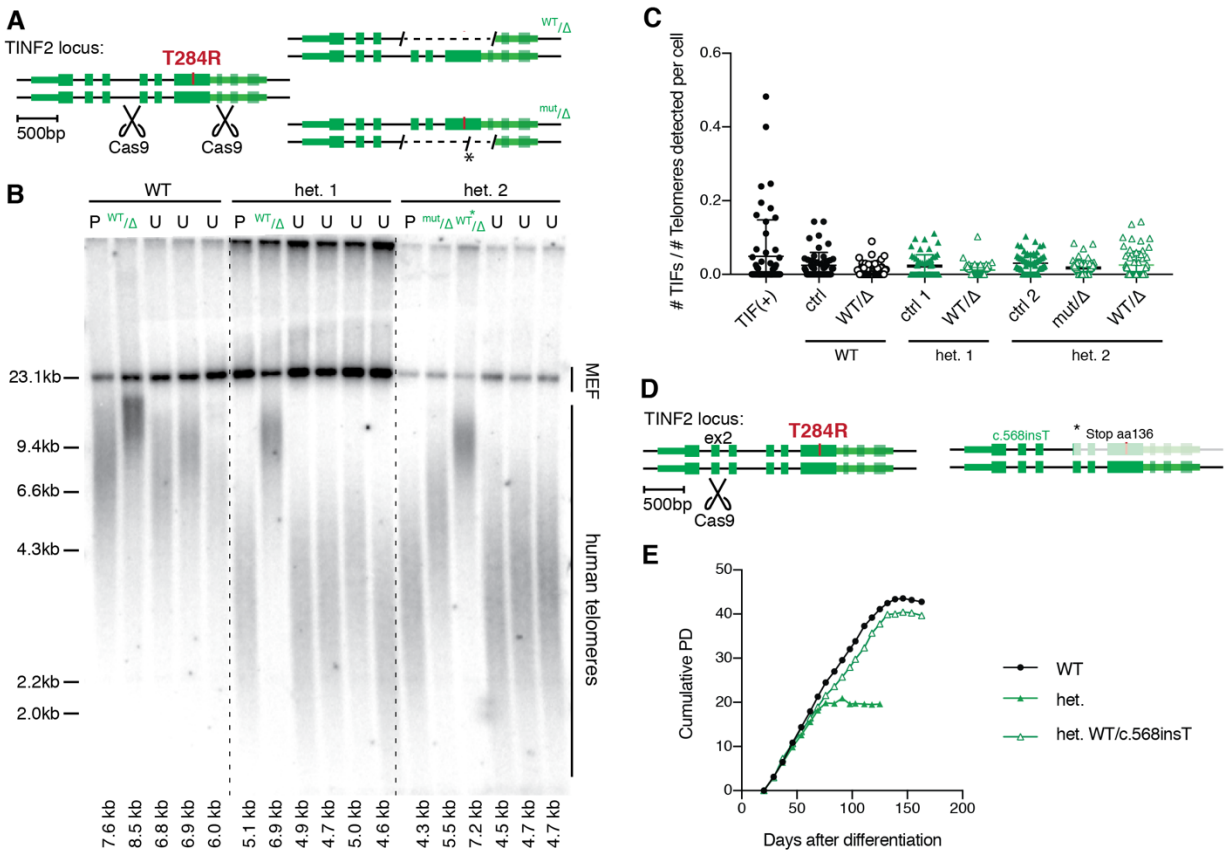
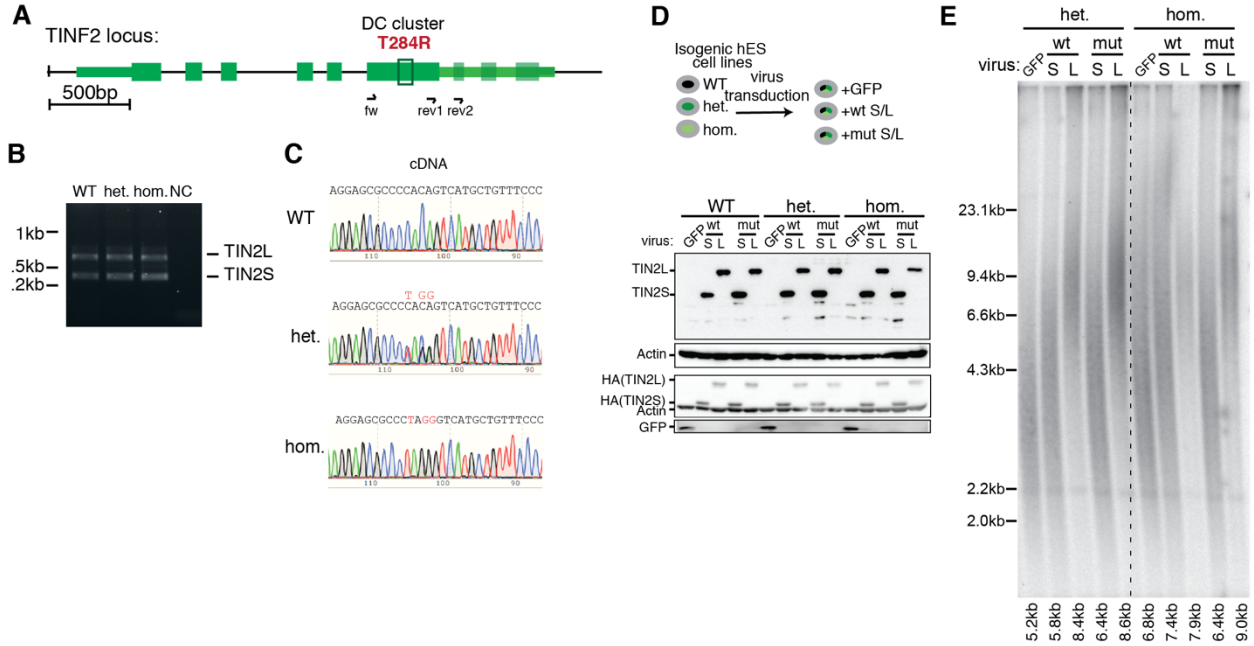
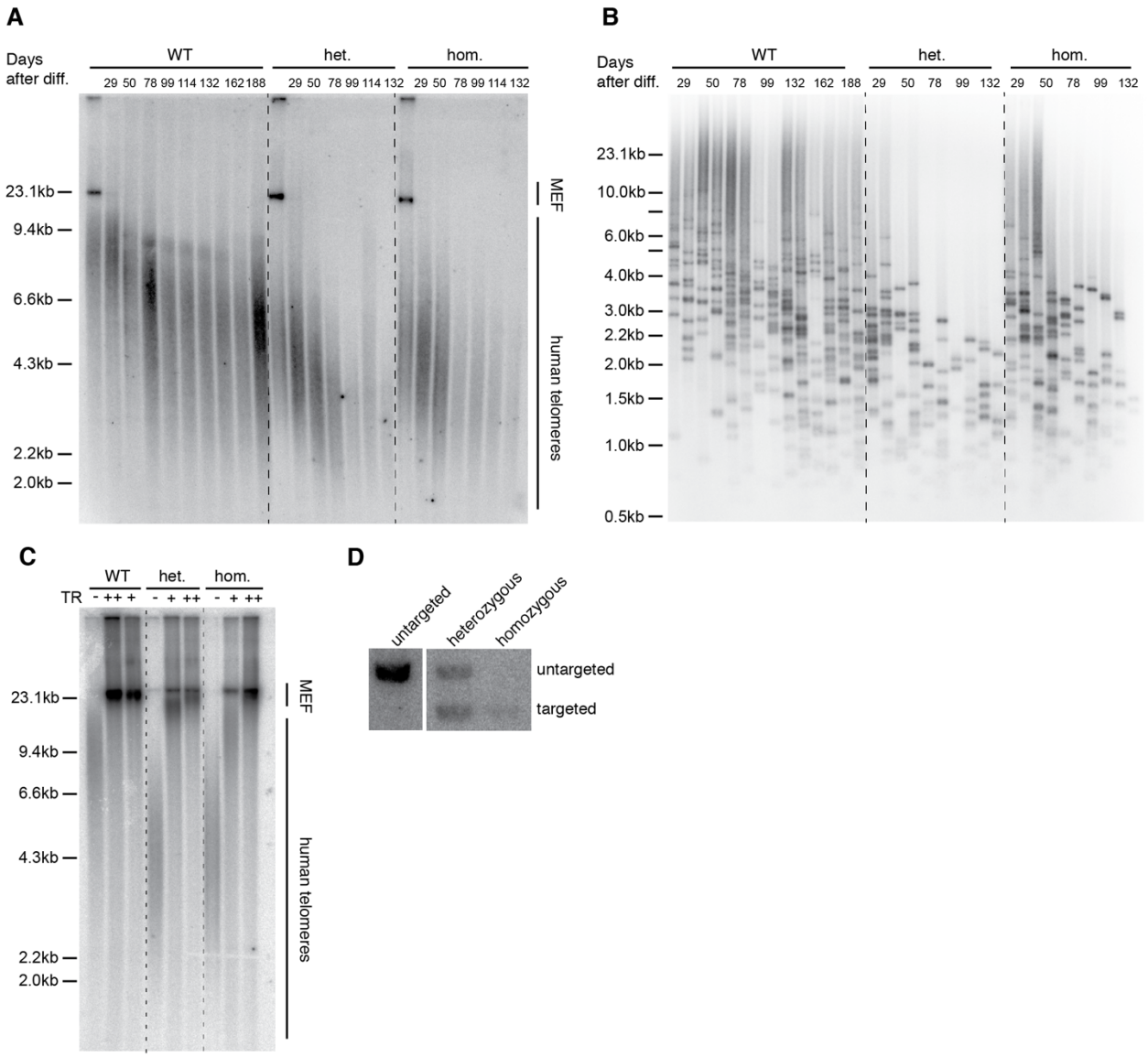


Figure 4-3: Loss of one copy of TIN2 leads to telomere elongation and restores normal proliferative capacity *(A) Schematic overview of the TINF2 locus with Cas9 cut sites in exon 4 and exon 7 for generation of a null allele. Possible outcomes of a heterozygous targeting event are: WT/KO and mut/KO. (B) Telomere length analysis following targeting of wild-type and heterozygous hESCs. Genotype of hemizygous cell lines is marked above each lane. (P = parental cell line, U = untargeted cell line, *incomplete removal of targeted region) (C) Quantification of TIFs/detected telomeres per cell for control and hemizygous cell lines. TIF(+) positive control POT1 ΔPBD. (D) Schematic overview of the TINF2 locus with single Cas9 cut site in exon 2 to disrupt TIN2. (E) Growth curve of cumulative PDs over days after differentiation for wild-type, heterozygous and exon 2 targeted heterozygous cells disrupting the mutant allele.*

Supplemental Figures:

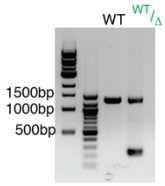


Supplemental Data Figure 4-1: *(A) Overview of TINF2 locus with primer pairs used for amplification of cDNA. (B) PCR products of primer pair fw+rev2 showing bands of different TIN2 isoforms for cDNA of WT, heterozygous and homozygous hESCs. (C) Chromatograms of Sanger Sequencing of PCR product of cDNA of WT, heterozygous and homozygous hESCs using primer pair fw+rev1. (D) Experimental overview of viral overexpression of TIN2 isoforms in WT, het and hom hESCs. Western blot analysis of TIN2 confirming overexpression in all cell lines with actin loading control. (E) Telomere length analysis of hESCs following overexpression of GFP (control), TIN2S$_{1-354}$ (S) and TIN2L$_{1-451}$ (L).*



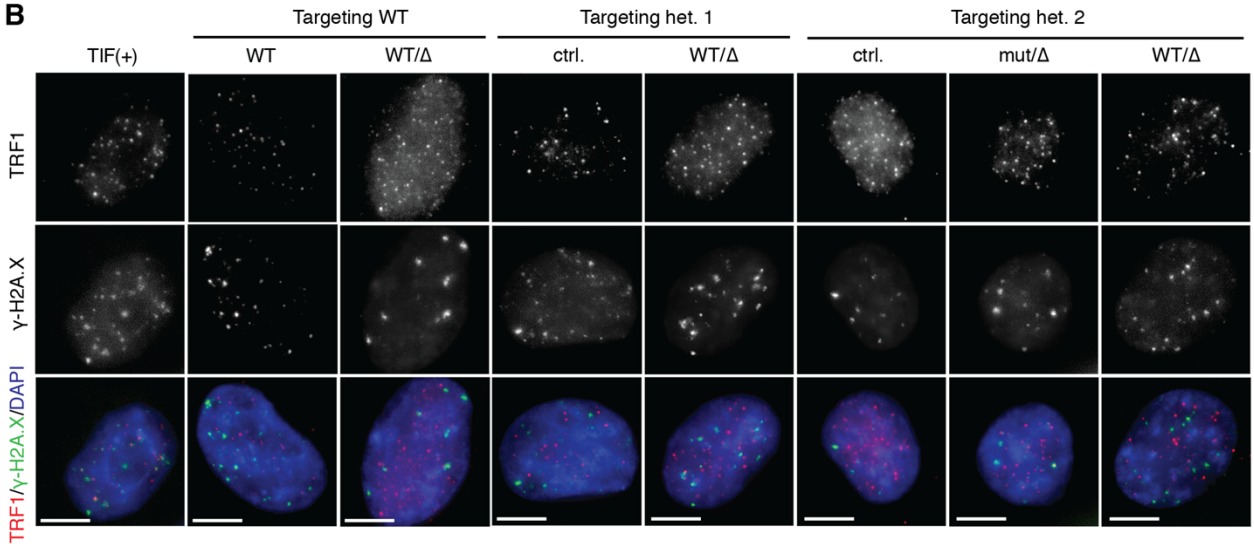
Supplemental Data Figure 4-2: *(A) Telomere length analysis by telomere restriction fragment blot of fibroblasts at indicated timepoints after differentiation. (B) Representative image of telomere length analysis by TeSLA of fibroblasts at indicated timepoint after differentiation, two lanes per timepoint. (C) Telomere length analysis after overexpression of hTR from the AAVS1 locus in wild-type, heterozygous and homozygous hESCs. (- untargeted, + heterozygous insertion, ++ homozygous insertion) (D) Representative Southern Blot of outside probe genotyping untargeted control, heterozygous and homozygous insertion after AAVS1 targeting as described in Hockemeyer et al. 2009 [105].*

A

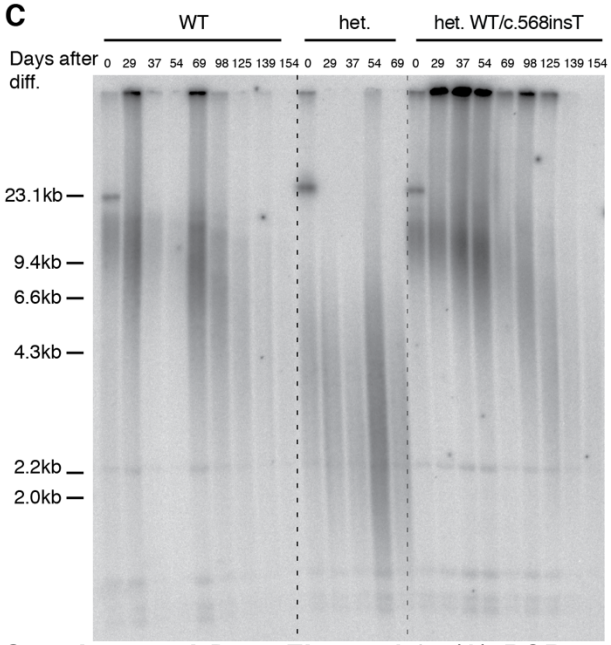


	Genotype	Junction	
Targeting WT	WT/Δ	exon 4 - exon 7	ATCTCCCCTG/AGGTAGTCTG
Targeting het. 1	WT/Δ	exon 4 - exon 7	ATCTCCCCTG/AGGTAGTCTG
Targeting het. 2	mut/Δ	exon 4 - exon 7	ATCTCCCCTG/AGGTAGTCTG
	WT/Δ	exon 4 - exon 6	CTCCCCTGCT/CCTCAGGGAC

B



C



Supplemental Data Figure 4-3: *(A) PCR genotyping strategy used to detect truncated TIN2 alleles. Table with the junctions after targeting in wild-type (WT) and heterozygous (het.) cell lines. (B) Representative IF images of indicated cell lines after targeting for exon 4-7 TIN2 deletion. (C) Telomere length analysis of wild-type (WT), heterozygous (het.) and heterozygous after exon 2 targeting cell lines at indicated time points following differentiation into fibroblasts.*

Material and Methods:

hESC culture and genome editing

Genome editing experiments were performed in WIBR#3 hESCs [103], NIH stem cell registry # 0079. Cell culture was carried out as previously described [104]. All targeting experiments in hESC were performed as previously described [105,106]. CAS9 and all sgRNAs were expressed using the pX330 plasmid [166].

TIN2 T284R Patient mutation editing:

1-2 x 10^7 hESCs were electroporated with 15μg of a CAS9 plasmid that contains a guide sequence (AGGGAAACAGCATGACTGTG), 35μg of a repair plasmid that contains a sequence leading to T284R mutation and a StyI restriction site, and 7.5μg of a GFP plasmid for fluorescence activated cell sorting. Genomic DNA of hES colonies arising from single cells were harvested for genotyping. Targeting was confirmed by PCR followed by restriction digest with StyI of the newly formed restriction site from genomic DNA. fw: CTGAGCCCATGGAACAGAA and rev: TTGTGCCCATGGCTAGGTCT (Expected size 327 bp).

Deletion of exon 4-7 of *TINF2*:

hESCs were co-electroporated with 15μg of two CAS9 plasmids, each containing guide sequences TGTTCAAGTTCCTACAGCAG and CCTGACTCAGACTACCTACC respectively, and 7.5ug of a GFP plasmid. Targeting was confirmed by PCR using the following primers (fw: GGCCACTAACCCACTTTTGA, rev: TGGCCATTTTCTTCCTCATC) and condition (Phusion, annealing temperature 63.4C, 1:15 min extension, expected sizes: 1275 bp WT band, exon 4-7 deletion: 218bp) from genomic DNA.

hTR overexpression:

hTR was overexpressed by targeting the AAVS1 locus of hESCs using neomycin selection as previously described[26] (Chiba et al. 2015).

Disruption of exon 2 of *TINF2*:

hESCs were co-electroporated with 15μg of a CAS9 plasmid containing guide sequence TCAGGACTTGGGCCCAAGGC and 7.5μg of a GFP plasmid. Targeting of exon 2 was confirmed by PCR (fw: GTAGGACCTGGAAGGGGAAA, rev: GATCCCGCACTATAGGTCCA) from genomic DNA. Allele specific genotyping was performed by cloning a long genomic DNA PCR product into PCR2.1 using NotI, HindIII: fw: GTAGGACCTGGAAGGGGAAA rev: GCAAGTCAACTGGGTTCTCC

Differentiation to fibroblast-like cells and growth curve

Fibroblast-like cells were derived from embryonic bodies (EBs). To form EBs hESC colonies were grown on petri dishes in fibroblast medium (DMEM [Lifetech]) supplemented with 15% FBessence [VWR], 1 mM glutamine [Lifetech], 1% non-essential

amino acids [Lifetech], and penicillin/streptomycin [Lifetech]). After 9 days EBs were transferred to tissue culture dishes to attach for 6 days. Fibroblast-like cells were passaged with Trypsin EDTA ([Lifetech], 0.25%), triturated into a single-cell suspension and plated on tissue culture dishes. Cells were trypsinized, counted and plated at a density of 500,000 cells per 10 cm dish. Medium was changed every 3-4 days and cells were passaged every 5-8 days. Growth curves are presented by plotting cumulative population doublings (PDs) against days after differentiation. All data analysis shown is in reference to the time after differentiation.

Generation of cDNA overexpression cell lines and viral infections

For TIN2 cDNA overexpression, the expressing vector along with lentiviral packaging vectors Delta-VPR and CMV-VSV-G were transfected into HEK293FT cells using calcium phosphate. The virus-containing supernatant was collected 48 and 72h post transfection and passed through a 0.45mm filter to eliminate cells. Target cells were plated in 6 well plates in mTesr media [Stemcell technologies] containing 2 μg/mL polybrene and ROCK inhibitor Y-27632 [Chemdea, 3.2 μg/mL]. After infection, the virus was removed, and cells were selected with puromycin on resistant DR4 feeder cells[167] (Tucker 1997). Cells were validated for protein expression via immunoblotting.

cDNA expression analysis

RNA was extracted with TRIzol [Lifetech] and treated with DNaseI [NEB]. 600 ng RNA were converted to cDNA with the qScript Reverse Transcriptase [Quantabio] and random and poly(A) priming. 2 μl cDNA from the qScript reaction mixture was used for the detection of the TIN2 transcripts. PCR with Phusion Polymerase [NEB], GC Buffer.

Primers for detecting all isoforms: fw: CTAGCTGGCCGACACTTCAA rev: CACAGAGACGGAGGACACAC

Primers for detecting mutant/wt allele expression: fw: GGACCATCTTCAAGGACGCA rev: CATGGCTAGGTCTGCTGTGT

Telomeric repeat amplification protocol

PCR-based telomeric repeat amplification protocol (TRAP) was performed as previously described using TS (AATCCGTCGAGCAGAGTT) and ACX (GCGCGGCTTACCCTTACCCTTACCCTAACC) for amplification of telomeric repeats and TSNT (AATCCGTCGAGCAGAGTTAAAAGGCCGAGAAGCGAT) and NT (ATCGCTTCTCGGCCTTTT) as an internal control (*22*). Cell extract was generated using hypotonic Lysis buffer (HLB) (20 mM HEPES, 2 mM $MgCl_2$, 0.2 mM EGTA, 10% Glycerol, 1 mM DTT, 0.1 mM PMSF) supplemented with 0.5% CHAPS and samples were normalized using the Bradford assay (BioRad). 200 ng of total protein were used for detection of fibroblasts telomerase activity. For hESCs and cancer cell lines, a series of diluted lysate, 200, 40 and 8 ng were used. Throughout the figures, the same hESCs WT lysate was used as a standard. The TRAP products were resolved on 10% polyacrylamide /1xTAE gel. Dried gels were visualized by phosphor imaging.

Immunofluorescence staining/TIF analysis

hESCs were seeded on Matrigel covered coverslips one day prior to fixation by 2% paraformaldehyde in PBS followed by PBS washes. The fixed cells were permeabilized by 0.1% Triton x-100 in PBS and blocked in 3% v/v horse serum, 1mg/ml BSA, and 1mM EDTA in PBS. Fixed cells were incubated in primary antibodies (TRF1 raised in rabbit against amino acid residues 17-41 [Chinapeptide], γ-H2AX [Millipore 05-636], TIN2 [Novus 59B288.1]) diluted in the blocking solution followed by PBS washes and incubated in diluted secondary antibodies [Donkey anti-Rabbit A-21206 and Goat ani-Mouse A21235 ThermoFisher Scientific]. Coverslips were stained with DAPI and mounted using ProLong Gold Antifade Mountant [ThermoFisher Scientific].

Z-stack images of the samples were taken using Nikon Eclipse TE2000-E Widefield EpiFluorescence microscope with ANDOR Zyla sCMOS camera. TIFs were scored blindly from the maximum projection images by detecting colocalization of TRF1 and γH2Ax using an ImageJ plugin ComDet v0.3.7 (Cell Biology Group of Utrecht University).

Immunoblotting

Protein samples were extracted in RIPA buffer. After heating to 95 °C for 5 min they were resolved by SDS-PAGE. The protein was then transferred to PVDF membrane and subsequently incubated with the indicated antibodies diluted in 5% milk in TBST. Antibodies used are the following: TIN2 [custom-made antibody raised against peptide sequence CVRDPKATKQDLRKIL-NH2, Chinapeptide], HA [Thermo Fisher Scientific 32-6700], Actin [Abcam 8226]. After washing with TBST, the membrane was visualized using ECL [Bio-Rad 1705061].

Detection of telomere length

Genomic DNA was extracted using phenol chloroform following overnight Proteinase K digestion (0.25mg/mL) and resuspended in TE buffer. Genomic DNA was digested with MboI, AluI and RNaseA overnight at 37 °C. The resulting DNA was normalized and 2µg of DNA was run on 0.75% agarose [Seakem ME Agarose, Lonza], dried under vacuum for 2hr at 50 °C, denatured in 0.5M NaOH, 1.5M NaCl for 30 min, shaking at 25°C, neutralized with 1M Tris pH6.0, 2.5M NaCl shaking at 25 °C, 2x for 15 min. Then the gel was pre-hybridized in Church's buffer (1% BSA, 1mM EDTA, 0.5M $NaP0_4$ pH7.2, 7% SDS) for 1hr at 55 °C before adding a ^{32}P-end-labeled $(T_2AG_3)_3$ telomeric probe. The gel was washed 3x 30min in 4x SSC at 50°C and 1x 30 min in 4x SSC + 0.1% SDS at 25°C before exposing on a phosphorimager screen.

TeSLA (Telomere shortest length assay)

TeSLA was performed as described previously with slight modifications [168]. Briefly, genomic DNA was extracted using phenol chloroform following overnight proteinase K digestion (0.25mg/mL). Purified DNA was resolved in TE buffer and quantified. 50ng of isolated genomic DNA were used per sample for the ligation reaction.

Then DNA was diluted to insert 40pg per PCR reaction. 8 PCR reactions were run out per sample and quantified. PCRs were run on 0.75% Agarose gels as described for telomere length analysis by telomere restriction fragment assay and detected by in-gel hybridization with a ^{32}P-end-labeled $(T_2AG_3)_3$ telomeric probe. Quantification of the blots was performed using the Matlab plugin provided in the original publication [168].

Chapter 5: Discussion and future directions

Portions of this chapter were published as “Lorbeer FK, Hockemeyer D: TERT promoter mutations and telomeres during tumorigenesis. *Curr Opin Genet Dev* 2020, **60**:56–62.” [1]. It has been reproduced here in part with full permission of the authors.

Summary

Advances in high-throughput telomere length measurement methods and the expansion of possibilities for genome-wide genotyping have helped identify a large number of genetic variants associated with disease and telomere length. The current challenge remains to gain a mechanistic understanding of the connections between disease phenotypes, genetics, and telomere length in order to be able to develop therapeutic strategies. The study of specific mutations in an isogenic hESC model system with physiological regulation of telomerase and telomere length has allowed us to contrast the initial effects of mutations on telomere length homeostasis and integrity and model disease progression longitudinally.

Our study of TPMs and their effects on immortality and telomere length give insights into how long telomeres can be promoting cancer risk, but telomerase expressing TPM tumors have extremely short telomeres. In dysplastic nevi, the precursor stage of melanoma, we confirmed our hypothesis that TPMs are selected for when telomeres become short and telomere shortening acts as a tumor suppressor mechanism during melanoma formation. Moving from cancer to the short telomere disease, DC, our study of a TIN2-DC mutant highlights the importance of identifying in which cell type the mutations initially affect telomere length. Our study also provides an experimental approach for identifying therapeutic strategies aimed at alleviating the adverse effects of the disease mutations. The congruency with/differences to other studies, as well as possibilities for intervention in both diseases will be discussed below.

Why do cancer cells with TPMs generally have short telomeres and what are the implications?

Despite elevated *TERT* expression, TPM cancers have short telomeres compared to matched healthy controls. Sequencing-derived length estimates show that telomeres were shorter in TPM samples compared to matched normal samples in glioma [92], clear cell renal cell carcinoma [169], and melanoma [44]. In the aforementioned TCGA cancer sequencing data of 31 cancer types, telomere length estimates of TPM tumors were lower than those of matched wild-type control samples for almost all analyzed cancer types [48]. The short telomeres of TPM cancers could suggest that TPMs are a late event of tumorigenesis, when telomeres are exhausted. However, TPMs occur during the early stages of tumorigenesis in glioma, hepatocellular carcinoma, and melanoma.

In glioblastoma TPMs are potentially even the earliest genetic event of cancer formation. A comparison of samples from the tumor-free subventricular zone (SVZ), the tumor, as well as matching normal tissue found that the non-tumorous SVZ samples already harbor TPMs and could be the site of origin of the cancer [119]. Similarly, TPMs

were shown to be the most frequent somatic genetic alteration in HCC and also the first recurrent gene somatically mutated in preneoplastic cirrhotic lesions [170]. Multi-region sequencing of multiple regenerative nodules (cancer precursor) and tumor samples from several patients further showed that TPMs are the initial and essential step for HCC carcinogenesis, as their frequency increased with the stepwise progression from dysplastic nodule to carcinoma [171,172].

In cutaneous melanoma, TPMs are found frequently (~70% of all cases [45]). For these cancers, samples from matched precancerous lesions as well as tumors have been analyzed for genetic aberrations and telomere length. Here, based on allele frequency, TPMs are among the earliest events of tumor formation and occur before the critical bi-allelic cell-cycle checkpoint inactivation [91,120]. Measurements of relative telomere length by quantitative telomere FISH of patient samples with known genetic history, showed that telomeres shortened in patient samples even after acquisition of TPMs [88]. Why then are telomeres short, if TPMs are acquired at a time when telomeres are expected to still be long?

We resolved this conundrum by employing an hESC model comparing isogenic TPM-harboring and wild-type hESCs following differentiation (Chapter 2). When differentiated into fibroblasts, wild-type hESCs become telomerase-negative. In a comparison of differentiated wild-type and mutant cells into fibroblasts, the presence of TPMs did – similar to the wild-type – not prohibit telomere shortening, matching the patient data. Analysis of *TERT* expression dynamics showed that the transcriptional upregulation of *TERT* was gradual and only occurred when critically short telomeres were accumulating [88]. Therefore, immortalization of precancerous cells by TPMs can be described as a two-step process, in which during the first phase of tumorigenesis, TPMs can be acquired but do not prohibit telomere shortening and are not intrinsically cancerous. In the second phase, TPMs convey a selective advantage, potentially only when all telomeres have become critically short (Figure 2-4). In the classic crisis model telomeres become critically short following the inactivation of the DNA damage response and cells can emerge from this state by acquiring a mechanism to stabilize telomeres [94]. The early occurrence of TPMs before the loss of checkpoint genes in melanoma, glioblastoma and HCC, as well as the gradual upregulation of telomerase expression challenge the idea of immortalization of TPM cancers by emergence of cells from a “classic” crisis.

TERT promoter mutations in precursor lesions

With this re-thinking of the “classic” crisis model, it remained an open question when during tumorigenesis TPMs are selected for and when/if telomere shortening plays a major role in tumor suppression. By assessing TPM status and telomere length in dysplastic nevi, the precursor stage of melanoma, we found that TPMs were already detectable and that dysplastic melanocytes with TPMs had shorter telomeres than those without TPMs (Chapter 3). The fact that telomeres in TPM-positive nevi were relatively shorter than those in wild-type nevi, provide evidence that telomere shortening acts as a

tumor suppressor mechanism in nevi and that melanocytes often depend on TPMs to overcome replicative senescence. Further evidence that telomere shortening in nevi indeed contributes to tumor suppression comes from associative studies of telomere length and nevus count: higher nevus numbers have been linked to longer telomeres [173] and an increased nevus count is an established risk factor for melanoma development [174]. In agreement with the results from our previous study (Chapter 2), longer telomeres would not only allow melanocytes to undergo more cell divisions but also allow for the sufficient upregulation of telomerase expression. One possible mechanism could be that *TERT* expression from the mutant promoter is further enhanced by active mitogen-activated protein (MAP) kinase signaling, which is widely active in dysplastic nevi due to additional presence of a driver mutation. This mechanism is mediated by the upregulation of different ETS factors such as GABP [175] as well as ETV1, ETV4 and ETV5, which have all been shown to bind the mutant *TERT* promoter [176].

Molecular mechanisms of the mutant TERT promoter and ETS factor binding: An unresolved issue

To date, as TPMs are unique in their high prevalence as non-coding mutations and early occurrence across cancer types, there has been a chase for the molecular mechanism of ETS-binding to the mutant TERT promoter as a potentially attractive drug target. GABPα was the first ETS factor identified binding to the TPM [101] and was independently validated in a study showing that TPMs lead to monoallelic expression of the mutant allele, with allele-specific changes in active histone marks upon GABPα depletion [177,178]. GABPα enhanced expression of TERT by mediating long-range interactions of the mutant *TERT* promoter. Upon GABPα silencing, these interactions as well as the active histone marks found in the promoter decreased [179]. However, our model system using hESCs lacking the endogenous cooperative ETS binding sites required for tetramerization showed that cells with TPMs still had higher TERT levels when other ETS sites were missing. This provides additional evidence that even without the GABPα/β tetramerization on the mutant *TERT* promoter ETS factor binding could stimulate TERT expression [88].

Subsequent experiments found that the formation of the GABPα/β tetramer on the mutant *TERT* promoter specifically required the GABPβ1L isoform [180]. The disruption of GABPβ1L initially resulted in telomere shortening and cell death in cancer cells with TPMs. Cells depleted of the GABPβ1L isoform eventually continued to proliferate both *in vitro* and in *in vivo* xenografts again suggesting redundancy in ETS factor binding to the mutant *TERT* promoter. Different studies have provided further evidence that other ETS factors can bind the mutant *TERT* promoter and drive expression: Glioma cell line experiments found that the -124C/T and -146C/T TPM to not be functionally identical. The -146C/T mutation was bound cooperatively by ETS1/2 and p52, thereby stimulating TERT expression via non-canonical NFκB signaling [181]. Similarly, in thyroid cancer the ETS factor ETV5 can bind and activate TPMs [182]. An ATAC-Seq chromatin assay confirmed

heterozygosity and differential accessibility of the mutated allele in a TCGA data set of 23 different cancer types. Motif analysis of the ATAC-Seq peaks yielded the ETS family members ELF1 or ELF2 as binding factors of the *de novo* binding site [183]. In nuclear extracts from melanoma cell lines ELF1 can bind the mutant promoter as detected by mass-spectrometry. In *in vitro* binding assays ELF1 also bound the mutant *TERT* promoter but competed for binding with the higher affinity GABPα/β tetramer on the endogenous ETS binding sites [184]. Taken together, these studies suggest that the ubiquitously expressed GABPα/β plays a role for expression from the mutant promoter, but other ETS factors compete for binding and consequently can also drive TERT expression from the mutant promoter.

Targetability and therapeutic relevance of TPMs: Short telomeres as a vulnerability

While the redundancy of ETS factor binding and the inherent difficulty of targeting a non-coding mutation remain an unresolved challenge in targeting TPMs therapeutically, telomerase inhibition has long been explored as a therapeutic strategy to interfere with telomere elongation and immortalization in cancer cells (reviewed in [185]). Most of the clinical evaluation for TERT inhibition performed to date preceded the discovery of TPMs. This is important to note, as the outcome of an early clinical trial of the telomerase inhibitor, Imetelstat, revealed a trend towards an improvement in median progression-free survival and overall survival of patients with shorter telomeres compared to patients with long or medium average telomere length [186]. The finding that cancer cells with TPMs generally have very short telomeres and proliferate for an extended period of time with marginal telomerase levels [88] raises the intriguing possibility that telomerase inhibition will be an effective intervention in cells with TPMs. Therefore, revisiting telomerase inhibition as a cancer intervention should be revisited.

Acutely, it seems important to revisit the therapeutic potential of chemical inhibition of telomerase activity in cancer cells with TPMs. It will be critical to study the shortening dynamics and TERT expression throughout tumorigenesis for each cancer type in a time-resolved manner in order to successfully exploit TPMs as a potential therapeutic target. Knowing when during tumorigenesis *TERT* promoter mutant cells outgrow non-mutant cells will aide finding a therapeutic window when cells are most vulnerable for such telomerase inhibition. Combining whole genome sequencing data and information on telomere length from different stages of cancer development will provide the guidance necessary for finding prognostic markers and more effective treatments.

Long telomeres? Short telomeres?

Long telomeres pre-dispose for cancer formation. Shortening telomeres in combination with telomerase inhibition could be an Achilles heel of developing cancers. Once malignancy is reached, long telomeres and a high nevus count, which is also associated with long telomeres, are of favorable prognostic value for melanoma survival [187,188]. The seemingly contradictory effects of telomere length and telomere maintenance, have on the disease can be reconciled by taking into account the telomerase status and the stage of disease progression in the affected cell: In telomerase-

negative cells long telomeres extend the cellular lifespan until replicative senescence, which increases the risk of transformation. Once replicative senescence is overcome, e.g. by TPM-mediated *TERT* expression, relatively longer telomeres become potentially beneficial by protecting telomeres from fusions [99].

Similarly, DC patients, who have extremely short constitutional telomeres, suffer from an increased cancer risk. It is assumed that the increased risk of cancer formation in DC patients is driven by the extended proliferation of telomerase-positive cells with extremely short telomeres, which fuels genomic instability and drives cancer formation [96,100]. In blood cells of some DC patients, with mutations in the coding region of *TERT*, TPMs were found on the wild-type allele of *TERT.* These TPMs likely act as a compensatory mechanism, resulting in higher telomerase expression and thereby telomere protection, without resulting in cancer [189].

We find that generating a TIN2-DC mutation in hESCs led to telomere shortening without deprotection of telomeres in hESCs and resulted in a marked decrease in the proliferative capacity of telomerase-negative daughter cells. In light of the increased risk of cancer formation by long telomeres, the challenge of envisioning a treatment for DC, is to find a way to increase telomere length in the stem cell compartment specifically. Such a stem cell therapy would restore the replicative potential for regeneration without increasing the risk of cancer formation in telomerase-negative tissues.

References

1. Lorbeer FK, Hockemeyer D: **TERT promoter mutations and telomeres during tumorigenesis**. *Curr Opin Genet Dev* 2020, **60**:56–62.

2. de Lange T: **How Telomeres Solve the End-Protection Problem**. *Science* 2009, **326**:948.

3. Karlseder J, Broccoli D, Dai Y, Hardy S, de Lange T: **p53- and ATM-dependent apoptosis induced by telomeres lacking TRF2**. *Science* 1999, **283**:1321–1325.

4. Takai H, Smogorzewska A, Lange T de: **DNA Damage Foci at Dysfunctional Telomeres**. *Curr Biol* 2003, **13**:1549–1556.

5. Greider CW, Blackburn EH: **Identification of a specific telomere terminal transferase activity in Tetrahymena extracts**. *Cell* 1985, **43**:405–413.

6. Hayflick L, Moorhead PS: **The serial cultivation of human diploid cell strains**. *Exp Cell Res* 1961, **25**:585–621.

7. Steinert S, Shay JW, Wright WE: **Transient Expression of Human Telomerase Extends the Life Span of Normal Human Fibroblasts**. *Biochem Biophys Res Commun* 2000, **273**:1095–1098.

8. Vaziri H, Benchimol S: **Reconstitution of telomerase activity in normal human cells leads to elongation of telomeres and extended replicative life span**. *Curr Biol CB* 1998, **8**:279–282.

9. Bodnar AG, Ouellette M, Frolkis M, Holt SE, Chiu CP, Morin GB, Harley CB, Shay JW, Lichtsteiner S, Wright WE: **Extension of life-span by introduction of telomerase into normal human cells**. *Science* 1998, **279**:349–352.

10. Ouellette MM, Liao M, Herbert BS, Johnson M, Holt SE, Liss HS, Shay JW, Wright WE: **Subsenescent telomere lengths in fibroblasts immortalized by limiting amounts of telomerase**. *J Biol Chem* 2000, **275**:10072–10076.

11. Jiang XR, Jimenez G, Chang E, Frolkis M, Kusler B, Sage M, Beeche M, Bodnar AG, Wahl GM, Tlsty TD, et al.: **Telomerase expression in human somatic cells does not induce changes associated with a transformed phenotype**. *Nat Genet* 1999, **21**:111–114.

12. Hockemeyer D, Collins K: **Control of telomerase action at human telomeres**. *Nat Struct Mol Biol* 2015, **22**:848–852.

13. Kabir S, Hockemeyer D, de Lange T: **TALEN gene knockouts reveal no requirement for the conserved human shelterin protein Rap1 in telomere protection and length regulation**. *Cell Rep* 2014, **9**:1273–1280.

14. van Steensel B, de Lange T: **Control of telomere length by the human telomeric protein TRF1**. *Nature* 1997, **385**:740–743.

15. Smogorzewska A, van Steensel B, Bianchi A, Oelmann S, Schaefer MR, Schnapp G, de Lange T: **Control of human telomere length by TRF1 and TRF2**. *Mol Cell Biol* 2000, **20**:1659–1668.

16. Loayza D, de Lange T: **POT1 as a terminal transducer of TRF1 telomere length control**. *Nature* 2003, **423**:1013–1018.

17. Sexton AN, Regalado SG, Lai CS, Cost GJ, O'Neil CM, Urnov FD, Gregory PD, Jaenisch R, Collins K, Hockemeyer D: **Genetic and molecular identification of three human TPP1 functions in telomerase action: recruitment, activation, and homeostasis set point regulation**. *Genes Dev* 2014, **28**:1885–1899.

18. Nandakumar J, Bell CF, Weidenfeld I, Zaug AJ, Leinwand LA, Cech TR: **The TEL patch of telomere protein TPP1 mediates telomerase recruitment and processivity**. *Nature* 2012, **492**:285–289.

19. Frank AK, Tran DC, Qu RW, Stohr BA, Segal DJ, Xu L: **The Shelterin TIN2 Subunit Mediates Recruitment of Telomerase to Telomeres**. *PLOS Genet* 2015, **11**:e1005410.

20. Chen L-Y, Redon S, Lingner J: **The human CST complex is a terminator of telomerase activity**. *Nature* 2012, **488**:540–544.

21. Touzot F, Callebaut I, Soulier J, Gaillard L, Azerrad C, Durandy A, Fischer A, Villartay J-P de, Revy P: **Function of Apollo (SNM1B) at telomere highlighted by a splice variant identified in a patient with Hoyeraal–Hreidarsson syndrome**. *Proc Natl Acad Sci* 2010, **107**:10097–10102.

22. Wright WE, Piatyszek MA, Rainey WE, Byrd W, Shay JW: **Telomerase activity in human germline and embryonic tissues and cells**. *Dev Genet* 1996, **18**:173–179.

23. Yui J, Chiu CP, Lansdorp PM: **Telomerase activity in candidate stem cells from fetal liver and adult bone marrow**. *Blood* 1998, **91**:3255–3262.

24. Chiu C-P, Dragowska W, Kim NW, Vaziri H, Yui J, Thomas TE, Harley CB, Lansdorp PM: **Differential Expression of Telomerase Activity in Hematopoietic Progenitors from Adult Human Bone Marrow**. *STEM CELLS* 1996, **14**:239–248.

25. Cristofari G, Lingner J: **Telomere length homeostasis requires that telomerase levels are limiting**. *EMBO J* 2006, **25**:565–574.

26. Chiba K, Johnson JZ, Vogan JM, Wagner T, Boyle JM, Hockemeyer D: **Cancer-associated TERT promoter mutations abrogate telomerase silencing**. *eLife* 2015, **4**:e07918.

27. Weinrich SL, Pruzan R, Ma L, Ouellette M, Tesmer VM, Holt SE, Bodnar AG, Lichtsteiner S, Kim NW, Trager JB, et al.: **Reconstitution of human telomerase with the template RNA component hTR and the catalytic protein subunit hTRT**. *Nat Genet* 1997, **17**:498–502.

28. Avilion AA, Piatyszek MA, Gupta J, Shay JW, Bacchetti S, Greider CW: **Human Telomerase RNA and Telomerase Activity in Immortal Cell Lines and Tumor Tissues**. *Cancer Res* 1996, **56**:645–650.

29. Yi X, Shay JW, Wright WE: **Quantitation of telomerase components and hTERT mRNA splicing patterns in immortal human cells**. *Nucleic Acids Res* 2001, **29**:4818–4825.

30. Khattar E, Tergaonkar V: **Transcriptional Regulation of Telomerase Reverse Transcriptase (TERT) by MYC**. *Front Cell Dev Biol* 2017, **5**.

31. Lin S-Y, Elledge SJ: **Multiple Tumor Suppressor Pathways Negatively Regulate Telomerase**. *Cell* 2003, **113**:881–889.

32. Günes C, Rudolph KL: **The Role of Telomeres in Stem Cells and Cancer**. *Cell* 2013, **152**:390–393.

33. Kim NW, Piatyszek MA, Prowse KR, Harley CB, West MD, Ho PL, Coviello GM, Wright WE, Weinrich SL, Shay JW: **Specific association of human telomerase activity with immortal cells and cancer**. *Science* 1994, **266**:2011–2015.

34. Horikawa I, Barrett JC: **cis-Activation of the Human Telomerase Gene (hTERT) by the Hepatitis B Virus Genome**. *JNCI J Natl Cancer Inst* 2001, **93**:1171–1173.

35. Sung W-K, Zheng H, Li S, Chen R, Liu X, Li Y, Lee NP, Lee WH, Ariyaratne PN, Tennakoon C, et al.: **Genome-wide survey of recurrent HBV integration in hepatocellular carcinoma**. *Nat Genet* 2012, **44**:765–769.

36. Peifer M, Hertwig F, Roels F, Dreidax D, Gartlgruber M, Menon R, Krämer A, Roncaioli JL, Sand F, Heuckmann JM, et al.: **Telomerase activation by genomic rearrangements in high-risk neuroblastoma**. *Nature* 2015, **526**:700–704.

37. Valentijn LJ, Koster J, Zwijnenburg DA, Hasselt NE, van Sluis P, Volckmann R, van Noesel MM, George RE, Tytgat GAM, Molenaar JJ, et al.: ***TERT* rearrangements are frequent in neuroblastoma and identify aggressive tumors**. *Nat Genet* 2015, **47**:1411–1414.

38. Zhao Y, Wang S, Popova EY, Grigoryev SA, Zhu J: **Rearrangement of Upstream Sequences of the hTERT Gene During Cellular Immortalization**. *Genes Chromosomes Cancer* 2009, **48**:963–974.

39. Horn S, Figl A, Rachakonda PS, Fischer C, Sucker A, Gast A, Kadel S, Moll I, Nagore E, Hemminki K, et al.: **TERT Promoter Mutations in Familial and Sporadic Melanoma**. *Science* 2013, **339**:959–961.

40. Huang FW, Hodis E, Xu MJ, Kryukov GV, Chin L, Garraway LA: **Highly Recurrent TERT Promoter Mutations in Human Melanoma**. *Science* 2013, **339**:957–959.

41. Griewank KG, Murali R, Schilling B, Schimming T, Möller I, Moll I, Schwamborn M, Sucker A, Zimmer L, Schadendorf D, et al.: **TERT Promoter Mutations Are Frequent in Cutaneous Basal Cell Carcinoma and Squamous Cell Carcinoma**. *PLOS ONE* 2013, **8**:e80354.

42. Heidenreich B, Nagore E, Rachakonda PS, Garcia-Casado Z, Requena C, Traves V, Becker J, Soufir N, Hemminki K, Kumar R: **Telomerase reverse transcriptase promoter mutations in primary cutaneous melanoma**. *Nat Commun* 2014, **5**.

43. Huang FW, Hodis E, Xu MJ, Kryukov GV, Chin L, Garraway LA: **Highly Recurrent TERT Promoter Mutations in Human Melanoma**. *Science* 2013, **339**:957–959.

44. Hayward NK, Wilmott JS, Waddell N, Johansson PA, Field MA, Nones K, Patch A-M, Kakavand H, Alexandrov LB, Burke H, et al.: **Whole-genome landscapes of major melanoma subtypes**. *Nature* 2017, **545**:175–180.

45. Akbani R, Akdemir KC, Aksoy BA, Albert M, Ally A, Amin SB, Arachchi H, Arora A, Auman JT, Ayala B, et al.: **Genomic Classification of Cutaneous Melanoma**. *Cell* 2015, **161**:1681–1696.

46. Sizemore GM, Pitarresi JR, Balakrishnan S, Ostrowski MC: **The ETS family of oncogenic transcription factors in solid tumours**. *Nat Rev Cancer* 2017, **17**:337–351.

47. Killela PJ, Reitman ZJ, Jiao Y, Bettegowda C, Agrawal N, Diaz LA, Friedman AH, Friedman H, Gallia GL, Giovanella BC, et al.: **TERT promoter mutations occur frequently in gliomas and a subset of tumors derived from cells with low rates of self-renewal**. *Proc Natl Acad Sci* 2013, **110**:6021–6026.

48. Barthel FP, Wei W, Tang M, Martinez-Ledesma E, Hu X, Amin SB, Akdemir KC, Seth S, Song X, Wang Q, et al.: **Systematic analysis of telomere length and somatic alterations in 31 cancer types**. *Nat Genet* 2017, **49**:349–357.

49. Fredriksson NJ, Ny L, Nilsson JA, Larsson E: **Systematic analysis of noncoding somatic mutations and gene expression alterations across 14 tumor types**. *Nat Genet* 2014, **46**:1258–1263.

50. Frenck RW, Blackburn EH, Shannon KM: **The rate of telomere sequence loss in human leukocytes varies with age**. *Proc Natl Acad Sci* 1998, **95**:5607–5610.

51. Iwama H, Ohyashiki K, Ohyashiki JH, Hayashi S, Yahata N, Ando K, Toyama K, Hoshika A, Takasaki M, Mori M, et al.: **Telomeric length and telomerase activity vary with age in peripheral blood cells obtained from normal individuals**. *Hum Genet* 1998, **102**:397–402.

52. Rufer N, Brümmendorf TH, Kolvraa S, Bischoff C, Christensen K, Wadsworth L, Schulzer M, Lansdorp PM: **Telomere Fluorescence Measurements in Granulocytes and T Lymphocyte Subsets Point to a High Turnover of Hematopoietic Stem Cells and Memory T Cells in Early Childhood**. *J Exp Med* 1999, **190**:157–168.

53. Son NH, Murray S, Yanovski J, Hodes RJ, Weng N: **Lineage-specific telomere shortening and unaltered capacity for telomerase expression in human T and B lymphocytes with age**. *J Immunol Baltim Md 1950* 2000, **165**:1191–1196.

54. Friedrich U, Griese E, Schwab M, Fritz P, Thon K, Klotz U: **Telomere length in different tissues of elderly patients**. *Mech Ageing Dev* 2000, **119**:89–99.

55. Savage SA: **Beginning at the ends: telomeres and human disease**. *F1000Research* 2018, **7**:524.

56. Rachakonda S, Kong H, Srinivas N, Garcia-Casado Z, Requena C, Fallah M, Heidenreich B, Planelles D, Traves V, Schadendorf D, et al.: **Telomere length, telomerase reverse transcriptase promoter mutations, and melanoma risk**. *Genes Chromosomes Cancer* 2018, **57**:564–572.

57. Aoude LG, Pritchard AL, Robles-Espinoza CD, Wadt K, Harland M, Choi J, Gartside M, Quesada V, Johansson P, Palmer JM, et al.: **Nonsense Mutations in the Shelterin Complex Genes ACD and TERF2IP in Familial Melanoma**. *JNCI J Natl Cancer Inst* 2014, **107**.

58. Alter BP, Baerlocher GM, Savage SA, Chanock SJ, Weksler BB, Willner JP, Peters JA, Giri N, Lansdorp PM: **Very short telomere length by flow fluorescence in situ**

hybridization identifies patients with dyskeratosis congenita. *Blood* 2007, **110**:1439–1447.

59. Alter BP, Rosenberg PS, Giri N, Baerlocher GM, Lansdorp PM, Savage SA: **Telomere length is associated with disease severity and declines with age in dyskeratosis congenita**. *Haematologica* 2012, **97**:353–359.

60. Alter BP, Giri N, Savage SA, Peters JA, Loud JT, Leathwood L, Carr AG, Greene MH, Rosenberg PS: **Malignancies and survival patterns in the National Cancer Institute inherited bone marrow failure syndromes cohort study**. *Br J Haematol* 2010, **150**:179–188.

61. Alter BP, Giri N, Savage SA, Rosenberg PS: **Cancer in dyskeratosis congenita**. *Blood* 2009, **113**:6549–6557.

62. Alter BP, Giri N, Savage SA, Rosenberg PS: **Cancer in the National Cancer Institute inherited bone marrow failure syndrome cohort after fifteen years of follow-up**. *Haematologica* 2018, **103**:30–39.

63. Rode L, Nordestgaard BG, Bojesen SE: **Long telomeres and cancer risk among 95 568 individuals from the general population**. *Int J Epidemiol* 2016, **45**:1634–1643.

64. Iles MM, Bishop DT, Taylor JC, Hayward NK, Brossard M, Cust AE, Dunning AM, Lee JE, Moses EK, Akslen LA, et al.: **The Effect on Melanoma Risk of Genes Previously Associated With Telomere Length**. *JNCI J Natl Cancer Inst* 2014, **106**:dju267.

65. Zou P, Gu A, Ji G, Zhao L, Zhao P, Lu A: **The TERT rs2736100 Polymorphism and Cancer Risk: A Meta-analysis Based on 25 Case-Control Studies**. *BMC Cancer* 2012, **12**:7.

66. Bojesen SE, Pooley KA, Johnatty SE, Beesley J, Michailidou K, Tyrer JP, Edwards SL, Pickett HA, Shen HC, Smart CE, et al.: **Multiple independent variants at the TERT locus are associated with telomere length and risks of breast and ovarian cancer**. *Nat Genet* 2013, **45**:371–384.

67. Han J, Qureshi AA, Prescott J, Guo Q, Ye L, Hunter DJ, De Vivo I: **A prospective study of telomere length and the risk of skin cancer**. *J Invest Dermatol* 2009, **129**:415–421.

68. Nan H, Du M, Vivo ID, Manson JE, Liu S, McTiernan A, Curb JD, Lessin LS, Bonner MR, Guo Q, et al.: **Shorter Telomeres Associate with a Reduced Risk of Melanoma Development**. *Cancer Res* 2011, **71**:6758–6763.

69. Johnson JZ, Hockemeyer D: **Human stem cell-based disease modeling: prospects and challenges**. *Curr Opin Cell Biol* 2015, **37**:84–90.

70. Huang D-S, Wang Z, He X-J, Diplas BH, Yang R, Killela PJ, Meng Q, Ye Z-Y, Wang W, Jiang X-T, et al.: **Recurrent TERT promoter mutations identified in a large-scale study of multiple tumour types are associated with increased TERT expression and telomerase activation**. *Eur J Cancer Oxf Engl 1990* 2015, **51**:969–976.

71. Mosrati MA, Willander K, Falk IJ, Hermanson M, Höglund M, Stockelberg D, Wei Y, Lotfi K, Söderkvist P: **Association between TERT promoter polymorphisms and acute myeloid leukemia risk and prognosis**. *Oncotarget* 2015, **6**:25109–25120.

72. Shimoi T, Yoshida M, Kitamura Y, Yoshino T, Kawachi A, Shimomura A, Noguchi E, Yunokawa M, Yonemori K, Shimizu C, et al.: **TERT promoter hotspot mutations in breast cancer**. *Breast Cancer Tokyo Jpn* 2018, **25**:292–296.

73. Cárcano FM, Vidal DO, van Helvoort Lengert A, Neto CS, Queiroz L, Marques H, Baltazar F, da Silva Martinelli CM, Soares P, da Silva ECA, et al.: **Hotspot TERT promoter mutations are rare events in testicular germ cell tumors**. *Tumour Biol J Int Soc Oncodevelopmental Biol Med* 2016, **37**:4901–4907.

74. Liu X, Wu G, Shan Y, Hartmann C, von Deimling A, Xing M: **Highly prevalent TERT promoter mutations in bladder cancer and glioblastoma**. *Cell Cycle* 2013, **12**:1637–1638.

75. Harland M, Petljak M, Robles-Espinoza CD, Ding Z, Gruis NA, van Doorn R, Pooley KA, Dunning AM, Aoude LG, Wadt KAW, et al.: **Germline TERT promoter mutations are rare in familial melanoma**. *Fam Cancer* 2016, **15**:139–144.

76. Shi J, Yang XR, Ballew B, Rotunno M, Calista D, Fargnoli MC, Ghiorzo P, Bressac-de Paillerets B, Nagore E, Avril MF, et al.: **Rare missense variants in POT1 predispose to familial cutaneous malignant melanoma**. *Nat Genet* 2014, **46**:482–486.

77. Robles-Espinoza CD, Harland M, Ramsay AJ, Aoude LG, Quesada V, Ding Z, Pooley KA, Pritchard AL, Tiffen JC, Petljak M, et al.: **POT1 loss-of-function variants predispose to familial melanoma**. *Nat Genet* 2014, **46**:478–481.

78. Calvete O, Martinez P, Garcia-Pavia P, Benitez-Buelga C, Paumard-Hernández B, Fernandez V, Dominguez F, Salas C, Romero-Laorden N, Garcia-Donas J, et al.: **A mutation in the POT1 gene is responsible for cardiac angiosarcoma in TP53-negative Li-Fraumeni-like families**. *Nat Commun* 2015, **6**:8383.

79. Vulliamy TJ, Walne A, Baskaradas A, Mason PJ, Marrone A, Dokal I: **Mutations in the reverse transcriptase component of telomerase (TERT) in patients with bone marrow failure**. *Blood Cells Mol Dis* 2005, **34**:257–263.

80. Vulliamy T, Marrone A, Goldman F, Dearlove A, Bessler M, Mason PJ, Dokal I: **The RNA component of telomerase is mutated in autosomal dominant dyskeratosis congenita**. *Nature* 2001, **413**:432–435.

81. Yamaguchi H, Baerlocher GM, Lansdorp PM, Chanock SJ, Nunez O, Sloand E, Young NS: **Mutations of the human telomerase RNA gene (TERC) in aplastic anemia and myelodysplastic syndrome**. *Blood* 2003, **102**:916–918.

82. Tsakiri KD, Cronkhite JT, Kuan PJ, Xing C, Raghu G, Weissler JC, Rosenblatt RL, Shay JW, Garcia CK: **Adult-onset pulmonary fibrosis caused by mutations in telomerase**. *Proc Natl Acad Sci U S A* 2007, **104**:7552–7557.

83. Aalbers AM, Kajigaya S, van den Heuvel-Eibrink MM, van der Velden VHJ, Calado RT, Young NS: **Human telomere disease due to disruption of the CCAAT box of the TERC promoter**. *Blood* 2012, **119**:3060–3063.

84. Savage SA, Giri N, Baerlocher GM, Orr N, Lansdorp PM, Alter BP: **TINF2, a Component of the Shelterin Telomere Protection Complex, Is Mutated in Dyskeratosis Congenita**. *Am J Hum Genet* 2008, **82**:501–509.

85. Gupta MP, Talcott KE, Kim DY, Agarwal S, Mukai S: **Retinal findings and a novel TINF2 mutation in Revesz syndrome: Clinical and molecular correlations with pediatric retinal vasculopathies**. *Ophthalmic Genet* 2017, **38**:51–60.

86. Guo Y, Kartawinata M, Li J, Pickett HA, Teo J, Kilo T, Barbaro PM, Keating B, Chen Y, Tian L, et al.: **Inherited bone marrow failure associated with germline mutation of ACD, the gene encoding telomere protein TPP1**. *Blood* 2014, **124**:2767–2774.

87. Takai H, Jenkinson E, Kabir S, Babul-Hirji R, Najm-Tehrani N, Chitayat DA, Crow YJ, Lange T de: **A POT1 mutation implicates defective telomere end fill-in and telomere truncations in Coats plus**. *Genes Dev* 2016, doi:10.1101/gad.276873.115.

88. Chiba K, Lorbeer FK, Shain AH, McSwiggen DT, Schruf E, Oh A, Ryu J, Darzacq X, Bastian BC, Hockemeyer D: **Mutations in the promoter of the telomerase gene TERT contribute to tumorigenesis by a two-step mechanism**. *Science* 2017, **357**:1416–1420.

89. Greider CW, Blackburn EH: **The telomere terminal transferase of tetrahymena is a ribonucleoprotein enzyme with two kinds of primer specificity**. *Cell* 1987, **51**:887–898.

90. Jafri MA, Ansari SA, Alqahtani MH, Shay JW: **Roles of telomeres and telomerase in cancer, and advances in telomerase-targeted therapies**. *Genome Med* 2016, **8**:69.

91. Shain AH, Yeh I, Kovalyshyn I, Sriharan A, Talevich E, Gagnon A, Dummer R, North J, Pincus L, Ruben B, et al.: **The Genetic Evolution of Melanoma from Precursor Lesions**. *N Engl J Med* 2015, **373**:1926–1936.

92. Ceccarelli M, Barthel FP, Malta TM, Sabedot TS, Salama SR, Murray BA, Morozova O, Newton Y, Radenbaugh A, Pagnotta SM, et al.: **Molecular Profiling Reveals Biologically Discrete Subsets and Pathways of Progression in Diffuse Glioma**. *Cell* 2016, **164**:550–563.

93. Nagore E, Heidenreich B, Rachakonda S, Garcia-Casado Z, Requena C, Soriano V, Frank C, Traves V, Quecedo E, Sanjuan-Gimenez J, et al.: **TERT promoter mutations in melanoma survival**. *Int J Cancer* 2016, **139**:75–84.

94. Maciejowski J, de Lange T: **Telomeres in cancer: tumour suppression and genome instability**. *Nat Rev Mol Cell Biol* 2017, **18**:175–186.

95. Artandi SE, DePinho RA: **A critical role for telomeres in suppressing and facilitating carcinogenesis**. *Curr Opin Genet Dev* 2000, **10**:39–46.

96. Lin TT, Norris K, Heppel NH, Pratt G, Allan JM, Allsup DJ, Bailey J, Cawkwell L, Hills R, Grimstead JW, et al.: **Telomere dysfunction accurately predicts clinical outcome in chronic lymphocytic leukaemia, even in patients with early stage disease**. *Br J Haematol* 2014, **167**:214–223.

97. Borah S, Xi L, Zaug AJ, Powell NM, Dancik GM, Cohen SB, Costello JC, Theodorescu D, Cech TR: **TERT promoter mutations and telomerase reactivation in urothelial cancer**. *Science* 2015, **347**:1006–1010.

98. Capper R, Britt-Compton B, Tankimanova M, Rowson J, Letsolo B, Man S, Haughton M, Baird DM: **The nature of telomere fusion and a definition of the critical telomere length in human cells**. *Genes Dev* 2007, **21**:2495–2508.

99. Feldser DM, Hackett JA, Greider CW: **Telomere dysfunction and the initiation of genome instability**. *Nat Rev Cancer* 2003, **3**:623–627.

100. Plentz RR, Caselitz M, Bleck JS, Gebel M, Flemming P, Kubicka S, Manns MP, Rudolph KL: **Hepatocellular telomere shortening correlates with chromosomal instability and the development of human hepatoma**. *Hepatology* 2004, **40**:80–86.

101. Bell RJA, Rube HT, Kreig A, Mancini A, Fouse SD, Nagarajan RP, Choi S, Hong C, He D, Pekmezci M, et al.: **The transcription factor GABP selectively binds and activates the mutant TERT promoter in cancer**. *Science* 2015, **348**:1036–1039.

102. Min J, Shay JW: **TERT Promoter Mutations Enhance Telomerase Activation by Long-Range Chromatin Interactions**. *Cancer Discov* 2016, **6**:1212–1214.

103. Lengner CJ, Gimelbrant AA, Erwin JA, Cheng AW, Guenther MG, Welstead GG, Alagappan R, Frampton GM, Xu P, Muffat J, et al.: **Derivation of Pre-X Inactivation Human Embryonic Stem Cells under Physiological Oxygen Concentrations**. *Cell* 2010, **141**:872–883.

104. Soldner F, Hockemeyer D, Beard C, Gao Q, Bell GW, Cook EG, Hargus G, Blak A, Cooper O, Mitalipova M, et al.: **Parkinson's Disease Patient-Derived Induced Pluripotent Stem Cells Free of Viral Reprogramming Factors**. *Cell* 2009, **136**:964–977.

105. Hockemeyer D, Soldner F, Beard C, Gao Q, Mitalipova M, DeKelver RC, Katibah GE, Amora R, Boydston EA, Zeitler B, et al.: **Efficient targeting of expressed and silent genes in human ESCs and iPSCs using zinc-finger nucleases**. *Nat Biotechnol* 2009, **27**:851–857.

106. Hockemeyer D, Wang H, Kiani S, Lai CS, Gao Q, Cassady JP, Cost GJ, Zhang L, Santiago Y, Miller JC, et al.: **Genetic engineering of human pluripotent cells using TALE nucleases**. *Nat Biotechnol* 2011, **29**:731–734.

107. Chiba K, Vogan JM, Wu RA, Gill MS, Zhang X, Collins K, Hockemeyer D: **Endogenous Telomerase Reverse Transcriptase N-Terminal Tagging Affects Human Telomerase Function at Telomeres In Vivo**. *Mol Cell Biol* 2017, **37**.

108. Sergé A, Bertaux N, Rigneault H, Marguet D: **Dynamic multiple-target tracing to probe spatiotemporal cartography of cell membranes**. *Nat Methods* 2008, **5**:687–694.

109. Ryu J, Hong SS, Horn BKP, Freeman DM, Mermelstein MS: **Multibeam interferometric illumination as the primary source of resolution in optical microscopy**. *Appl Phys Lett* 2006, **88**:171112.

110. Serrano M, Lin AW, McCurrach ME, Beach D, Lowe SW: **Oncogenic ras provokes premature cell senescence associated with accumulation of p53 and p16INK4a**. *Cell* 1997, **88**:593–602.

111. Lin AW, Barradas M, Stone JC, van Aelst L, Serrano M, Lowe SW: **Premature senescence involving p53 and p16 is activated in response to constitutive MEK/MAPK mitogenic signaling**. *Genes Dev* 1998, **12**:3008–3019.

112. Michaloglou C, Vredeveld LCW, Soengas MS, Denoyelle C, Kuilman T, van der Horst CMAM, Majoor DM, Shay JW, Mooi WJ, Peeper DS: **BRAFE600-associated senescence-like cell cycle arrest of human naevi**. *Nature* 2005, **436**:720–724.

113. Bartkova J, Rezaei N, Liontos M, Karakaidos P, Kletsas D, Issaeva N, Vassiliou L-VF, Kolettas E, Niforou K, Zoumpourlis VC, et al.: **Oncogene-induced senescence is part of the tumorigenesis barrier imposed by DNA damage checkpoints**. *Nature* 2006, **444**:633–637.

114. Di Micco R, Fumagalli M, Cicalese A, Piccinin S, Gasparini P, Luise C, Schurra C, Garre' M, Nuciforo PG, Bensimon A, et al.: **Oncogene-induced senescence is a DNA damage response triggered by DNA hyper-replication**. *Nature* 2006, **444**:638–642.

115. Harley CB, Futcher AB, Greider CW: **Telomeres shorten during ageing of human fibroblasts**. *Nature* 1990, **345**:458–460.

116. Allsopp RC, Vaziri H, Patterson C, Goldstein S, Younglai EV, Futcher AB, Greider CW, Harley CB: **Telomere length predicts replicative capacity of human fibroblasts**. *Proc Natl Acad Sci U S A* 1992, **89**:10114–10118.

117. Zhang A, Zheng C, Lindvall C, Hou M, Ekedahl J, Lewensohn R, Yan Z, Yang X, Henriksson M, Blennow E, et al.: **Frequent Amplification of the Telomerase Reverse Transcriptase Gene in Human Tumors**. *Cancer Res* 2000, **60**:6230–6235.

118. Peifer M, Hertwig F, Roels F, Dreidax D, Gartlgruber M, Menon R, Krämer A, Roncaioli JL, Sand F, Heuckmann JM, et al.: **Telomerase activation by genomic rearrangements in high-risk neuroblastoma**. *Nature* 2015, **526**:700–704.

119. Lee JH, Lee JE, Kahng JY, Kim SH, Park JS, Yoon SJ, Um J-Y, Kim WK, Lee J-K, Park J, et al.: **Human glioblastoma arises from subventricular zone cells with low-level driver mutations**. *Nature* 2018, **560**:243–247.

120. Shain AH, Joseph NM, Yu R, Benhamida J, Liu S, Prow T, Ruben B, North J, Pincus L, Yeh I, et al.: **Genomic and Transcriptomic Analysis Reveals**

Incremental Disruption of Key Signaling Pathways during Melanoma Evolution. *Cancer Cell* 2018, **34**:45-55.e4.

121. Tsao H, Bevona C, Goggins W, Quinn T: **The transformation rate of moles (melanocytic nevi) into cutaneous melanoma: a population-based estimate**. *Arch Dermatol* 2003, **139**:282–288.

122. Shitara D, Nascimento MM, Puig S, Yamada S, Enokihara MMSS, Michalany N, Bagatin E: **Nevus-associated melanomas: clinicopathologic features**. *Am J Clin Pathol* 2014, **142**:485–491.

123. Carr J, Mackie RM: **Point mutations in the N-ras oncogene in malignant melanoma and congenital naevi**. *Br J Dermatol* 1994, **131**:72–77.

124. Bauer J, Curtin JA, Pinkel D, Bastian BC: **Congenital melanocytic nevi frequently harbor NRAS mutations but no BRAF mutations**. *J Invest Dermatol* 2007, **127**:179–182.

125. Krauthammer M, Kong Y, Bacchiocchi A, Evans P, Pornputtapong N, Wu C, McCusker JP, Ma S, Cheng E, Straub R, et al.: **Exome sequencing identifies recurrent mutations in *NF1* and RASopathy genes in sun-exposed melanomas**. *Nat Genet* 2015, **47**:996.

126. Hodis E, Watson IR, Kryukov GV, Arold ST, Imielinski M, Theurillat J-P, Nickerson E, Auclair D, Li L, Place C, et al.: **A Landscape of Driver Mutations in Melanoma**. *Cell* 2012, **150**:251–263.

127. Maldonado JL, Fridlyand J, Patel H, Jain AN, Busam K, Kageshita T, Ono T, Albertson D, Pinkel D, Bastian BC: **Determinants of BRAF mutations in primary melanoma**. *J Natl Cancer Inst* 2003, **95**:1878–90.

128. Menzies AM, Haydu LE, Visintin L, Carlino MS, Howle JR, Thompson JF, Kefford RF, Scolyer RA, Long GV: **Distinguishing Clinicopathologic Features of Patients with V600E and V600K BRAF-Mutant Metastatic Melanoma**. *Clin Cancer Res* 2012, **18**:3242–3249.

129. Akbani R, Akdemir KC, Aksoy BA, Albert M, Ally A, Amin SB, Arachchi H, Arora A, Auman JT, Ayala B, et al.: **Genomic Classification of Cutaneous Melanoma**. *Cell* 2015, **161**:1681–1696.

130. Pollock PM, Harper UL, Hansen KS, Yudt LM, Stark M, Robbins CM, Moses TY, Hostetter G, Wagner U, Kakareka J, et al.: **High frequency of BRAF mutations in nevi**. *Nat Genet* 2003, **33**:19–20.

131. Kumar R, Angelini S, Snellman E, Hemminki K: **BRAF mutations are common somatic events in melanocytic nevi**. *J Invest Dermatol* 2004, **122**:342–8.

132. Poynter JN, Elder JT, Fullen DR, Nair RP, Soengas MS, Johnson TM, Redman B, Thomas NE, Gruber SB: **BRAF and NRAS mutations in melanoma and melanocytic nevi**. *Melanoma Res* 2006, **16**:267–73.

133. Wu J, Rosenbaum E, Begum S, Westra WH: **Distribution of BRAF T1799A(V600E) mutations across various types of benign nevi: implications for melanocytic tumorigenesis**. *Am J Dermatopathol* 2007, **29**:534–7.

134. MacKie RM, English J, Aitchison TC, Fitzsimons CP, Wilson P: **The number and distribution of benign pigmented moles (melanocytic naevi) in a healthy British population**. *Br J Dermatol* 1985, **113**:167–174.

135. Kittler H, Pehamberger H, Wolff K, Binder M: **Follow-up of melanocytic skin lesions with digital epiluminescence microscopy: Patterns of modifications observed in early melanoma, atypical nevi, and common nevi**. *J Am Acad Dermatol* 2000, **43**:467–476.

136. Hayward NK, Wilmott JS, Waddell N, Johansson PA, Field MA, Nones K, Patch A-M, Kakavand H, Alexandrov LB, Burke H, et al.: **Whole-genome landscapes of major melanoma subtypes**. *Nature* 2017, **advance online publication**.

137. Hewitt G, Jurk D, Marques FDM, Correia-Melo C, Hardy T, Gackowska A, Anderson R, Taschuk M, Mann J, Passos JF: **Telomeres are favoured targets of a persistent DNA damage response in ageing and stress-induced senescence**. *Nat Commun* 2012, **3**:708.

138. Suram A, Kaplunov J, Patel PL, Ruan H, Cerutti A, Boccardi V, Fumagalli M, Di Micco R, Mirani N, Gurung RL, et al.: **Oncogene-induced telomere dysfunction enforces cellular senescence in human cancer precursor lesions**. *EMBO J* 2012, **31**:2839–2851.

139. Elder DE, Murphy GF, Pathology (U.S.) AFI of: *Melanocytic tumors of the skin*. Armed Forces Institute of Pathology; 1991.

140. Bertuch AA: **The molecular genetics of the telomere biology disorders**. *RNA Biol* 2015, **13**:696–706.

141. Townsley DM, Dumitriu B, Young NS: **Bone marrow failure and the telomeropathies**. *Blood* 2014, **124**:2775–2783.

142. Heiss NS, Knight SW, Vulliamy TJ, Klauck SM, Wiemann S, Mason PJ, Poustka A, Dokal I: **X-linked dyskeratosis congenita is caused by mutations in a highly conserved gene with putative nucleolar functions**. *Nat Genet* 1998, **19**:32–38.

143. Mitchell JR, Wood E, Collins K: **A telomerase component is defective in the human disease dyskeratosis congenita**. *Nature* 1999, **402**:551–555.

144. Knight SW, Heiss NS, Vulliamy TJ, Greschner S, Stavrides G, Pai GS, Lestringant G, Varma N, Mason PJ, Dokal I, et al.: **X-Linked Dyskeratosis Congenita Is Predominantly Caused by Missense Mutations in the DKC1 Gene**. *Am J Hum Genet* 1999, **65**:50–58.

145. Marrone A, Walne A, Tamary H, Masunari Y, Kirwan M, Beswick R, Vulliamy T, Dokal I: **Telomerase reverse-transcriptase homozygous mutations in autosomal recessive dyskeratosis congenita and Hoyeraal-Hreidarsson syndrome**. *Blood* 2007, **110**:4198–4205.

146. Walne AJ, Vulliamy T, Marrone A, Beswick R, Kirwan M, Masunari Y, Al-Qurashi F, Aljurf M, Dokal I: **Genetic heterogeneity in autosomal recessive dyskeratosis congenita with one subtype due to mutations in the telomerase-associated protein NOP10**. *Hum Mol Genet* 2007, **16**:1619–1629.

147. Vulliamy T, Beswick R, Kirwan M, Marrone A, Digweed M, Walne A, Dokal I: **Mutations in the telomerase component NHP2 cause the premature ageing syndrome dyskeratosis congenita**. *Proc Natl Acad Sci U S A* 2008, **105**:8073–8078.

148. Zhong F, Savage SA, Shkreli M, Giri N, Jessop L, Myers T, Chen R, Alter BP, Artandi SE: **Disruption of telomerase trafficking by TCAB1 mutation causes dyskeratosis congenita**. *Genes Dev* 2011, **25**:11–16.

149. Tummala H, Walne A, Collopy L, Cardoso S, de la Fuente J, Lawson S, Powell J, Cooper N, Foster A, Mohammed S, et al.: **Poly(A)-specific ribonuclease deficiency impacts telomere biology and causes dyskeratosis congenita**. *J Clin Invest* 2015, **125**:2151–2160.

150. Ballew BJ, Yeager M, Jacobs K, Giri N, Boland J, Burdett L, Alter BP, Savage SA: **Germline mutations of regulator of telomere elongation helicase 1, RTEL1, in Dyskeratosis congenita**. *Hum Genet* 2013, **132**:473–480.

151. Kocak H, Ballew BJ, Bisht K, Eggebeen R, Hicks BD, Suman S, O'Neil A, Giri N, Maillard I, Alter BP, et al.: **Hoyeraal-Hreidarsson syndrome caused by a germline mutation in the TEL patch of the telomere protein TPP1**. *Genes Dev* 2014, **28**:2090–2102.

152. Savage SA, Giri N, Jessop L, Pike K, Plona T, Burdett L, Alter BP: **Sequence analysis of the shelterin telomere protection complex genes in dyskeratosis congenita**. *J Med Genet* 2011, **48**:285–288.

153. Ye JZ-S, Donigian JR, van Overbeek M, Loayza D, Luo Y, Krutchinsky AN, Chait BT, de Lange T: **TIN2 binds TRF1 and TRF2 simultaneously and stabilizes the TRF2 complex on telomeres**. *J Biol Chem* 2004, **279**:47264–47271.

154. Jz Y, T de L: **TIN2 Is a Tankyrase 1 PARP Modulator in the TRF1 Telomere Length Control Complex**. *Nat Genet* 2004, **36**.

155. Takai KK, Kibe T, Donigian JR, Frescas D, de Lange T: **Telomere protection by TPP1/POT1 requires tethering to TIN2**. *Mol Cell* 2011, **44**:647–659.

156. Walne AJ, Vulliamy T, Beswick R, Kirwan M, Dokal I: **TINF2 mutations result in very short telomeres: analysis of a large cohort of patients with dyskeratosis congenita and related bone marrow failure syndromes**. *Blood* 2008, **112**:3594–3600.

157. Sarper N, Zengin E, Kılıç SÇ: **A child with severe form of dyskeratosis congenita and TINF2 mutation of shelterin complex**. *Pediatr Blood Cancer* 2010, **55**:1185–1186.

158. Xin Z-T, Ly H: **Characterization of interactions between naturally mutated forms of the TIN2 protein and its known protein partners of the shelterin complex**. *Clin Genet* 2012, **81**:301–302.

159. Yang D, He Q, Kim H, Ma W, Songyang Z: **TIN2 Protein Dyskeratosis Congenita Missense Mutants Are Defective in Association with Telomerase**. *J Biol Chem* 2011, **286**:23022–23030.

160. Frescas D, Lange T de: **A TIN2 dyskeratosis congenita mutation causes telomerase-independent telomere shortening in mice**. *Genes Dev* 2014, **28**:153–166.

161. Nelson ND, Dodson LM, Escudero L, Sukumar AT, Williams CL, Mihalek I, Baldan A, Baird DM, Bertuch AA: **The C-Terminal Extension Unique to the Long Isoform of the Shelterin Component TIN2 Enhances Its Interaction with TRF2 in a Phosphorylation- and Dyskeratosis Congenita Cluster-Dependent Fashion**. *Mol Cell Biol* 2018, **38**.

162. Pike AM, Strong MA, Ouyang JPT, Greider CW: **TIN2 Functions with TPP1/POT1 To Stimulate Telomerase Processivity**. *Mol Cell Biol* 2019, **39**.

163. Balakumaran A, Mishra PJ, Pawelczyk E, Yoshizawa S, Sworder BJ, Cherman N, Kuznetsov SA, Bianco P, Giri N, Savage SA, et al.: **Bone marrow skeletal stem/progenitor cell defects in dyskeratosis congenita and telomere biology disorders**. *Blood* 2015, **125**:793–802.

164. Fok WC, Shukla S, Vessoni AT, Brenner KA, Parker R, Sturgeon CM, Batista LFZ: **Posttranscriptional modulation of TERC by PAPD5 inhibition rescues hematopoietic development in dyskeratosis congenita**. *Blood* 2019, **133**:1308–1312.

165. Boyle JM, Hennick KM, Regalado SG, Vogan JM, Zhang X, Collins K, Hockemeyer D: **Telomere length set point regulation in human pluripotent stem cells critically depends on the shelterin protein TPP1**. *bioRxiv* 2018, doi:10.1101/298778.

166. Cong L, Ran FA, Cox D, Lin S, Barretto R, Habib N, Hsu PD, Wu X, Jiang W, Marraffini LA, et al.: **Multiplex Genome Engineering Using CRISPR/Cas Systems**. *Science* 2013, **339**:819–823.

167. Tucker KL, Wang Y, Dausman J, Jaenisch R: **A transgenic mouse strain expressing four drug-selectable marker genes**. *Nucleic Acids Res* 1997, **25**:3745–3746.

168. Lai T-P, Zhang N, Noh J, Mender I, Tedone E, Huang E, Wright WE, Danuser G, Shay JW: **A method for measuring the distribution of the shortest telomeres in cells and tissues**. *Nat Commun* 2017, **8**:1–14.

169. Mitchell TJ, Turajlic S, Rowan A, Nicol D, Farmery JHR, O'Brien T, Martincorena I, Tarpey P, Angelopoulos N, Yates LR, et al.: **Timing the Landmark Events in the Evolution of Clear Cell Renal Cell Cancer: TRACERx Renal**. *Cell* 2018, **173**:611-623.e17.

170. Nault JC, Mallet M, Pilati C, Calderaro J, Bioulac-Sage P, Laurent C, Laurent A, Cherqui D, Balabaud C, Zucman-Rossi J, et al.: **High frequency of telomerase reverse-transcriptase promoter somatic mutations in hepatocellular carcinoma and preneoplastic lesions**. *Nat Commun* 2013, **4**:2218.

171. Kim SK, Takeda H, Takai A, Matsumoto T, Kakiuchi N, Yokoyama A, Yoshida K, Kaido T, Uemoto S, Minamiguchi S, et al.: **Comprehensive analysis of genetic aberrations linked to tumorigenesis in regenerative nodules of liver cirrhosis**. *J Gastroenterol* 2019, **54**:628–640.

172. Nault JC, Calderaro J, Tommaso LD, Balabaud C, Zafrani ES, Bioulac-Sage P, Roncalli M, Zucman-Rossi J: **Telomerase reverse transcriptase promoter**

mutation is an early somatic genetic alteration in the transformation of premalignant nodules in hepatocellular carcinoma on cirrhosis. *Hepatology* 2014, **60**:1983–1992.

173. Bataille V, Kato BS, Falchi M, Gardner J, Kimura M, Lens M, Perks U, Valdes AM, Bennett DC, Aviv A, et al.: **Nevus Size and Number Are Associated with Telomere Length and Represent Potential Markers of a Decreased Senescence In vivo**. *Cancer Epidemiol Prev Biomark* 2007, **16**:1499–1502.

174. Emery JD, Usher-Smith JA, Walter FM: **Predicting the Risk of Melanoma**. *JAMA Dermatol* 2016, **152**:875–877.

175. Liu R, Zhang T, Zhu G, Xing M: **Regulation of mutant TERT by BRAF V600E/MAP kinase pathway through FOS/ GABP in human cancer**. *Nat Commun* 2018, **9**:1–13.

176. Song YS, Yoo S-K, Kim HH, Jung G, Oh A-R, Cha J-Y, Kim S-J, Cho SW, Lee KE, Seo J-S, et al.: **Interaction of BRAF-induced ETS factors with mutant TERT promoter in papillary thyroid cancer**. *Endocr Relat Cancer* 2019, doi:10.1530/ERC-17-0562.

177. Huang FW, Bielski CM, Rinne ML, Hahn WC, Sellers WR, Stegmeier F, Garraway LA, Kryukov GV: **TERT promoter mutations and monoallelic activation of TERT in cancer**. *Oncogenesis* 2015, **4**:e176–e176.

178. Stern JL, Theodorescu D, Vogelstein B, Papadopoulos N, Cech TR: **Mutation of the TERT promoter, switch to active chromatin, and monoallelic TERT expression in multiple cancers**. *Genes Dev* 2015, **29**:2219–2224.

179. Akıncılar SC, Khattar E, Boon PLS, Unal B, Fullwood MJ, Tergaonkar V: **Long-Range Chromatin Interactions Drive Mutant TERT Promoter Activation**. *Cancer Discov* 2016, **6**:1276–1291.

180. Mancini A, Xavier-Magalhães A, Woods WS, Nguyen K-T, Amen AM, Hayes JL, Fellmann C, Gapinske M, McKinney AM, Hong C, et al.: **Disruption of the β1L Isoform of GABP Reverses Glioblastoma Replicative Immortality in a TERT Promoter Mutation-Dependent Manner**. *Cancer Cell* 2018, **34**:513-528.e8.

181. Li Y, Zhou Q-L, Sun W, Chandrasekharan P, Cheng HS, Ying Z, Lakshmanan M, Raju A, Tenen DG, Cheng S-Y, et al.: **Non-canonical NF-κB signalling and ETS1/2 cooperatively drive C250T mutant TERT promoter activation**. *Nat Cell Biol* 2015, **17**:1327–1338.

182. Bullock M, Lim G, Zhu Y, Åberg H, Kurdyukov S, Clifton-Bligh RJ: **The ETS Factor ETV5 Activates the Mutant TERT Promoter in Thyroid Cancer**. *Thyroid Off J Am Thyroid Assoc* 2019, doi:10.1089/thy.2018.0314.

183. Corces MR, Granja JM, Shams S, Louie BH, Seoane JA, Zhou W, Silva TC, Groeneveld C, Wong CK, Cho SW, et al.: **The chromatin accessibility landscape of primary human cancers**. *Science* 2018, **362**.

184. Makowski MM, Willems E, Fang J, Choi J, Zhang T, Jansen PWTC, Brown KM, Vermeulen M: **An interaction proteomics survey of transcription factor binding at recurrent TERT promoter mutations**. *PROTEOMICS* 2016, **16**:417–426.

185. Shay JW: **Role of Telomeres and Telomerase in Aging and Cancer**. *Cancer Discov* 2016, **6**:584–593.

186. Chiappori AA, Kolevska T, Spigel DR, Hager S, Rarick M, Gadgeel S, Blais N, Von Pawel J, Hart L, Reck M, et al.: **A randomized phase II study of the telomerase inhibitor imetelstat as maintenance therapy for advanced non-small-cell lung cancer**. *Ann Oncol* 2015, **26**:354–362.

187. Ribero S, Davies JR, Requena C, Carrera C, Glass D, Rull R, Vidal-Sicart S, Vilalta A, Alos L, Soriano V, et al.: **High nevus counts confer a favorable prognosis in melanoma patients**. *Int J Cancer* 2015, **137**:1691–1698.

188. Rachakonda S, Srinivas N, Mahmoudpour SH, Garcia-Casado Z, Requena C, Traves V, Soriano V, Cardelli M, Pjanova D, Molven A, et al.: **Telomere length and survival in primary cutaneous melanoma patients**. *Sci Rep* 2018, **8**:10947.

189. Maryoung L, Yue Y, Young A, Newton CA, Barba C, Oers NSC van, Wang RC, Garcia CK: **Somatic mutations in telomerase promoter counterbalance germline loss-of-function mutations**. *J Clin Invest* 2017, **127**:982–986.